


Spatial and temporal integration in
the substrate for self-stimulation of
the lateral hypothalamus in the rat

Dwayne C. Schindler

A Thesis
in
The Department
of
Psychology

Presented in Partial Fullfillment of the Requirements
for the degree of Master of Arts at
Concordia University
Montreal, Quebec, Canada
August 1983

© Dwayne C. Schindler ~



ABSTRACT

SPATIAL AND TEMPORAL INTEGRATION IN THE SUBSTRATE FOR SELF-STIMULATION OF THE LATERAL HYPOTHALAMUS IN THE RAT

Dwayne C. Schindler

Two experiments were conducted to test a mathematical model of how electrical stimulation of the brain results in behaviour directed toward obtaining more stimulation. The model proposes that the trade-off function¹ relating the reciprocal of the number of pulses ($1/N$) and the current (I) is linear over some range of values. Furthermore, the slope of the function is sub-divided into three anatomical and electrophysiological variables, two of which are functions of either pulse or train duration. It was hypothesized that these experiments would not only test the model, but also shed light on the current integrating properties of the directly stimulated tissue, and aid in characterizing the network responsible for post-synaptic integration. Twelve male rats bearing chronic electrodes aimed at the lateral hypothalamus were trained to self-stimulate. In the strength-duration experiment, train duration was held

constant and pulse duration was varied. At each pulse duration, I/N and I were traded off. A similar procedure was employed in the charge-duration experiment, except pulse duration was held constant and train duration was varied. Most of the gross predictions of the model were supported. However, some of the finer predictions were not. Since estimates of the minimum current may be inaccurate, an unbiased estimate of the chronaxie for the strength-duration function could not be calculated. The form of the charge-duration function was linear, a finding consistent with previous results. It would appear that the model contributes to understanding how stimulation parameters affect the activity of the substrate for self-stimulation.

Acknowledgements

I would like to express my appreciation to Dr. Peter Shizgal, my thesis supervisor, without whose help none of this would have been possible. In spite of my snail's pace, he had the patience and understanding to let me evolve in my own time. I would like to thank Dr. Barbara Woodside for her comments concerning the need to build better bridges across the chasms of the early drafts and the need to make the material more accessible. While it can be said that the Faculty and Staff of the Department of Psychology exist to help students, I think they deserve honourable mention for supporting my excesses.

I would like to thank Cathy Bielaiew and George Fouriezios for sharing with me much more than just their knowledge of psychology. Their friendship has been and is important to me.

I would like to thank Sue Schenk for all the tricks that she taught me. Also, I would like to thank David Morton for helping me tame several computer monsters. To all the other people in our lab, I would like to thank you for having been reasonable when I wasn't.

Finally, I would like to thank Hiedi and my parents for supporting me when I needed it most.

I would also like to thank the National Science and Engineering Research Council for having funded much of this research.

Table of Contents

	Page
Introduction	1
I. Rationale for Studying BSR	2
II. A Model of the BSR Substrate	14
a) The minimal model	14
b) The cable model	15
c) The integrator	18
d) The combined model	22
III. Strength-duration experiments	29
a) Testing the model	40
b) Distinguishing between two hypotheses	43
c) A non-arbitrary, strength-duration curve	58
IV. Charge-duration experiments	59
a) Testing the model	60
b) A charge-duration curve	62
Summary	65
Method	68
Subjects	68
Apparatus	69
Procedure	69
Initial training and selection	69
Strength-duration experiments	71
Charge-duration experiments	74
Histology	77

Table of Contents

	Page
Results	78
I. Figures	78
Strength-duration experiments	78
Required number determinations	78
Required current determinations	79
Charge-duration experiments	87
Required number determinations	87
Required current determinations	92
II. Data analysis	99
III. Statistical analysis	113
Strength-duration experiments	113
Required number determinations	113
Required current determinations	117
Charge-duration experiments	127
Required number determinations	127
Required current determinations	134
IV. Histology	144

Table of Contents

	Page
Discussion	147
I. The $1/N$ versus I trade-off functions	149
Linearity	150
The slope	151
$I_0(d)$	153
$(1/N)_0$	156
I_{min}	158
$(1/N)_c$	161
The fate of the principal predictions: A summary	162
II. Multiple firing versus multiple sub-populations	164
III. A non-arbitrary, strength-duration curve	170
IV. The charge-duration curve	170
V. Overview	176
Reference notes	180
References	181

List of Figures

Figure		Page
1	Predicted linear relationship between $1/N$ and I given a constant level of performance.	24
2	Resistor-capacitor network models of the neural membrane.	31
3	Idealized strength-duration curve.	33
4	Predictions of the extended model for short pulse durations when train duration is constant and pulse duration is varied.	44
5	Behaviourally-derived strength-duration curve given multiple sub-populations.	50
6	Electrophysiologically- and behaviourally-derived strength-duration curves given multiple firing.	54
7	Predicted changes in the $1/N$ versus I trade-off functions for multiple sub-populations and multiple firing.	57
8	Predicted changes in the $1/N$ versus I trade-off functions when pulse duration is constant and train duration is varied.	63
9	The family of $1/N$ versus I trade-off functions for subjects run in the required number strength-duration experiment.	80-86
10	The family of $1/N$ versus I trade-off functions for subjects run in the required current strength-duration experiment.	88-89

List of Figures

Figure	Page
11 The family of $1/N$ versus I trade-off functions for subjects run in the required current strength-duration experiment shown using a limited abscissal range.	90-91
12 The family of $1/N$ versus I trade-off functions for subjects run in the required number charge-duration experiment.	93-98
13 The family of $1/N$ versus I trade-off functions for subjects run in the required current charge-duration experiment.	100-103
14 The family of $1/N$ versus I trade-off functions for subjects run in the required current charge-duration experiment shown using a limited abscissal range.	104-107
15 Strength-duration curves based on I_{min} and the slope for a subject from the required number variant.	128
16 Strength-duration curves based on I_{min} and the slope for a subject from the required current variant.	129
17 Charge-duration functions for two subjects: one from the required number variant and the other from the required current variant.	146
18 Electrode placements.	148

List of Tables

Table	Page
1. Notation.	9-11
2 Chronaxies and the number of data points used to determine the chronaxies for the charge-duration experiment.	111
3 Slope and y-intercept values derived from the required number strength-duration experiment.	114
4 Mean minimum current values derived from the required number strength-duration experiment.	116
5 The x-intercept derived from the required number strength-duration experiment.	118
6 The $(1/N)c$ values derived from the required number strength-duration experiment.	119
7 Data derived from the required current strength-duration experiment.	120
8 Chronaxie and rheobase estimates for the strength-duration function derived from fitting a hyperbola or an exponential to I_{min} -pulse duration values.	125
9 Chronaxie and rheobase estimates for the strength-duration function derived from fitting a hyperbola or an exponential to $(slope-1)$ -pulse duration values.	126
10 Slope and y-intercept values derived from the required number charge-duration experiment.	130
11 Mean minimum current values derived from the required number charge-duration experiment.	132

List of Tables

Table	Page
12. Mean current values corresponding to a frequency of 400 hertz derived from the required number charge-duration experiment.	133
13. The x-intercept derived from the required number charge-duration experiment.	135
14. The $(1/N)c$ values derived from the required number charge-duration experiment.	136
15. The slope and y-intercept values derived from the required current charge-duration experiment.	138
16. Mean minimum current values derived from the required current charge-duration experiment.	139
17. Mean current values corresponding to a frequency of 400 hertz derived from the required current charge-duration experiment.	140
18. The x-intercept values derived from the required current charge-duration experiment.	141
19. The $(1/N)c$ values derived from the required current charge-duration experiment.	143
20. Chronaxie estimates for the charge-duration functions based on the effective charge and the total charge.	145

The objective of the present series of experiments was to characterize the neural substrate that subserves the rewarding effects of electrical brain stimulation.

Specifically, these experiments were designed to test a recently proposed mathematical model (Gallistel, Shizgal, and Yeomans, 1981) which relates two stimulation parameters through the use of anatomical and physiological constructs. If the model were found to adequately describe the relationship between these parameters, then it could be used to estimate some of the strength-duration characteristics of the neurons subserving brain stimulation reward (BSR). These estimates could then be used in electrophysiological recording studies to aid in discriminating between those neurons that most likely subserve reward and those that subserve other functions. They could also be used to describe the spatio-temporal integrating characteristics of the reward substrate.

The introductory discussion below is divided into four parts. The first deals with the rationale for employing the BSR paradigm to study the neurophysiological basis of learning and motivation. Next, the mathematical model proposed by Gallistel et al. (1981) is developed. This model relates the reciprocal of the number of stimulation pulses ($1/N$) to the current (I) through the use of physiological

constructs. The two subsequent parts investigate the dependence of the function relating $1/N$ to I on the duration of stimulation pulses and trains. These sections explain how physiological characteristics of the reward substrate might be inferred from the form of these dependencies.

I. Rationale for Studying BSR

The discovery that rats would perform operant behaviour for electrical stimulation of certain brain regions (Olds and Milner, 1954) provided an impetus for the study of the neurophysiological basis of learning and motivation. It was felt that this technique would facilitate the exploration of the neural mechanisms involved in naturally occurring appetitive behaviours. The notion that there is a link between self-stimulation and behaviours such as feeding (Hoebel, 1968; Hoebel, 1969; Hoebel, 1975; Hoebel and Teitelbaum, 1962; Hoebel and Thompson, 1969; Margules and Olds, 1962) and copulation (Caggiula and Hoebel, 1966) has received consistent empirical support.

For example, Hoebel (1975) has reviewed the work leading to the proposal that lateral hypothalamic neurons that support feeding also support self-stimulation. As noted by Hoebel (1975), there are several lines of research that lead to this conclusion. First, there is the fact that electrodes aimed at the lateral hypothalamus (LH) that

support self-stimulation can also support feeding behaviour. Second, it was found that postingestional factors such as osmotic and gastric loads depress both feeding and self-stimulation behaviours. Third, when the subject was satiated, it was found that self-stimulation behaviour was depressed but that stimulation-escape behaviour was increased. Additional support stemmed from the demonstration that appetite suppressants such as phenylpropanolamine also suppressed self-stimulation. All these lines of research point out factors that affect feeding and self-stimulation in a parallel manner.

Support for a relation between BSR and natural rewards has also come from the area of electrophysiology. Rolls, Burton, and Mora (1980) performed a series of experiments aimed at analyzing neuronal activity related to BSR and to feeding in rhesus and squirrel monkeys. First, these authors implanted arrays of stimulating electrodes aimed at various brain sites. After the subjects had been taught to self-stimulate, the activity of single neurons were recorded in the LH, amygdala, orbital frontal cortex, and the globus pallidus when stimulation was applied at the self-stimulation sites. Of particular interest was that neurons in the LH were activated from several of the self-stimulation sites. Rolls et al. (1980) concluded that in the monkey there is a highly interconnected set of self-stimulation sites. That is, stimulation applied at one self-stimulation site can elicit activity in neurons at other

self-stimulation sites.

In the same study, Rolls et al. (1980) assessed the effect of food presentation on the activity of a large sample of neurons trans-synaptically driven by stimulation at BSR sites. It was found that 104 neurons, or about 14 percent of the sample, showed activity changes associated with the presentation of food stimuli. Increases in activity occurred only when the subject was hungry. That is, increases in the activity of the neurons occurred only when the food was rewarding. It was concluded that there are neurons within the monkey brain that receive input from both food reward and BSR.

In summary, the current literature is consistent with a link between BSR and naturally occurring motivational phenomena. Thus, it does not seem unrealistic to expect that research involving these naturally occurring phenomena would have a two-fold effect. First, it would enhance our knowledge of the neurological basis of these phenomena and second, it may eventually permit the development of treatment procedures for disorders involving these phenomena.

It has been proposed that a detailed understanding of the mechanisms subserving BSR might come from a circuit diagram that details the trajectories of the neurons subserving self-stimulation and the pattern of their

synaptic connections. The use of neural circuit diagrams as mechanistic explanations for behaviour has been implemented successfully in invertebrate neurobiology (Kandel, 1970; Pearson, 1976; Roeder, 1976).

In order to derive a circuit diagram for BSR, it is necessary to distinguish the neural elements subserving BSR from other neurons that are activated by the stimulation electrode. Gallistel et al. (1981) have recently outlined a four stage approach to this problem. The first stage consists of establishing behaviourally derived trade-off functions that impose quantitative constraints on the neural substrate. Trade-off functions describe how much of a change in one parameter is necessary to compensate for a change in another parameter so as to maintain a constant level of behaviour (Edmonds, Stellar, and Gallistel, 1974). The second stage involves trying to explain the derived trade-off functions in terms of the physiological and anatomical properties of neurons. Recording the activity of candidate neurons and tracing their trajectories is the work of stage three. Finally, stage four involves sifting through the data from stage three and choosing the neurons with characteristics similar to those defined by the behaviourally derived trade-off functions.

An application of the four-stage approach advocated by Gallistel et al. (1981) in the area of BSR may be seen in the following experiment. Yeomans (1975) trained rats to

press a lever in order to obtain electrical stimulation of the posterior hypothalamus. Stimulation consisted of cathodal pulse pairs. The first pulse in a pair is called the conditioning pulse (C-pulse) while the second pulse is called the test pulse (T-pulse). It was found that as the C-T interval increased, the number of pulse pairs necessary to maintain a constant level of performance first increased and then decreased. Thus a trade-off function was established relating the number of pulse pairs to the C-T interval. By using the appropriate scaling techniques, Yeomans was able to compute the relative effectiveness of the T-pulse as a function of the C-T interval.

As noted above, stage two of this approach involves trying to explain these results in anatomical and physiological terms. With reference to the findings of the electrophysiological recording studies done by Erlanger and Gasser, Yeomans was able to account for the progressive changes in the curve relating T-pulse effectiveness to C-T interval in terms of local potential summation and the absolute and relative refractory periods of neurons. Local potential summation occurs when the depolarization caused by the T-pulse elicits action potentials in neurons that underwent sub-threshold depolarizations as a result of the C-pulse. Yeomans proposed that if the sharp decay in the relative effectiveness of the T-pulse was due to local potential summation then axonal stimulation was probably responsible for the rewarding affect. Yeomans' data

suggested that the recovery of excitability in these axons occurs for the most part between 0.4 and 1.2 msec. Thus, the results of these trade-off functions place quantitative constraints on the directly stimulated substrate for BSR. Candidate reward neurons must manifest electrophysiological characteristics similar to those determined by Yeomans (1975) or another physiological explanation of his behavioural data must be found.

As may be noted in the example above, the use of trade-off functions to characterize the neural substrate subserving reward has been and still is a cornerstone of the psychophysical approach to the study of BSR. Since this method, pioneered by Deutsch and Gallistel, plays such a fundamental role in the interpretation of experimental findings, the rationale for employing trade-off functions is explored below in more detail.

Trade-off functions have long been used in physiological and psychophysiological experiments. For example, many aspects of the excitability cycle of neurons were inferred from behaviourally derived trade-off functions many years before the advent of the cathode ray tube and vacuum tube amplifier that permitted a more direct observation of these phenomena (see Gallistel, 1975a for a historical review).

The power of trade-off functions is that their use

permits a characterization of the substrate around the electrode tip even though the experimenter may be observing behaviour many steps removed from the actual point of stimulation. How this is possible will be developed below. The symbols employed in this discussion and throughout this paper are listed in Table 1.

One of the assumptions underlying physiological experiments on the neural substrate for BSR is that the avidity of the behaviour (B) is a function of the rewarding impact (Re) of the stimulation. Hence,

$$B = f(\text{Re}, -). \quad (1)$$

The dash after reward signifies that behaviour is not a function of reward alone. Certain performance factors such as the level of arousal, the health of the animal, the task difficulty, and the time of day must also be considered. If the contribution of these performance variables is fixed by holding constant the home environment and experimental procedure, then behaviour is assumed to vary solely as a function of reward.

The rewarding aspect of the stimulation is itself a function of the stimulus parameters (S), which are: the pulse duration (d), train duration (D), current (I), and the number of pulses (N). Thus,

Table 1

Notation

<u>Symbol</u>	<u>Definition</u>
B	Behaviour emitted by a subject
c	Chronaxie of the strength-duration function for pulses (units = seconds)
C	Chronaxie of the strength-duration function for trains (units = seconds)
G _s	Specific capacitance of the membrane
d	Pulse duration (units = seconds)
D	Train duration (units = seconds)
E	Level of excitation
f(Re,-)	Function relating behaviour to the rewarding aspect of stimulation and performance factors
F	Frequency of the stimulation pulses
F _{max}	Maximum frequency at which a reward relevant neuron can be fired
g(S)	Function relating the stimulation parameters to the rewarding aspects of the stimulation
h(Nf)	Monotonic function relating the output of the integrator to the level of excitation
I	Current (units = microamperes)
I _{min}	Minimum current that elicits a criterial level of performance (units = microamperes)
I _o (d)	Wasted current (units = microamperes)
I _r	Rheobasic current (units = microamperes)

Table 1 (cont'd)

<u>Symbol</u>	<u>Definition</u>
k	Scalar constant that relates the number of stimulated neurons to the stimulation current (units = reward relevant neurons per microamperes)
$k_1(d)$	Current-distance constant for reward relevant neurons (units = microamperes per square millimeter)
k_2	Packing constant (units = number of reward relevant neurons per square millimeter)
$N(d, D, I)$	Number of stimulation pulses required to elicit criterial performance
$(1/N)c$	The $1/N$ value corresponding to the intersection of the linear portion of the $1/N$ versus I trade-off function and the vertical line from I_{min} (units = (pulses)-1)
$(1/N)o$	The y-intercept of the $1/N$ versus I trade-off function (units = (pulses)-1)
$N_f(D)$	Number of neuronal firings required to produce a criterial level of excitation at the output of the integrator
$N_n(d, I)$	Number of neurons stimulated by a given current intensity and pulse duration
Q	Total charge (units = microcoulombs)
Q'	Effective charge (units = microcoulombs)
Q_0'	Impulse charge. Charge necessary to bring the system to threshold given an infinitesimally short train duration
r	Rheobase of the strength-duration function for pulses (units = microamperes)
R	Rheobase of the strength-duration function for trains (units = microcoulombs/second)

Table 1 (cont'd)

<u>Symbol</u>	<u>Definition</u>
R_e	Rewarding effect of stimulation
R_s	Specific resistance of the membrane
S	Stimulation parameters
τ	Time constant of the membrane
ΔV	Change in transmembrane potential produced by the stimulating current
$w_1(d, F)$	Weighting factor expressing the effectiveness of the stimulation pulses as a function of their frequency and the number of firings per pulse
$w_2(d, I)$	Weighting factor expressing the spatial density of the reward relevant neurons to the packing constant within the effective radius of excitation defined by the pulse duration and the current

$$R_e = g(S).$$

(2)

Equations 1 and 2 may be combined so that behaviour may be seen as an indirect function of the stimulus parameters.

Thus,

$$B = f(g(S)).$$

(3)

When a constant behavioural output is demanded from the subject, it is assumed that the level of reward is also constant. As noted above, a trade-off function for two stimulus parameters details those pairs of values that result in a constant level of behavioural performance. If f were monotonic, then the rewarding value would be constant for all pairs of values comprising the trade-off function. This would allow one to see through f . That is, it would be as if behaviour were a direct rather than an indirect function of the stimulation parameters. The function f would be monotonic if it could be demonstrated that a monotonic relationship existed between one of the input variables (for example, d , D , I , or N) and the final output (B). Using the runway paradigm, such a relationship has been demonstrated over a substantial range of all four input variables (Edmonds et al., 1974; Gallistel, 1978; Matthews, 1977). Therefore, provided that performance factors are held

constant, the trade-off function reflects only g ; that is, it reflects only those processes that translate the stimulus parameters into some level of excitation mediating reward (Gallistel, 1974). This allows the researcher to assume that the relationship portrayed by the trade-off function reflects some aspect of the system subserving reward. Therefore, such trade-off functions impose quantitative constraints that any candidate system must be able to account for if it is to be considered as the BSR substrate.

The power of trade-off functions to link behavioural observations to neuronal functioning can best be portrayed by research in the area of vision. For example, one of the reasons that the isomerization of rhodopsin is accepted as the first stage in scotopic perception is the compelling concordance of behavioural and neurochemical trade-off between the wavelength and intensity of light that produce equivalent effects (Cornsweet, 1970).

Given the multitude of neurons directly driven by the stimulating electrode, one or two characteristics may not be enough to distinguish reward neurons from among the other sub-populations excited by the stimulation electrode. However, with a list of electrophysiological characteristics, a researcher doing single unit recording studies may more critically select candidate reward neurons. Once neurons matching the quantitative constraints imposed by the behaviourally derived trade-off functions have been

found, they may be injected with a tracer dye. Mapping studies of this nature will aid in clarifying the pathway of the relevant fibres and provide information concerning where cell bodies and terminal endings are located. By progressively mapping various stages of the pathway, this approach may lead toward a neural circuit diagram that, as explained earlier, may provide the basis for a mechanistic explanation of reward and appetitive motivation. The research described below was designed to contribute to the characterization of the neural substrate subserving the rewarding aspects of brain stimulation by estimating the temporal and spatial integrating characteristics of reward relevant neurons.

II. A Model of the BSR Substrate

a) The minimal model

Employing a minimal number of assumptions, Gallistel (1978) proposed a model of how electrical stimulation of the brain results in behaviour directed toward obtaining more stimulation. The first assumption is that the stimulation excites neurons within the immediate vicinity of the electrode tip. The reward relevant neurons that are driven by the stimulation are defined as the "first-stage" neurons. Second, it is assumed that the first-stage neurons are not the immediate cause of reinforcement but rather form a cable

along which the signal is transmitted. The excitation arising from the electrical stimulation flows into a neural network (referred to as the integrator) that sums the postsynaptic effects of the action potentials over space and time. Next, through a conversion process, the peak output of the integrator is recorded in an engram. The engram is responsible for the enduring effect of the stimulation and probably contains some representation of the magnitude of the reward and of the conditions under which the reward was obtained. Finally, the behaviour of the subject is determined by the engram from previous trials, the effect of the priming stimulation, and other performance factors such as the level of arousal, the health of the subject, and difficulty of the task.

The sections below present a more detailed analysis of the cable and the integrator that arises from the work of Shizgal, Howlett, and Corbett (Note 4) and Gallistel et al. (1981).

b) The cable model

The cable model details further the first assumption of the minimal model. Hawkins (cited in Gallistel, 1975b) has noted that the simplest assumptions predict that the number of stimulated neurons should be a scalar function of current. Thus,

$$N_n = k \times I, \quad (4)$$

where N_n = the number of stimulated neurons,

k = a scalar constant (units = neurons per uampere),

and I = current (units = uampere).

The effectiveness of any current is a function of the duration over which it is applied. However, for the sake of simplicity, this argument will first be included only in Equation 12.

Shizgal et al. (Note 4) have argued that not all of the stimulating current is effective in exciting neurons. Rather, some of the current is wasted due to the destruction of tissue by the electrode. Thus, according to Shizgal et al. (Note 4), the number of stimulated neurons is better modelled as a linear function of current rather than as a scalar function. In addition, these authors expressed the slope of the function in anatomical and physiological terms. Their version of Equation 4 is as follows:

$$N_n = k_2 / k_1 (I - I_0), \quad (5)$$

where N_n = number of stimulated neurons,

k_2 = the packing constant (units = number of reward relevant neurons per square millimeter),

k_1 = the current-distance constant for reward relevant neurons (units = uamperes per square millimeter),

I = the total current (units = uamperes),

and I_0 = the waste current (units = uamperes).

The constant, k_1 , determines the spread of current for reward relevant neurons. As is the case for currents, this constant is a function of the pulse duration. However, for the sake of simplicity, this argument will first be included only in Equation 12.

The term, k_2/k_1 , in Equation 5 represents the number of reward relevant neurons per microampere. In other words, Shizgal et al. (Note 4) have divided the scalar constant, k , of Equation 4 into two terms. The use of two constants leads to certain testable hypotheses. For example, one could aim electrodes at sites where the density of the reward relevant neurons is believed to differ. The model would predict that the functions relating the number of neurons to the current would differ with respect to slope and y-intercept.

The factor, $I - I_0$, is the corrected current. That is, it denotes the effective component of the total current set by the experimenter. The multiplication of the effective current by the two constants in Equation 5 yields an estimate of the number of stimulated neurons.

c) The integrator

The integrator, which corresponds to the second stage of the minimal model proposed by Gallistel (1978), is hypothesized to sum the postsynaptic effects of the action potentials from the first stage neurons both spatially and temporally.

Empirical support for the hypothesis that some mechanism must temporally integrate action potentials comes from Ward (1959). It has been found that rats will not press a lever for a single stimulation pulse regardless of its intensity (Ward, 1959). Rather, a series of pulses (defined as a train of stimulation) must be delivered.

Empirical support for the hypothesis that some mechanism must spatially integrate action potentials comes from Gallistel (1974). He found that over a wide range of values, a decrease or an increase in the number of pulses (N) within a train of electrical stimulation could be compensated for by an appropriate change in current. It may be recalled that a change in the current would either increase or decrease the field of excitation and result in a change in the number of stimulated neurons. From these results, Gallistel (1974) reasoned that the output of the integrator depends solely on the total number of action potentials arriving via the cable during a given time period. Thus, 100 different neurons firing 10 action

potentials each would produce the same reward as 10 neurons firing 100 action potentials each. This idea was developed independently by Yeomans (1975).

The simplest assumption about how the system integrates neural activity is that the level of excitation (E) rises with the number of neuronal firings (Nf) in the cable. Thus,

$$E = h(Nf), \quad (6)$$

where h is a monotonic function.

The number of firings, Nf, is a function of the pulse duration (d), the train duration (D), and the current (I). For the sake of simplicity, these arguments will first be included only in Equation 12.

The number of firings elicited by short stimulation pulses is the product of the number of pulses (N) and the number of stimulated neurons (Nn). Thus,

$$Nf = N \times Nn. \quad (7)$$

The number of stimulated neurons is a function of pulse duration (d) and current (I). However, for the sake of simplicity, these arguments will first be included only in Equation 12.

By solving for the reciprocal of the number of pulses ($1/N$), the equation becomes

$$1/N = 1/N_f \times N_n. \quad (8)$$

Edmonds et al. (1974) proposed that the integrator summed postsynaptic potentials whose strength decayed as a function of time. That is, it was hypothesized that the integrator was leaky. If so, charging the integrator would be analogous to filling a leaky bucket with glasses of water. This type of process tends to be characteristic of many neuronal systems involving one or more synapses.

Since the initial formulation of the leaky integrator model, an alternative has been proposed that is based on perfect integration above a threshold input rate (Gallistel et al., 1981). This other model was advanced to deal more parsimoniously with certain research findings that cannot be explained exclusively by a simple leaky integrator model. This issue will be dealt with at greater length in the discussion section. The model to be presented here is the leaky integrator since a) it can be argued that the other models are not easily portrayed by simple neurophysiological mechanisms, b) that deviation from a leaky integrator model may reflect not only properties of the neural pathway transmitting the signal but also properties of a mnemonic process, and c) the most recent findings do not rule out

leaky integration of neural activity produced during stimulation trains.

As has been stated above, the build-up of excitation at the integrator resulting from trains of electrical pulses has been likened to the filling of a leaky bucket with glasses of water. As glasses of water are poured into the bucket some water leaks out. The amount of water left in the bucket from the preceding glass is a function of the time until the next glass is poured. It follows that as the time between subsequent glasses is increased the amount of leakage time is also increased. The more leakage time the greater the volume of water lost (that is, water that does not contribute to raising the level in the bucket). Therefore, a greater total volume of water would be needed to raise the water level to some criterion level when the glasses are poured in more slowly than when the glasses are poured in quickly.

In an analogous fashion, it may be reasoned that N pulses given over a short train duration would be more effective in raising the activity of the substrate to some level of excitation than if the same number of pulses were delivered over a longer duration. This would be due to the fact that given less time for leakage there would be more left of the effect of the preceding pulse to sum with the effect of the subsequent pulse. Hence, for a fixed number of pulses, increasing the train duration increases the leak

time. To compensate for the increased leakage, an increase in the number of pulses is required to maintain a criterial level of excitation.

In summary, the cable model details how the number of stimulated neurons is determined by the current. The integrator sums firings in the cable over space and time. The combined model outlined below subsumes the cable model and the integrator; through the use of anatomical and physiological constructs, it links the stimulation parameters manipulated by the experimenter to their rewarding effect. This model predicts that the function mapping the current and the number of pulses required to hold the rewarding effect constant should vary in a systematic manner when the pulse duration (d) and train duration (D) are varied. By testing these predictions, the experiments below evaluate the strength of the model.

d) The combined model

Substituting Equation 5 in Equation 8, one obtains

$$1/N = 1/N_f \times k_2/k_1 (I - I_0), \quad (9)$$

which expresses the reciprocal of the number of pulses as a function of the effective current. Expanding Equation 9, one obtains

$$1/N = 1/Nf \times k_2/k_1 \times I - 1/Nf \times k_2/k_1 \times I_0. \quad (10)$$

Equation 10 shows the linear relationship between the reciprocal of the number of pulses and the total current.

Figure 1a graphically illustrates the relationship that would be expected if the experimenter set the train duration, the pulse duration, and the current and then determined the number of pulses required to maintain a constant level of performance. The slope of the graph would be equivalent to the coefficient $(1/Nf \times k_2/k_1)$ of the total current in Equation 10, while the negative y-intercept would equal $1/Nf \times k_2/k_1 \times I_0$. Thus, Shizgal et al. (Note 4) predict a result similar to that of Gallistel (1974) except that the function is linear rather than scalar. That is, the hypothesized function does not pass through the origin due to the "wasted" current, the current that does not elicit any neural activity.

Shizgal (Note 3) has proposed that at extreme currents the linear relationship between $1/N$ and I breaks down. To take into account the non-linear trends, Shizgal has proposed introducing two weighting factors. This would modify Equation 9 to become

$$1/N = w_1(d,F)/Nf \times k_2/k_1 \times ((w_2(d,I) \times I) - I_0). \quad (11)$$

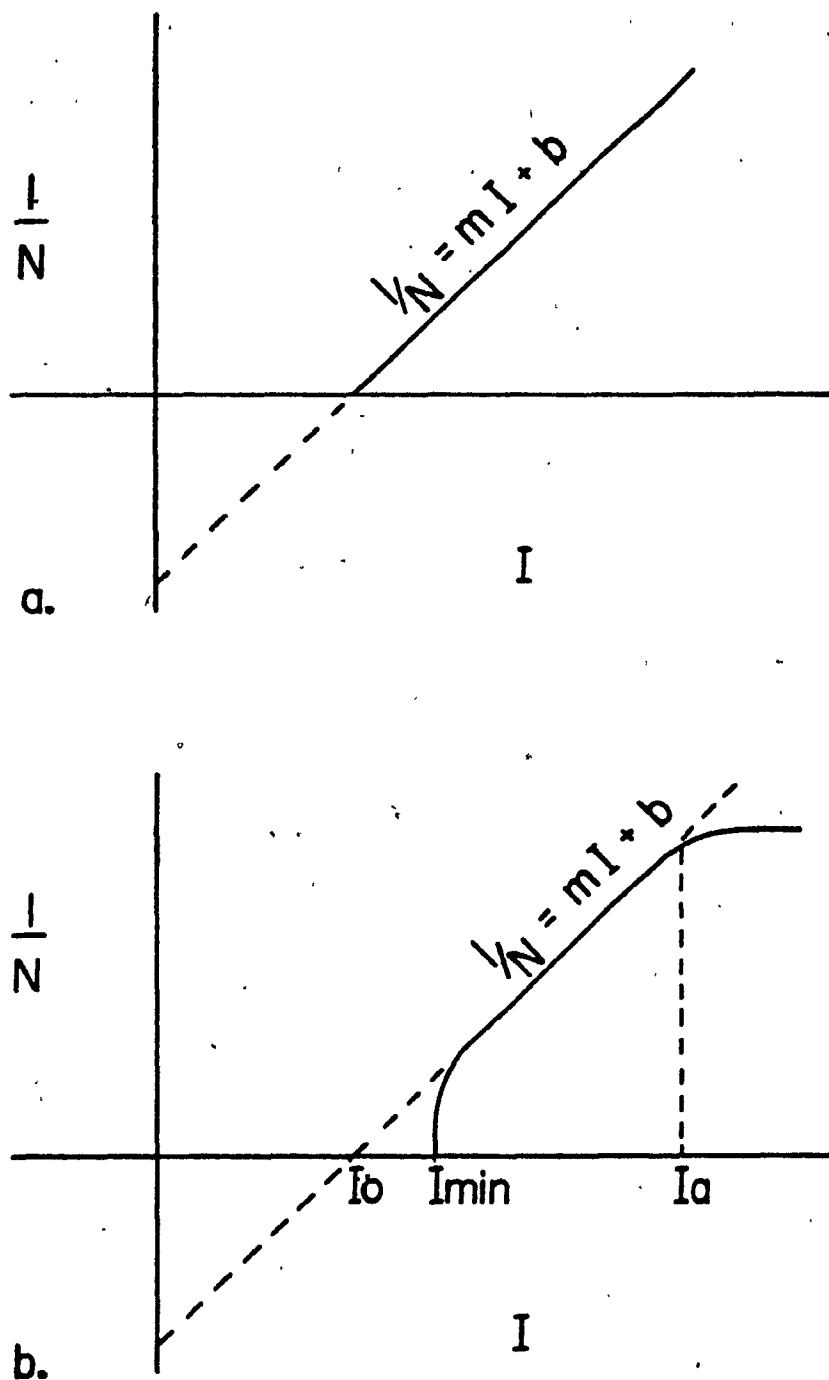


Figure 1. The upper panel (a) represents the predicted linear relationship between $1/N$ versus I given a constant level of performance. The lower panel (b) represents the predicted effects of high and low frequency roll-offs on the $1/N$ versus I trade-off function.

where $w_1(d,F)$ is a weighting factor expressing the effectiveness of stimulation pulses as a function of their frequency and duration while $w_2(d,I)$ relates the spatial density of the reward relevant neurons to the field of excitation defined by the pulse duration (d) and the current. When each pulse is fully effective, the function $w_1(d,F)$ is given a weight of one. However, as noted earlier, neurons are unable to follow very high frequencies; also, at low frequencies the effectiveness of each pulse may be reduced since there must be some interpulse spacing that cannot be bridged by the integrator. Thus, the weight would be less than one at either very high or very low frequencies. In addition, long pulse durations may elicit multiple action potentials from each reward relevant axon. If this hypothesis were correct, then a long stimulation pulse that excited a given region would be more effective in eliciting firings than a shorter pulse that excited the same region. Therefore, the weighting factor would be assigned some value greater than one (Shizgal, Note 3).

The packing constant, k_2 , describes the number of reward relevant fibres per square millimeter. The use of a constant to describe this quantity implies that there are no major inhomogeneities in the distribution of the reward related neurons within the stimulated field. This assumption is probably violated least when both the electrode tip and the surface defined by the field of excitation lie within the cable. Thus, the function $w_2(d,I)$ would be given a

weight of one and the factor k_2/k_1 would roughly describe the relationship between increments in current and increments in the number of reward neurons recruited. However, if the density of fibres started to thin out as a function of their distance from the electrode tip, then the function $w_2(d, I)$ would decrease to denote the diminished recruitment of relevant fibres (Shizgal, Note 3). This is graphically portrayed in Figure 1b by the rounding of the linear portion of the $1/N$ versus I trade-off function at the points I_a and I_{min} . Yeomans, Pearce, Wen, and Hawkins (Note 6) have proposed a geometric model to account for the non-linear trend in the $1/N$ versus I trade-off functions. This model takes into account the distance of the electrode from the center of the bundle and predicts the form of $w_2(d, I)$.

Equation 11 presents the $1/N$ versus I trade-off function that is the basis for the present research. However, for the sake of simplicity, the arguments of each variable except for the weighting factors have been modified. When the relationship between each component of Equation 11 and the various stimulation parameters are detailed, the predictions following from the model proposed by Shizgal et al. (Note 4) may be more readily conceived.

As mentioned earlier, the number of pulses is a function of the pulse duration, the current, and the train duration. The first weighting factor expresses the effectiveness of stimulation pulses as a function of their

frequency and duration. Following from the model of the leaky integrator proposed by Gallistel (1974), the required number of firings must be a function of train duration. That is, the number of stimulation pulses required to raise the output of the integrator to a given level will increase with train duration. The packing constant, k_2 , expresses a spatial arrangement and is not affected by the stimulation parameters. However, the current-distance constant, k_1 , which describes the effective spread of current is a function of the duration over which it is applied. This is so because of leaky integration of charge in the membranes of the stimulated cells (refer to the following section). The second weighting factor relates the spatial density of the reward relevant neurons to the field of excitation defined by the pulse duration and the current. The waste current, I_0 , which represents a spatial aspect of the stimulation current is also a function of the pulse duration. That is, the area in which a current stimulates neurons is a function not only of the intensity of the current but also of the time over which it is applied. The total current, I , is set by the experimenter. Thus, Equation 11 may be expanded and rewritten as

$$\begin{aligned} 1/N(d,D,I) &= w_1(d,F)/Nf(D) \times k_2/k_1(d) \times (w_2(d,I) \times I) \\ &- w_1(d,F)/Nf(D) \times k_2/k_1(d) \times I_0(d). \end{aligned} \quad (12)$$

Equation 12 expresses the relationship between the commonly varied stimulation parameters through the use of various

anatomical and physiological factors; it forms the theoretical basis for the experimental manipulations outlined below.

To test the combined model, a series of trade-off functions relating the reciprocal of the required number of pulses ($1/N$) to the current (I) were determined. According to the theory outlined earlier, it is assumed that the various combinations of $1/N$ and I that meet the constant behavioural criterion produce the same peak signal at the output of the integrator. If this assumption is correct, than any across-session changes in the trade-off functions can be attributed to the effects of the parameter that is varied across sessions. Specifically, in the strength-duration experiments, the pulse duration was varied across sessions while the train duration was held constant. It was hypothesized that an analysis of the changes in the relationship between $1/N$ and I as pulse duration was varied would shed light on the current integrating properties of the directly stimulated tissue. In the charge-duration experiments, the train duration was varied across sessions while the pulse duration was held constant. It was hypothesized that an analysis of the changes in the relationship between $1/N$ and I as train duration was varied would characterize the network responsible for post-synaptic integration.

III. Strength-duration experiments

The experiments in which pulse duration was manipulated were undertaken with three aims in mind. The first objective was to test the accuracy of the model in predicting the dependence of the I/N versus I trade-off function on pulse duration. A second objective concerned the discrepancy between behaviourally and electrophysiologically derived strength-duration estimates. Two hypotheses have been formulated to account for these discrepancies. Since the model predicts distinct results for each hypothesis, it could be used to choose between the two. Finally, the model was employed in an attempt to establish a strength-duration curve that would not be dependent on an arbitrary selection of stimulation parameters.

These objectives will be dealt with more completely below. First, it is necessary to discuss the relevant neurophysiological concepts. Of particular interest is the difference between the expected strength-duration estimates for single units and a population of neurons.

The passive electrical behaviour of the neural membrane has been likened to that of a parallel resistor-capacitor network (Lapicque, 1907). This model is shown graphically in Figure 2a. If this model were correct, then the passive rise or decay of an externally created potential would be

exponential. Thus, the time course of the change in membrane potential produced by a constant current flowing through the membrane would be described by the following equation:

$$\Delta V = IR_s(1 - e^{-\frac{I R_s d}{C_s}}) \quad (13)$$

where ΔV is the change in membrane potential created by the passage of the transmembrane current

I is the current intensity

R_s is the specific resistance of the membrane

d is the the duration of the stimulation pulse

and C_s is the specific capacitance of the membrane.

When the pulse duration is equal to the product of the specific resistance and capacitance of the membrane, then the voltage will attain 63 percent of its maximum value. This value has been designated the time constant (τ) of the membrane. Providing that the exponential model is correct, then τ specifies the passive electrical properties of the membrane.

When d approaches infinity, V approaches IR_s . If I_r (the asymptotic current) is defined as the current for a pulse of infinite duration, then Equation 13 becomes

$$I_r = V / R_s. \quad (14)$$

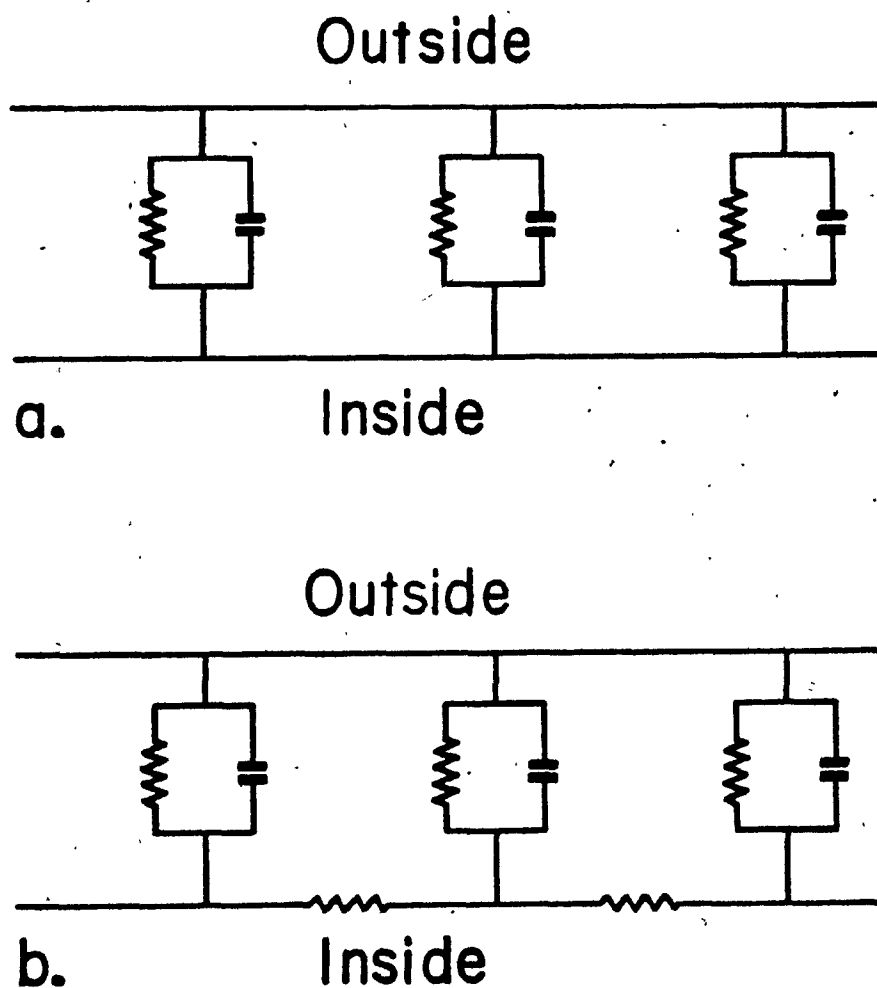


Figure 2. Resistor-capacitor network models of the neural membrane. The upper panel (a) represents the model for a cell with an equipotential interior. The lower panel (b) represents the model for a cell with significant intracellular resistance to current flow.

By combining Equations 13 and 14 and rearranging terms, one obtains

$$I = I_r / (1 - e^{-\frac{I_r C_s}{I}}). \quad (15)$$

Equation 15 provides a means of estimating τ . A trade-off experiment can be performed where the duration of the stimulation pulse is varied and the threshold current for eliciting an action potential is determined. The elicitation of an action potential would be equivalent to requiring a critical voltage change provided no accommodation occurred (see below). The resultant curve, which relates the threshold current and the duration of the stimulating pulse, is known as the strength-duration curve and is shown in Figure 3.

Lapicque (1907) described the strength-duration curve in terms of two parameters, the rheobase and the chronaxie. The rheobase was defined in the same way as I_r - the minimum current necessary to elicit an action potential given an infinitely long stimulation duration. The chronaxie was defined as the pulse duration at which the threshold current was twice as great as the rheobase. Thus, the rheobase represents the threshold current below which stimulation pulses, regardless of their duration, are unable to excite the neuron. The chronaxie was viewed as a reflection of the time course of charge integration in the membrane. If the

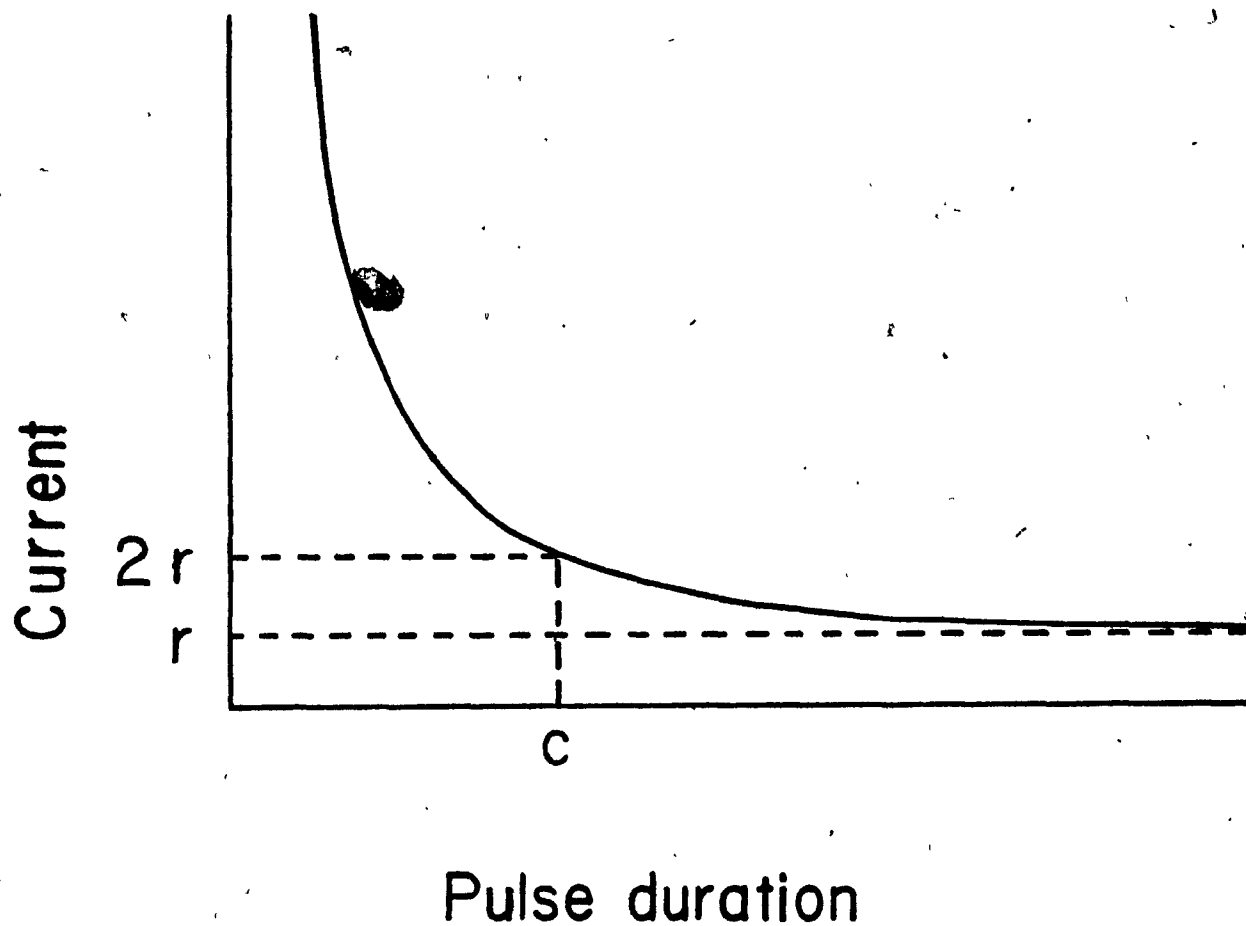


Figure 3. Idealized strength-duration curve. The horizontal asymptote is called the rheobase (r), while the duration at which the current is twice rheobase is called the chronaxie.

strength-duration curve were exponential, then the chronaxie would be equal to a multiple of the time constant. Determination of the rheobase and the chronaxie from strength-duration curves has become a standard practice since the preliminary work done by Lapicque (1907). This may have reflected the belief that these values represent fundamental electrical characteristics of the membrane and hence can be used to describe and distinguish different types of neurons. An example of this is the work done by Lucas (1917) on the mechanism underlying claw closure in Astacus. Lucas (1917) determined strength-duration curves for the two types of claw closure, a rapid, twitch-like closure and a slow contraction. That is, he varied the duration of the current and determined the threshold current required to produce each of the claw closures. He found that the strength-duration curve for the twitch yielded a chronaxie of .0012 sec. while the strength-duration curve for the slow closure yielded a chronaxie of .0028 sec. On the basis of these data, Lucas (1917) proposed that there must be two distinct sub-populations triggering claw closure in Astacus: one responsible for the slow contraction and one responsible for the twitch-like closure.

This ability to establish quantitative constraints on the neural elements responsible for effects of electrical stimulation renders determination of the rheobasic current and the chronaxie pertinent to research on brain stimulation reward. That is, determination of these two values might

contribute to the identification of reward relevant fibres by means of electrophysiological recordings. However, the rheobase is not only affected by the threshold of the neurons but also by their spatial relationship to the electrode. In contrast, the chronaxie is regarded as more closely tied to the intrinsic characteristics of the neuron and therefore is more suitable for purposes of comparison across experiments and stimulation sites (Rushton, 1935).

While the exponential function adequately describes the empirically derived data for short pulse durations, the same is not necessarily true for longer pulse durations. These deviations suggest that the model represented by Figure 2a is an oversimplification. Theoretical grounds for deviations from an exponential relationship have been explored in detail by Noble and Stein (1966).

The model in Figure 2a is appropriate only in special circumstances, for example, in spherical cells. In such cells, resistance to intracellular current flow is negligible when compared to the resistance to transmembrane current flow. Thus, the passive electrical behaviour of the cell as a whole is specified by a single time constant computed by lumping the parallel resistances and capacitances that represent each patch of membrane. If the parallel resistance and capacitance of each patch of membrane are the same, then the time constant of the cell membrane as a whole is equivalent to the time constant of

any given patch.

While this may be the case for a spherical cell, the same is not true for a cylindrical axon. Due to the relatively small diameter of the axon, the axoplasm exerts a resistance to current flow that, although smaller than the transmembrane resistance, cannot be ignored. Thus, the simple network shown in Figure 2a must be modified to include the axoplasmic resistance (see Figure 2b) between each membrane patch. It is also necessary to revise Equation 15, because the time course of the voltage changes induced by a current pulse in network 2b differs from the simple exponential behaviour of network 2a. The cable theory (Hodgkin and Rushton, 1946) that describes the behaviour of network 2b is beyond the scope of this thesis. Nonetheless, the differences between networks 2a and 2b can be summarized here by considering the simple case when the duration of the current pulse equals the product of the specific resistance and capacitance of the membrane. In that case, the transmembrane voltage across the model membrane described by Figure 2a will reach 63 percent of its asymptotic value at the end of the pulse while the voltage across the model membrane described by Figure 2b will attain 84 percent of its asymptotic value.

A second reason for deviation from simple exponential behaviour concerns the non-linearities in the current-voltage relation. That is, in modelling a patch of membrane

as a resistor-capacitor network, it was assumed that the resistor had a constant value independent of the value of voltage and time. However, the work done by Hodgkin, Huxley, and Katz (1952; Hodgkin and Huxley, 1952a,b,c) has shown that this assumption is incorrect and that the resistance of the membrane varies as a function of voltage and time. Consequently, the strength-duration relationship cannot be perfectly fit by a single exponential.

Hodgkin and Huxley (1952b) also showed that activation of ion gates did not occur instantaneously. Rather, activation of these gates takes a finite time. Therefore, even after the threshold value has been attained, charge continues to flow during the interval in which the gates are changing state. This is equivalent to adding a measuring device to the models in Figure 2 that registered transmembrane voltage changes after a time delay. Such a delay would alter the strength-duration curve obtained by trading off the current and duration required for the measuring device to register a fixed voltage change.

Finally, Hill (1936) has pointed out that a cell accommodates to sustained changes in transmembrane voltage. For example, the transmembrane voltage that must be attained to elicit an action potential increases during prolonged depolarization. This means that with long duration pulses, a greater current is needed to elicit an action potential than if there were no accommodation. Therefore, the total charge

necessary to excite the neuron increases more quickly with pulse duration than would be expected from the simple exponential model. One can imagine the membrane potential trying to reach a slowly receding threshold. Not only will the time it takes to approach the threshold increase but so will the total amount of energy expended.

To summarize, the neural membrane has been likened to a parallel resistor-capacitor network. In such a system, the passive decay of an externally, created potential is exponential. There are at least four reasons why the parallel resistor-capacitor model is oversimplified and hence that deviations from exponential behaviour are predicted. First, this model does not take into account axoplasmic resistance. Second, the resistance of a patch of membrane varies as a function of voltage and time. Third, an action potential does not begin at the instant at which the threshold is attained. Finally, due to accommodation, the threshold value increases with prolonged depolarization.

As noted by Noble and Stein (1966), some of these deviations from exponential behaviour are compensatory. Hence, one might expect that the strength-duration curves for some neurons would be reasonably well fit by simple exponentials. Matthews (1978) obtained cathodal strength-duration curves for 27 single units driven by lateral hypothalamic stimulation. Eleven of the units were better fit by an exponential function while five were better fit by

a hyperbola. Eight units were fit equally well by both functions, whereas three were fit well by neither. It should be noted that the contribution of the four factors mentioned above may vary across cells and across different portions of the same cell. Consequently, strength-duration curves obtained for different cells or different regions of the same cell may differ in shape.

To this point, the discussion has focused on why the strength-duration curve for a single unit should not necessarily be expected to be represented by a single exponential function. The matter becomes even more complex when dealing with a population of neurons since the corresponding strength-duration curve represents a weighted sum of the characteristics of all the stimulated neural elements. There are at least two reasons why the population function may be more complicated than the function for single units. In one extreme case, the population function would be a composite of individual strength-duration functions with the same form but different time constants. In the other extreme case, the population function may be a composite of individual strength-duration curves that are each best represented by a different function.

On the basis of these considerations, one might question the utility of rheobase and chronaxie estimates in aiding researchers to characterize reward relevant fibres. That is, it may be asked whether parameters estimated from

the population strength-duration curves may aid in discriminating between single neurons. However, in spite of their limitations, the chronaxie and to a lesser extent the rheobase impose quantitative constraints upon the neural population under study. For instance, if a chronaxie estimate were behaviourally established for reward relevant fibres, then any candidate neuron monitored during electrophysiological studies would have to manifest a chronaxie value within the range of values compatible with the population curve. Otherwise, it would be assumed that the neuron being monitored subserved another function.

Having reviewed the biophysical bases of the strength-duration function, it will now be possible to elaborate on the three questions addressed by this series of experiments.

a) Testing the model

First, it was hypothesized that the model should predict the changes in the trade-off between $1/N$ versus I that arise when pulse duration is varied. To analyze the predicted changes, it will be necessary to return to the hypothesized relationship linking $1/N$ to I . With the train duration constant, it follows from Equation 12 that

$$\begin{aligned} 1/N(d,D,I) &= w_1(d,F)/Nf \times k_2/k_1(d) \times (w_2(d,I) \times I) \\ &- w_1(d,F)/Nf \times k_2/k_1(d) \times I_0(d). \end{aligned} \quad (16)$$

If the stimulation pulse elicits a single action potential per reward relevant neuron and the electrode tip is located within a homogeneous bundle, then Equation 16 becomes

$$\begin{aligned} 1/N(d,D,I) &= 1/Nf \times k_2/k_1(d) \times I \\ &- 1/Nf \times k_2/k_1 \times I_0(d). \end{aligned} \quad (17)$$

Of the three factors that comprise the slope of the trade-off function, only the current-distance constant should be affected by the manipulation of pulse duration. When a given current is applied over a longer time, it will recruit reward relevant fibres located on the fringe of the field of excitation that had previously undergone subthreshold depolarization. Thus, as pulse duration increases, the current may be decreased while maintaining a field of excitation of a given size. Mathematically, this would be represented by an increase in the slope of the function as pulse duration is increased.

As N approaches infinity, its reciprocal ($1/N$) approaches zero. The x-intercept may be determined by substituting this value in Equation 17. This reduces to

$$I = I_0(d). \quad (18)$$

The effectiveness of any current, however, is dependent upon the time interval during which it is applied. Thus, as the pulse duration is increased, the adjustment factor (I_0) should decrease. Therefore, increments in pulse duration should result in decreases in the size of the x-intercept.

The minimum current (I_{min}) is defined as the least current for a given pulse duration and train duration that will elicit behaviour. It represents the minimum region of the cable that can produce a criterial output when the constituent neurons are fired at their maximum rate. The minimum current should change in a manner analogous to the adjustment factor. That is, as pulse duration is varied, there should be pairs of minimum currents and pulse durations that fire the same minimum number of reward relevant neurons. The counter model (Edmonds, Stellar, & Gallistel, 1974; Gallistel, 1974) described above predicts that with train duration fixed, the same number of neurons must be fired by a given number of stimulation pulses if the level of excitation is to be maintained. Therefore, the reciprocal of the number of pulses corresponding to the intersection of the linear portion of the $1/N$ as I function and I_{min} should be constant for all pulse durations. As previously described, at the lowest currents the neurons are unable to follow perfectly the higher frequencies that are required to produce $Nf(D)$ firings. Since the increase in the number of stimulation pulses does not result in a

proportional increase in neuronal firings, the slope of the trade-off function increases until at currents less than I_{m1} , behaviour can no longer be elicited.

At higher currents, the function is expected to depart from linearity due to the thinning out of reward relevant fibres or a low frequency roll-off. It may be recalled that changes in pulse duration alter the effective radius of excitation. Therefore, the current at which these roll-offs occur should decrease as pulse duration is increased. These predictions are shown graphically in Figure 4.

b) Distinguishing between two hypotheses

As will be shown below, the chronaxie of the behavioural strength-duration curve can be misleading as a guide to the electrophysiological identification of the cable axons. The extended model provides a means for rectifying this. First, it enables the researcher to distinguish between two hypotheses proposed to account for the discrepancy between electrophysiologically and behaviourally derived strength-duration estimates. This was the second aim of the strength-duration experiments and will be discussed in the present section. Also, the extended model allows the influence of one of the hypothesized factors to be removed from the behavioural strength-duration curve. This was the third aim of the strength-duration experiments and will be discussed in the following section.

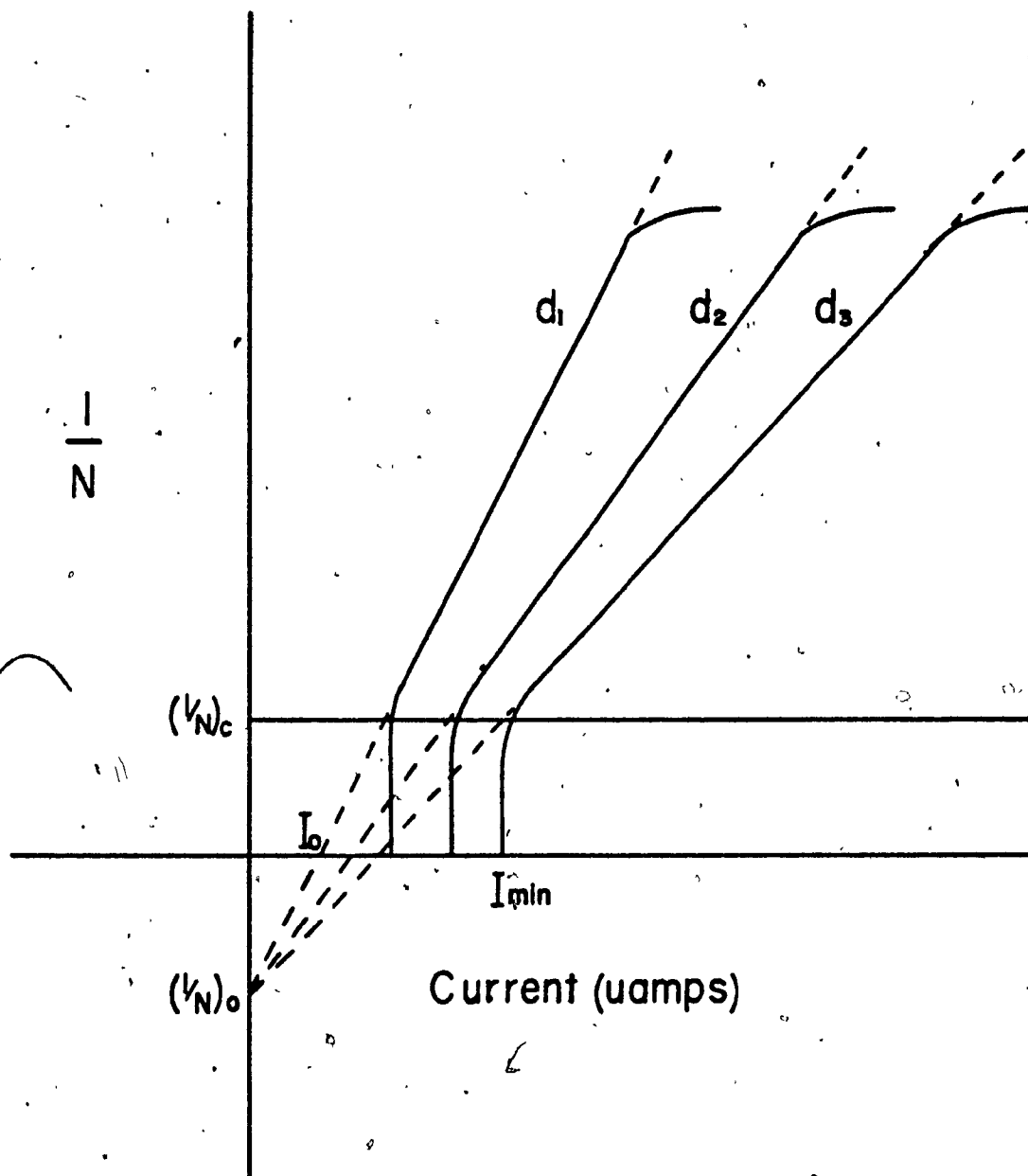


Figure 4. For short pulse durations, predictions of the extended model when train duration is constant and pulse duration is varied. Increments in pulse duration from d_3 to d_1 lead to increments in the slope of the $1/N$ versus I trade-off functions, decrements in I_{min} and I_o , and no changes in $(1/N)_o$, the y-intercept, or $(1/N)_c$, the $1/N$ value corresponding to the intersection of the linear portion of the trade-off function and a vertical line from I_{min} .

Recent conduction velocity estimates (Bielajew and Shizgal, 1982; Shizgal, Bielajew, Corbett, Skelton, and Yeomans, 1980) tend to support the hypothesis that among the reward relevant elements directly stimulated by MFB electrodes are small myelinated axons. In his summary of the neurophysiological literature, Ranck (1975) cited that chronaxie estimates for myelinated, single axons of the central nervous system cluster between 0.040 - 0.085 msec. These contrast sharply with the 0.9 - 3.0 msec values for the LH reward substrate that Matthews (1977) determined behaviourally. Matthews (1977) formulated two hypotheses that might account for these discrepancies. These will first be outlined briefly and then discussed in more detail.

The first hypothesis suggested by Matthews (1977) was that the stimulation excites a heterogeneous group of reward relevant elements. This could arise in one of two ways. First, the cable could be composed of several sub-populations of neurons with different chronaxies. Alternatively, the cable could be composed of a single population of neurons that have regionally varying chronaxies. For example, the chronaxies of the somata and the axons may differ. Since the model treats these two ideas equivalently, they are lumped together below under the rubric, "multiple sub-population hypothesis".

A second hypothesis suggested by Matthews (1977) was

that fibres mediating the rewarding effect might respond with more than a single action potential to pulses of long duration. This will be referred to as the multiple firing hypothesis. According to the extended model, the effects of varying the pulse duration on the family of $1/N$ versus I trade-off functions depends on which of Matthews' two hypotheses is correct. Hence, it may be possible to use the results of the experiment involving the manipulation of pulse duration to distinguish between the relative merits of these two hypotheses. Before looking at how the extended model may permit this differentiation, the development and relevance of the two hypotheses proposed by Matthews (1977) will be looked at in more detail.

Two of Matthews' (1977) findings are of particular relevance to the present work. First, he found the unexpectedly long chronaxie estimates mentioned above. Second, he found that most of the strength-duration curves continued to decrease even using pulses of 15 msec duration. That is, the strength-duration curves never reached an asymptote. This means that the required current could be further decreased with increments of pulse duration while still maintaining the criterial response.

It may be recalled that the chronaxie is the pulse duration corresponding to a current of twice rheobasic intensity. Therefore, the long chronaxie estimates may be related to the failure to reach rheobase. In that case, an

elucidation of the neural mechanisms responsible for the inability to reach rheobase might clarify the discrepancy between the behaviourally and the electrophysiologically derived chronaxie estimates. Both hypotheses formulated by Matthews can account for this discrepancy. In addition, these hypotheses highlight differences in the factors that may contribute to strength-duration function obtained in the behavioural and electrophysiological paradigms. To clarify this latter statement, it will be necessary to compare the electrophysiological and the behavioural procedures for determining strength-duration curves.

In the electrophysiological paradigm, the researcher selects a series of pulse durations and determines the minimal current that will elicit an action potential. In the behavioural paradigm, the researcher selects a series of pulse durations and determines the minimal current that will elicit a criterial level of performance. In many respects, the two paradigms are similar. That is, both paradigms use a series of pulse durations and determine the minimal current necessary to elicit a criterial output. However, in the behavioural paradigm, there are several intervening steps between the excitation at the electrode tip and the behavioural output. Because of these intervening steps, it is necessary to make several assumptions in the behavioural paradigm that are not necessary in the electrophysiological paradigm. In the behavioural paradigm, it is assumed that all combinations of pulse duration and current specified by

the strength-duration function fire the same neurons. It is also assumed that each stimulating pulse elicits a single action potential per reward relevant fibre. The hypotheses proposed by Matthews (1977) may be interpreted as questioning these assumptions.

The first hypothesis was that the cable is not comprised of a homogeneous population of fibres. If so, one would expect that the behaviourally derived strength-duration curve would be a weighted sum of one or more functions. Taking the simplest case, Matthews (1977) fit two single exponential functions to the data. One function was fit to the data for the short pulse durations while a second function was fit to the data for the long pulse durations. It was found that the two functions provided a more reasonable fit to the data than any single function. In comparing the chronaxie estimates from the two functions to values in Ranck's (1975) summary, Matthews (1977) hypothesized that the chronaxie estimate for the longer pulse durations might represent the recruitment of the somata of the reward relevant fibres. As noted above, the chronaxie value is sensitive to electrophysiological (activation time of the ion gates, accommodation, etc) and structural (cell diameter, etc) characteristics. Therefore, different parts of the same cell could yield different chronaxie values.

Figure 5 graphically represents how this hypothesis

could account for the continued decline of strength-duration curves derived in behavioural experiments. In this example, two time constants are used. These different time constants could be due to two distinct neural populations (for example, myelinated versus unmyelinated neurons) or due to two sites of impulse initiation (for example, axons versus cell bodies). In this example, short pulse durations predominantly stimulate elements with time constant A but also stimulate some elements with time constant B. However, with increments of pulse duration, there is sufficient time to activate more distant elements with the longer time constant. In effect, more reward relevant fibres per square millimeter are now stimulated. This has the same effect as changing the packing constant, k , in Equation 9. Therefore, the current can be further decremented while still stimulating the number of neurons required to produce the criterial level of excitation. In the multiple sub-population model, the behavioural curve approaches rheobase at the same time as the element with the longest chronaxie.

The second hypothesis proposed by Matthews (1977) dealt with the possibility that at long durations cable axons may respond with more than one action potential per pulse. According to both the counter model and empirical studies (e.g., Gallistel, Stellar, and Bubis 1974), an increase in the number of action potentials per pulse will have an effect on the integrator equivalent to an increase in the stimulation frequency. An increase in frequency requires a

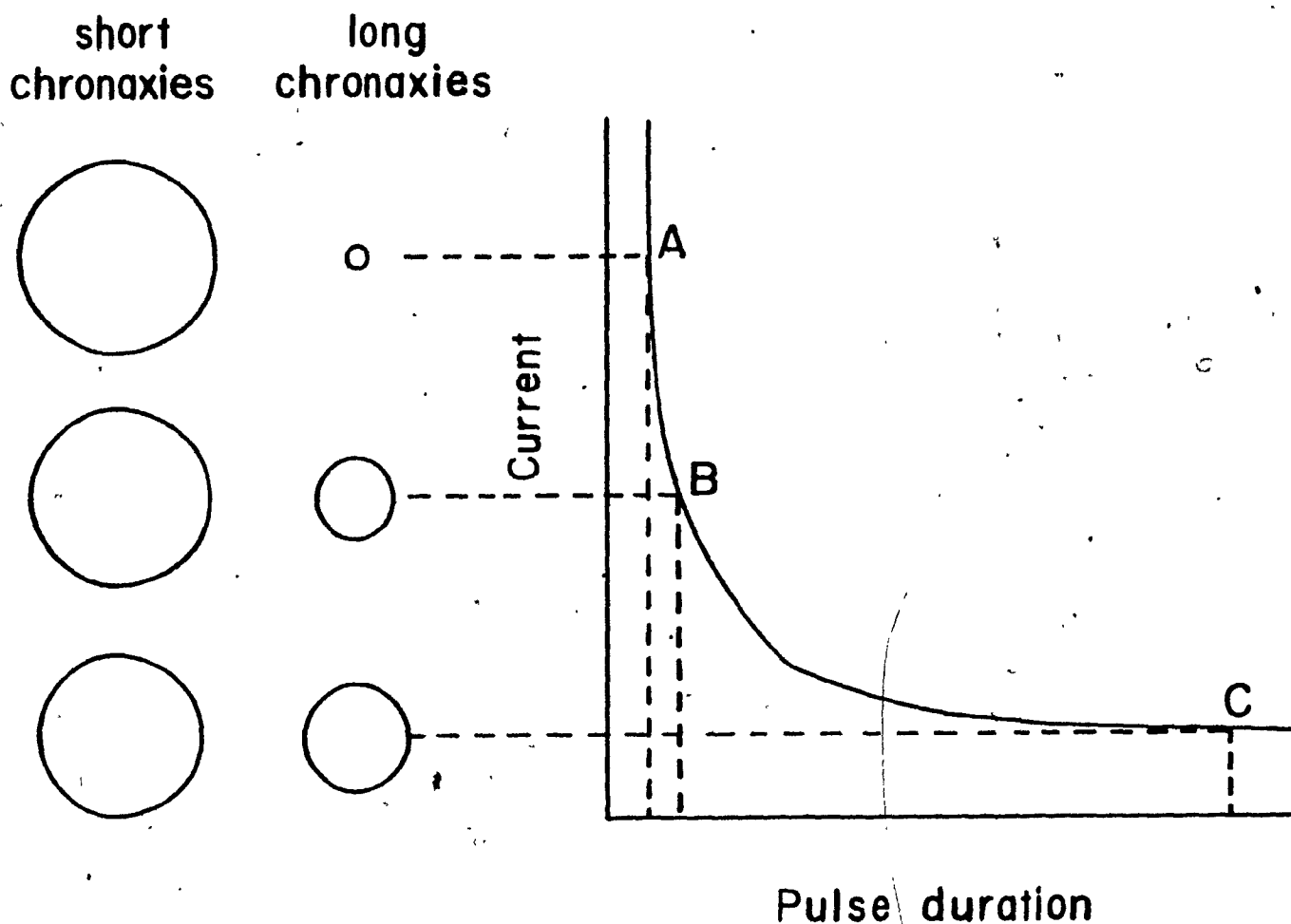


Figure 5. A model of how neural elements with differing chronaxies may contribute to a behaviourally-derived strength-duration curve. The size of each circle indicates the cross-sectional area of the cable in which a given population is fired. Assuming equal behavioural weights, a decrease or increase in one sub-population must be compensated for by a corresponding change in the other. At point A, an intense stimulus of short duration excites mainly those fibres with short chronaxies; whereas at point C, a less intense stimulus of longer duration fires relatively more fibres with long chronaxies.

decrease in the number of stimulated neurons, and hence, the current, in order to maintain a constant behavioural output. As pulse duration is increased, the required current will continue to drop until the relatively few remaining cable axons are firing at their maximum rate or until the pulse duration approaches the interpulse interval.

0

Figure 6 graphically represents how this hypothesis could account for the failure to reach rheobase, and hence, explain the unusually long chronaxies obtained in behavioural strength-duration experiments. Curve A represents the electrophysiological strength-duration function for a single neuron located at the very edge of the effective stimulation field. Curve B represents the behavioural strength-duration function for the entire population of reward relevant neurons passing through the effective field. For this example, it is assumed that all neurons in the cable have the same chronaxie.

At pulse duration a, the required current values obtained from the electrophysiological and the behavioural experiments are equal. As pulse duration is increased to b and c, the decrements in current required to hold constant the effect of stimulation are the same in the two experiments. As pulse duration is increased beyond c, the neurons begin to fire repetitively. Consequently, as pulse duration is increased to d, the decrements in current in the two experiments are no longer the same. The electro-

physiological curve is now approaching rheobase, and the required current changes little between pulse durations c and d. In contrast, in the behavioural experiment, the current may be substantially reduced because the increased discharge of the membrane capacitance is accompanied by an increased number of firings per pulse. After the pulse duration exceeds e, further increases in duration, fail to permit further reductions in current in the electrophysiological experiment. Due to multiple firing, the behavioural curve continues to drop after the electrophysiological curve has approached rheobase. In theory, the current required in the behavioural experiment may continue to decrease until the pulse duration approaches the interpulse interval. In practice, this could not be observed because lesions would be produced once the interval between the end of one pulse and the beginning of the next was too short to dissipate the charge on the electrode-brain interface that built up during the preceeding pulse.

These same events are shown schematically by the circles in Figure 6. The circles represent cross-sections of the effective stimulation fields produced by the currents and durations specified by the strength-duration curves. At pulse durations a to c, the effective fields of stimulation are equivalent in both experiments and the neuron, indicated by the black dot at the edge of the field, is fired. At pulse duration d, the size of the effective field in the electrophysiological experiment, indicated by the solid

circle, must be maintained if the neuron is to be fired. In contrast, in the behavioural experiment, the onset of multiple firing permits a reduction in the size of the effective field required to elicit behaviour. Simply stated, the contribution of the neuron, designated by the dot is no longer needed in the behavioural experiment, since neurons closer to the tip are compensating for its loss by firing more than once per pulse.

This example shows that the chronaxie of the behavioural curve can be misleading as a guide to the electrophysiological identification of the cable axons. To understand how the model may be able to distinguish between the two hypotheses outlined above, it will be necessary to return to Equation 12:

$$\begin{aligned} 1/N &= w_1(d,F)/Nf(D) \times k_2/k_1(d) \times (w_2(d,I) \times I) \\ &= w_1(d,F)/Nf(D) \times k_2/k_1(d) \times I_0(d). \end{aligned} \quad (12)$$

The weighting factor, $w_1(d,F)$, alters the relationship between the reciprocal of the number of pulses and the current under two conditions. The first condition involves the enhanced effectiveness of each pulse resulting from repetitive neural firing while the second concerns the decreased effectiveness due to the inability of the neurons to follow high stimulation frequencies.

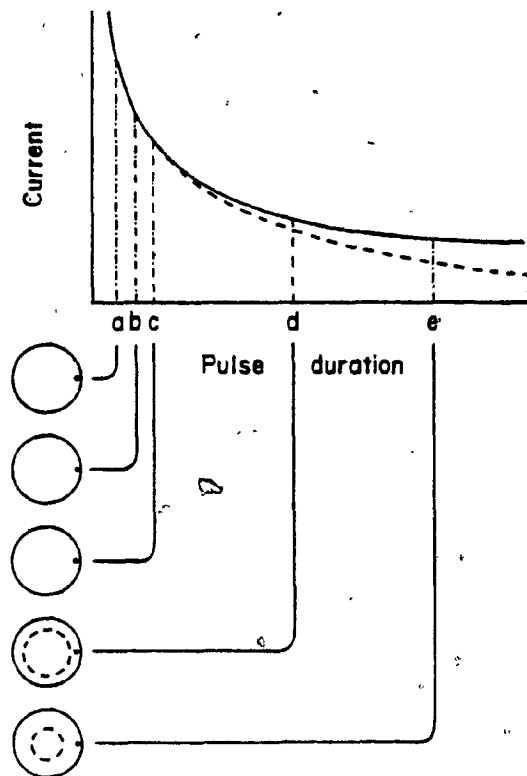


Figure 6. Hypothesized comparison of electrophysiologically- and behaviourally-derived strength-duration curves given a homogeneous population of reward neurons that fire repetitively during prolonged depolarization. As pulse duration is increased from a to c, equivalent decrements in current may be made in both the electrophysiological and behavioural experiments. For durations greater than c, the reward neurons fire repetitively for each pulse. At pulse duration e, the electrophysiological curve, denoted by the solid line, approaches rheobase, whereas the behavioural curve, denoted by the dashed line, continues to decrease. The circles corresponding to the five pulse durations detail the position of an axon, represented by the dot, relative to the stimulation fields used in the two strength-duration experiments. At pulse durations a to c, the size of the stimulation field for the two experiments are the same. At pulse durations d and e, the increase in frequency due to the multiple firing in the neurons near the tip necessitates a decrease in the number of neurons required to maintain a constant level of excitation in the behavioural experiment. A decrease in the required number of neurons is accomplished by decreasing the size of the stimulation field (dashed circle). The size of the stimulation field in the electrophysiological experiment (solid circle) must stay the same since it is defined by the current that is just sufficient to fire the axon.

At short pulse durations, the weighting factor assumes a value of unity over the linear portion of the $1/N$ versus I trade-off function. However, the increased effectiveness of each pulse due to repetitive firing at the longer pulse durations increases the value of $w_1(d, F)$. As noted above, increases in pulse duration lead to increases in the slope of the trade-off function. However, from Equation 12, it may be seen that increases in $w_1(d, F)$ would increase the slope to an even greater extent than would be expected if no repetitive firing occurred. In an analogous manner, the presence of the weighting factor in the term defining the y-intercept would increase that value as well.

When the neurons are responding at their maximum rate, F_{max} , further increases in the pulse duration are unable to produce any increase in the rate of responding. However, multiple firing should decrease the stimulation frequency necessary to reach F_{max} since each neuron fires several times per pulse. Such a decrease in the required number of pulses (N) would result in an upward shift of the point corresponding to the intersection of the linear portion of the $1/N$ versus I function and I_{min} .

Such changes could also be accounted for by the model that proposes a heterogeneous population of reward neurons. A discrepancy between predictions arises because the multiple firing model predicts that the x-intercept (I_0) and the minimum current at which behaviour may be elicited (I_{min})

should reach an asymptote (rheobase) before the slope. This is in contrast to the heterogeneous population model which predicts that these factors asymptote at the same pulse duration, the value at which the subpopulation with the longest chronaxie reaches rheobase. This may be understood by recalling that multiple firing reduces the number of pulses required to reach criterion but does not affect spatial variables such as I_{min} and I_o . Recruitment of additional sub-populations alters the $1/N$ versus I trade-off function in a manner similar to the predicted effects of changing the packing constant, k_2 . Manipulations of k_2 will affect not only I_{min} and I_o but also the slope. These predictions may be seen in Figures 7a and 7b.

Figure 7a shows the changes in the $1/N$ versus I trade-off functions that are expected if more than one action potential is elicited from the reward relevant fibres during prolonged depolarization. As the duration of the stimulation pulse increases from d_1 to d_3 , the values for the slope, I_{min} and I_o progressively change. However, at d_4 and d_5 where multiple firing occurs, the values for I_{min} and I_o remain constant whereas the slope continues to increase. Therefore, the strength-duration curves based on either I_{min} or I_o have a shorter chronaxie than a strength-duration curve based on the slope.

Figure 7b shows the family of $1/N$ versus I trade-off functions that is consistent with a cable made up of several

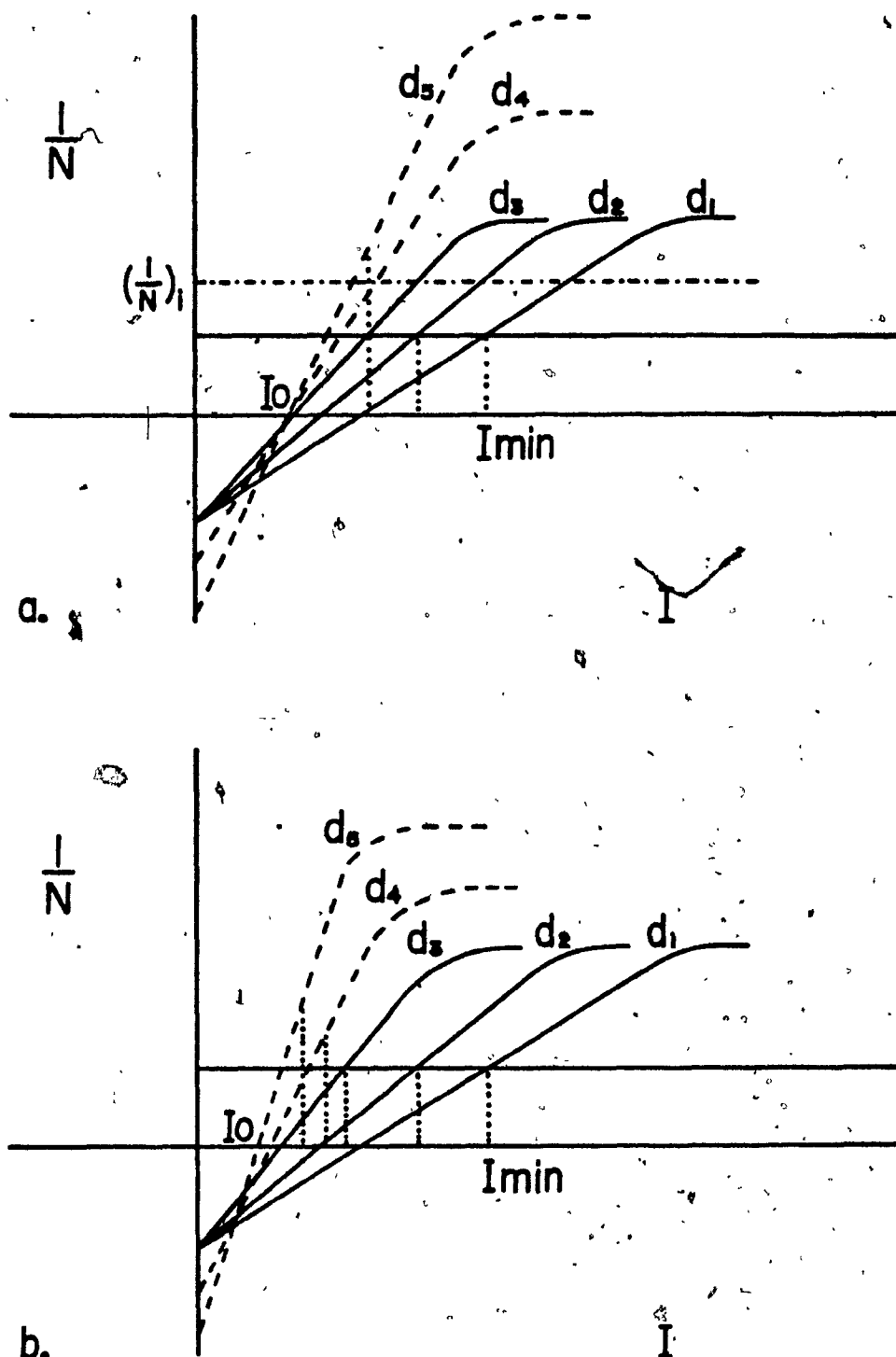


Figure 7. The upper panel (a) represents the effect of varying the pulse duration on the $1/N$ versus I trade-off functions according to the multiple firing hypothesis. As pulse duration increases from d_1 to d_5 , the slopes of the functions change. However, I_{min} and I_0 stop changing at d_3 . The lower panel (b) represents the predictions from a multiple sub-population model. As pulse duration changes, so do the values for the slope, I_{min} , and I_0 .

sub-populations of reward relevant fibres. As the pulse duration increases from d_1 to d_5 , the values for the slope, I_{min} , and I_0 continue to change. These changes continue until the element with the longest chronaxie reaches rheobase.

c) A non-arbitrary, strength-duration curve

The third aim of these experiments involving the manipulation of pulse duration was to establish a strength-duration curve that would not be dependent on an arbitrary selection of stimulation parameters. If the multiple firing hypothesis is correct, then chronaxie estimates obtained using frequencies that intersect the linear portion of the $1/N$ versus I trade-off function are biased, and the use of I_{min} , a current variable that is not affected by multiple firing, will yield a strength-duration curve more consistent with electrophysiologically derived curves.

To better understand this argument, it is necessary to briefly review the experimental procedure used by Matthews (1977). He arbitrarily selected a stimulation frequency and train duration; at each of a series of pulse durations, he then determined the current required to elicit a criterial behavioural response (half-maximum running speed). In terms of the present experiments, this is analogous to determining I for a particular value of $1/N$ for each of the $1/N$ versus I trade-off functions. This may be seen graphically in Figure

7a. The arbitrarily selected number of pulses is N_i (recall that frequency is the number of pulses per second). Since the slope continues to change across all pulse durations due to the influence of multiple firing, then no strength-duration curve would appear to reach rheobase. In fact, Matthews (1977) found that the required current continued to decrease even when the pulse duration exceeded 10 msec.

IV. Charge-duration experiments

The experiments involving manipulation of train duration had two objectives. These will be discussed briefly here and outlined in more detail below. First, the minimal model proposed by Gallistel (1978) and elaborated by Shizgal et al. (Note 4) predicts that the $1/N$ versus I trade-off functions should vary in a systematic manner as train duration is varied. The degree of correspondance between the predictions and the empirical results should reflect the model's ability to account for post-synaptic integration in the substrate for self-stimulation. A second objective of these experiments was to investigate the effects of corrections suggested by the extended model on the function that relates required charge to train duration. Other researchers (Gallistel, 1978; Huston, Mills, and Huston, 1974) have found that a linear function may be used to characterize the charge-duration relationship but their work has not taken into account the waste current proposed by Shizgal et al. (Note 4). The model predicts that inclusion

of this correction will not affect the linearity of the charge-duration function but will affect its parameters (Shizgal, Note 3).

a) Testing the model

The first aim was to determine whether the $1/N$ versus I trade-off functions varied in the systematic manner predicted by the extended model. These predictions may be derived from the function relating $1/N$ to I . When train duration is varied while pulse duration is held constant, Equation 12 reduces to

$$\begin{aligned} 1/N &= w_1(d, F)/Nf(D) \times k_2/k_1 \times (w_2(d, I) \times I) \\ &\quad - w_1(d, F)/Nf \times k_2/k_1 \times I_0. \end{aligned} \quad (19)$$

Over the linear portion of the curve, Equation 19 is further reduced to

$$1/N = 1/Nf(D) \times k_2/k_1 \times I - 1/Nf(D) \times k_2/k_1 \times I_0. \quad (20)$$

The essence of the leaky integrator model is that the number of neuronal firings that are necessary to maintain a constant level of excitation must increase as train duration increases. Increases in train duration increase leak time, and hence leakage. Consequently, the number of firings must be increased to compensate for the increased loss. Thus, as

train duration is increased, the reciprocal of the number of firings, $1/Nf(D)$, must decrease. Since this factor is part of both the slope and the intercept, these values should be affected by any manipulation of train duration. Specifically, increments of train duration should result in decrements of both the slope of the trade-off function and the y-intercept.

As the number of pulses approaches infinity, its reciprocal approaches zero. By substituting this in Equation 20, it reduces to

$$I = I_o. \quad (21)$$

Thus, all curves should pass through one x-intercept, I_o .

The counter model predicts that the minimum radius of excitation that will support criterial performance will be reached when the neurons are responding at their maximum firing rate (F_{max}). That is, at F_{max} , the number of reward-related neurons required to produce a criterial level of excitation is at a minimum. With pulse duration constant, the radius of excitation is determined by the current. As Edmonds et al. (1974) have shown, the required current decreases as train duration is increased at a fixed frequency. That is, the more time that is available when the frequency of input is fixed, the fewer reward relevant neurons that must be fired. Therefore, the current at which

F_{max} is reached, I_{min} , will decrease as train duration increases?

The number of pulses in a train is equal to the frequency (F) times the train duration plus one, or

$$N = D \times F + 1. \quad (22)$$

if F_{max} is the maximum stimulation frequency that the neurons may follow (assuming no fatigue effects at the longer train durations), then as D increases N will increase. Therefore, the value of $1/N$ at which F_{max} is attained will decrease as the train duration is increased. Figure 8 represents these predictions graphically.

b) A charge-duration curve

The second objective of these experiments was to investigate the form of the charge-duration relationship. A charge-duration function relates the required charge necessary to elicit a criterion behaviour to the duration of the stimulation train. The slope of this function is the rate of input necessary over a given interval to maintain criterial performance. The section below concerns the derivation of a charge-duration function from the extended model outlined earlier. This is followed by a review of charge-duration functions derived by other researchers.

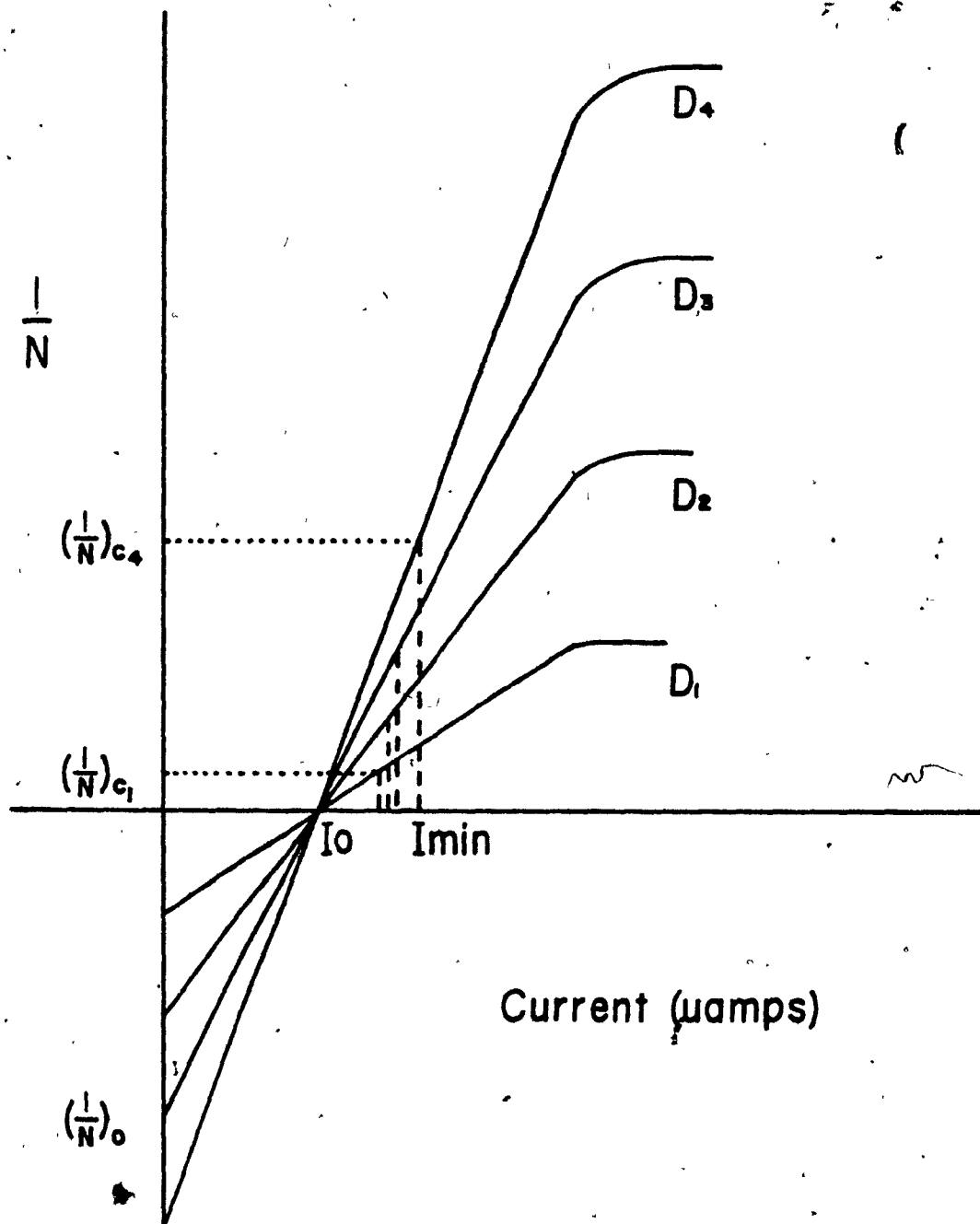


Figure 8. Predicted changes in the $1/N$ versus I trade-off functions when pulse duration is constant and train duration is varied. Increments in train duration from D_4 to D_1 lead to decrements in the slope of the trade-off function and $(1/N)_c$, increments in $(1/N)_o$, the y-intercept, and no change in I_0 , the x-intercept. The hyperbolic relationship between I_{min} and train duration is represented by the bunching of the vertical, dashed lines as train duration is increased from D_4 to D_1 .

The derivation of the charge-duration function in this experiment is based on Equation 20 which relates $1/N$ to I over the linear portion of the curve. If m is substituted for the slope, $1/N (D) \times k / k$, and the equation is then solved for the reciprocal of m , one obtains

$$1/m = N \times (I - I_0). \quad (23)$$

If both sides of the equation are multiplied by the pulse duration (d), then

$$d/m = d \times N \times (I - I_0). \quad (24)$$

The product, $d \times N \times (I - I_0)$, has the units microcoulombs and is denoted by Q' . According to the model, Q' is the effective electrical charge of the train of stimulation pulses for which the rat will self-stimulate. Thus, dividing the pulse duration by the slope of the best-fitting line relating $1/N$ and I yields an estimate of the effective charge needed to elicit criterial performance of a given train duration. By repeating this procedure at several train durations and by plotting the effective charge against train duration, one obtains a charge-duration function.

Huston et al. (1972) derived strength-duration functions for train durations using a paradigm developed by

Huston and Mills (cited in Huston et al., 1972). Using 100 Hertz sine wave stimulation, the current required to maintain a constant behavioural performance was determined for train durations ranging from 0.01 to 1.0 sec. When the mean threshold charge was plotted against train duration, a linear charge-duration function resulted.

Gallistel (1978) also derived a charge-duration function, but employed a different paradigm. In this experiment, rats were rewarded with trains of rectangular, cathodal pulses for running in an alley. Pulse duration and frequency were constant across sessions. The current required to elicit a criterial running speed was determined for trains of various duration (ranging between 0.1 and 20 sec). The results yielded a linear charge-duration function.

Neither Huston et al. (1972) nor Gallistel (1978) took into account the correction factor that has been advocated by Shizgal et al. (Note 4). The present investigation sought to determine what influence the effective current proposed by Shizgal et al. (Note 4) would have on the charge-duration function.

Summary

The objective of the present series of experiments was to contribute to the characterization of the neural substrate subserving BSR using the psychophysical approach

pioneered by Deutsch and Gallistel. With this approach, trade-off functions are obtained determining pairs of stimulation parameters that maintain a constant behavioural criterion. These trade-off functions impose quantitative constraints upon the neural substrate for the behaviour under investigation. A neural population must manifest electrophysiological characteristics similar to those established in the behavioural experiments if it is to be considered as a likely substrate for the behavioural effects of the stimulation.

The basis of the present research was the minimal model proposed by Gallistel (1978) and further elaborated by Shizgal et al. (Note 4). This extended model predicts the form of the trade-off functions that relate the commonly varied stimulation parameters.

The strength-duration and the charge-duration experiments were designed to test predictions of the extended model concerning the effect of varying pulse or train duration on the relationship between the number of stimulation pulses and the current. A second aim of the strength-duration experiments was to clarify the present discrepancy between behaviourally and electrophysiologically derived chronaxie estimates for BSR fibres. The final objective was to evaluate the form and parameters of the charge-duration function. Whereas previous work in this area was carried out using estimates of the total required

charge, the extended model suggests a means of calculating the effective portion of the required charge. Hence, it is of interest to determine how this correction affects the charge-duration function since this function constrains models of temporal integration in the reward substrate.

Specifically, the strength-duration and charge-duration experiments involve the determination of trade-off functions relating $1/N$ to I . That is, either $1/N$ or I is held constant and the required current or required number of pulses necessary to maintain a constant behavioural performance is determined. In the strength-duration experiments, the train duration is held constant while the pulse duration is varied across test sessions. In the charge-duration experiments, the pulse duration is held constant while the train duration is varied across test sessions.

Method

Subjects

The subjects were male rats from the Canadian Breeding Farms Ltd. Rat nos. 32, PC, 2B2, and 2G1 were of the Sprague Dawley strain whereas rat nos. B1, B2, G1, G2, N1, R2, Y1, NB1, and BL1 were of the Charles River strain. A normal 12 hour day/12 hour night cycle was maintained in the animal colony where the subjects were housed in individual wire mesh cages. Food (Purina rat chow) and water were available ad lib.

At the time of surgery, the subjects weighed 350-500 g. Each subject was anesthetized with sodium pentobarbital (Nembutal-60g/kg). With the incisor bar set at +5.0 mm, bilateral electrodes were aimed at the lateral hypothalamus (LH) using the following De Groot coordinates: 0.4 mm posterior to bregma, 1.7 mm lateral to the mid-sagittal suture, and 8.0 mm below dura. The electrodes were made from 250- μ m stainless steel wire and insulated with Formvar. The tips were bared of insulation in the process of honing them to a hemispherical shape. The current return consisted of four stainless steel screws fixed in the skull around which a thin wire was wrapped. The electrodes were cemented to the skull and the anchoring screws with dental acrylic. Before training procedures were begun, the subjects were allowed a one week period to recover from the surgery.

Apparatus

The chambers used in the training and the testing phases of the experiments were wooden boxes (28 cm x 27 cm x 69 cm) with a plexiglass front and two rodent levers (Lehigh Valley Electronics, 121-05) mounted on opposite sides, 4.5 centimeters above a wire mesh floor. Only one of the levers was employed during the experiments. All temporal parameters of the stimulation were controlled by digital pulse generators (Mundl, Note 1) while the current intensity was controlled by constant current amplifiers (Mundl, 1980). In order to prevent the build-up of charge at the brain-electrode interface, the outputs of the stimulators were shorted through a 1 k Ω resistor when no pulse was present. The stimulation current was monitored on an oscilloscope (D61a, Telequipment) by reading the voltage drop across a one percent precision 1 k Ω resistor in series with the electrode. To allow the animal to circle without twisting the leads, the connection between the electrode and the stimulator was routed through a mercury commutator (Leslie Manufacturing Corp., 590,592).

Procedure

Initial training and selection The first phase of training consisted in shaping the subjects to bar press for stimulation. Trains of pulses were delivered upon successively closer approximations to a bar press until the

desired behaviour was manifested. Each stimulation train lasted for 0.500 sec and consisted of 50 cathodal pulses (100 Hertz), 0.1 msec in duration, and 400 microamperes in amplitude. If subjects showed little tendency to approach the lever or manifested disruptive motor responses within the first three testing sessions, they were eliminated from the experiment.

Next, the subjects were taught to initiate bar pressing after being primed by five non-contingent trains of stimulation. Each bar press during the one minute period following priming resulted in the delivery of the stimulation train described above. Subjects had to maintain a rate of at least 50 bar presses per minute to pass into the stabilization phase of training.

Stabilization consisted of repeatedly determining the number of pulses required to produce a half-maximal response rate until the variance of the subject's performance fell within acceptable limits. These determinations consisted of systematically reducing the number of pulses while holding constant all the other stimulation parameters. During the first one minute component, a current intensity and a number of stimulation pulses were used that had previously produced vigorous bar pressing. On each subsequent trial, the number of pulses was reduced by 0.1 log₁₀ unit steps. This procedure continued until the subject emitted fewer than 10 responses on two successive trials. The number of responses for each

one minute component was then plotted against the number of pulses. The required number of pulses was derived by dropping a vertical line to the abscissa from the point on the rate-number curve corresponding to the half-maximum rate. The stability criterion was a range of required number values of no more than 0.1 log units for two consecutive training sessions, each consisting of approximately 12 determinations of the required number of pulses.

About 50 percent of the rats reached the data collection stage.

Strength-duration experiments

In these experiments, a series of number-current trade-off functions were determined. Pulse duration was held constant within each session but was varied across sessions. Train duration was held constant at 0.500 sec across all sessions. Pulse durations were selected so as to span a large range; the spacing between pulse durations was roughly logarithmic. Another factor that determined the combination of pulse durations employed for a given rat was the date of the subject's participation in the experiment. Subjects that participated in the early stages of the experiment were generally tested over more pulse durations than animals run later.

A cyclical order of presentation of the pulse durations was used across sessions. For example, rat no. B2 was run

with a pulse width of 0.09990 sec in the first session. On the next four sessions, the pulse durations were presented in the following order: 0.002500, 0.000500, 0.000250, and 0.000020 sec. In the next session the pulse duration was again 0.09990 sec and so on until all replications had been completed. It was assumed that this order of presentation would distribute the effect of any progressive behavioural change over all pulse durations. Usually, five sessions were run. The first sessions was discarded because variance tended to be high while the subject was accommodating to the experimental procedure.

Experimental sessions were run using one of two procedures for deriving the trade-off between the current and the number of pulses. The first variant, which was used for 7 subjects, consisted of a series of determinations of the required number of pulses. That is, the current intensity was set and the number of pulses was determined. In addition, two determinations of the required current were run at high stimulation frequencies. A determination of the required current was similar to a determination of the required number except that the number of pulses was set and the current intensity corresponding to the half-maximum rate of response was determined. The current determinations were run so that the lowest current that would elicit behaviour could be accurately determined. The second variant of the procedure involved only determinations of the required currents. This procedure was used to study more accurately

the relationship between number and current at low current intensities. Two subjects were run in the second set of experiments.

Any one session usually consisted of 6-14 determinations of the required number of pulses and/or determinations of the required current. The range over which these determinations were run was defined as follows: The smallest number of pulses tested was the value that elicited behaviour at the largest current employed in the experiment, 1600 microamperes. The maximum number of pulses was defined by one of two criteria. First, the smallest period (pulse onset to pulse onset) that was used was 1 msec. The second criterion employed was that the period had to be large enough so that there would be no build-up of charge at the brain-electrode interface. A build-up of charge was noted by a failure of the oscilloscope trace to return to baseline during the interpulse interval. The maximum duty cycle (pulse duration divided by the period) varied somewhat from subject to subject but was approximately 25 percent. Hence, the minimum period tested increased with the pulse duration.

When the first variant of the procedure was used, sessions started with a ten minute warm-up period consisting of two determinations of the required number of pulses; the current was set to an approximately mid-range intensity. This current intensity was also used for the first determination of the required number of pulses during the

data collection phase of the experiment. The second current intensity used was greater than the first while the third was less. This pattern of current intensity presentation was followed until the maximum current intensity employed had been reached at one extreme and a current intensity that did not elicit behaviour was reached at the other extreme. At this point, two required current determinations were also run using the largest and the second largest number of pulses possible given the aforementioned criteria (a period not less than 1 msec or a maximum duty cycle of approximately 25 percent). Finally, the required number of pulses was determined with the current set at the first value tested in that session. If there was a shift in the required number of pulses of more than $0.1 \log_{10}$ units between these two trials, then the data for that session were discarded on the grounds of insufficient stability in the subject's performance.

A similar procedure was employed for data collection in the second variant of the experiment with the exception that only required currents were determined and that the range of $1/N$ values used was smaller than in the first set of experiments. In this variant, train duration was held constant at 1.000 sec across all sessions.

Charge-duration experiments As in the strength-duration experiments, a series of number-current trade-off functions were determined. However, train duration was varied across

sessions while pulse duration was held constant at 0.1 msec.

As in the strength-duration experiments, a cyclical order of presentation was used so that the effect of any progressive behavioural change would be distributed over all the train durations. The five train durations employed, in their order of presentation, were: 0.500, 1.000, 0.250, 2.500, and 0.100 sec. Five sessions were usually run with the first session discarded.

Experimental sessions were run using one of two procedures for deriving the trade-off between the current and the number of pulses. The first variant, which was used for 6 subjects, consisted of a series of determinations of the required number of pulses. That is, the current was set and the number of pulses was determined. In addition, two determinations of the required current were run at high stimulation frequencies. The second variant of the experiment involved only determinations of the required currents. This procedure was used to study more accurately the relationship between number and current at low current intensities. Four subjects were run in the second procedure.

Any one session usually consisted of 6-14 determinations of the required number of pulses and/or determinations of the required current. The range over which these determinations were run was defined as follows: The smallest number of pulses tested was the value that elicited

behaviour at the largest current employed in the experiment, 600 microamperes. The maximum number of pulses was defined by one of two criteria. First, the smallest period (pulse onset to pulse onset) that was used was 1 msec. The second criterion employed was the maximum number of stimulation pulses that the pulse generator could produce. This corresponded to a value of 999 pulses. It was possible to use such high frequencies for all train durations since the pulse duration was so short that there was little build-up of charge at the brain-electrode interface.

When the first variant of the procedure was used, sessions started with a ten minute warm-up period consisting of two determinations of the required number of pulses; the current was set to an approximately mid-range intensity. This current intensity was also used for the first determination of the required number of pulses during the data collection phase of the experiment. The second current intensity used was greater than the first while the third was less. This pattern of current intensity presentation was followed until the maximum current intensity employed had been reached at one extreme and a current intensity that did not elicit behaviour was reached at the other extreme. At this point, two required current determinations were also run using the largest and the second largest number of pulses possible given the aforementioned criterion (a period not less than 1 msec). Finally, the required number of pulses was determined with the current set at the first

value tested in that session. If there was a shift in the required number of pulses of more than $0.1 \log_{10}$ units between these two trials, then the data for that session were discarded on the grounds of insufficient stability in the subject's performance.

A similar procedure was employed for data collection in the second variant of the experiment with the exception that only required currents were determined and that the range of $1/N$ values used was smaller than in the first variant of the experiment.

Histology

At the end of the experiment, the subjects were anesthetized with sodium pentobarbital (Nembutal-60 mg/kg) and then killed by exsanguination. After perfusion with 10 percent formalin, the brains were removed and then stored in 10 percent formalin for several days prior to sectioning. The brains were then blocked in the plane of electrode insertion and sliced in sections 40 μ m thick on a cryostat (at -18°C). The location of the electrode tips was verified with reference to the Pellegrino, Pellegrino, and Cushman (1970) stereotaxic atlas.

Results

This section is divided into four parts. The first part deals with the graphical representation of the data. Based in part upon an analysis of these graphs, the second part deals with the rationale for employing certain statistical analyses. The third part presents the statistical results themselves. The final part deals with the results of histology.

I. Figures

Strength-duration experiments

Required number determinations Figures 9a through 9g graphically represent the I/N versus I trade-off functions for the seven subjects run in this section of the strength-duration experiment. Each figure is composed of a series of panels. All but the lower right-hand panel represent the trade-off of the number of pulses and the current obtained with the single pulse duration indicated in the panel. The means of the required number determinations are represented by the squares while the means of the required current determinations are represented by the triangles. Except where it is smaller than the symbol, the 95 percent confidence interval around each mean is indicated as a vertical line passing through each square or as a horizontal line passing through each triangle. The line segment represents the line of best fit obtained from the

weighted least squares linear regression of $1/N$ on I over the range of values used in the required number determinations. The range of values included in each regression analysis was bounded by the lowest and highest currents tested across each pulse duration. The lower right-hand panel of each figure presents the line segments for the various $1/N$ versus I trade-off functions so that the progressive changes in the slopes and the I_{min} values may be more readily seen.

Required current determinations The results for the two subjects run in this version of the strength-duration experiment are shown graphically in Figures 10a and 10b. Each figure is composed of a series of panels. All but the lower right-hand panel represent the trade-off of the current and the number of pulses obtained with the single pulse duration indicated in the panel. The means of the required current determinations are represented by the triangles. Except where it is smaller than the symbol, the 95 percent confidence interval around each mean is indicated as a vertical line passing through each triangle. The line segment represents the line of best fit obtained from an iterative, weighted least squares linear regression of I on $1/N$. The iterative analysis and its rationale are described below. The lower right-hand panel of each figure presents the line segments for the various I versus $1/N$ trade-off functions so that the progressive changes in the slopes and the I_{min} values may be more readily seen.

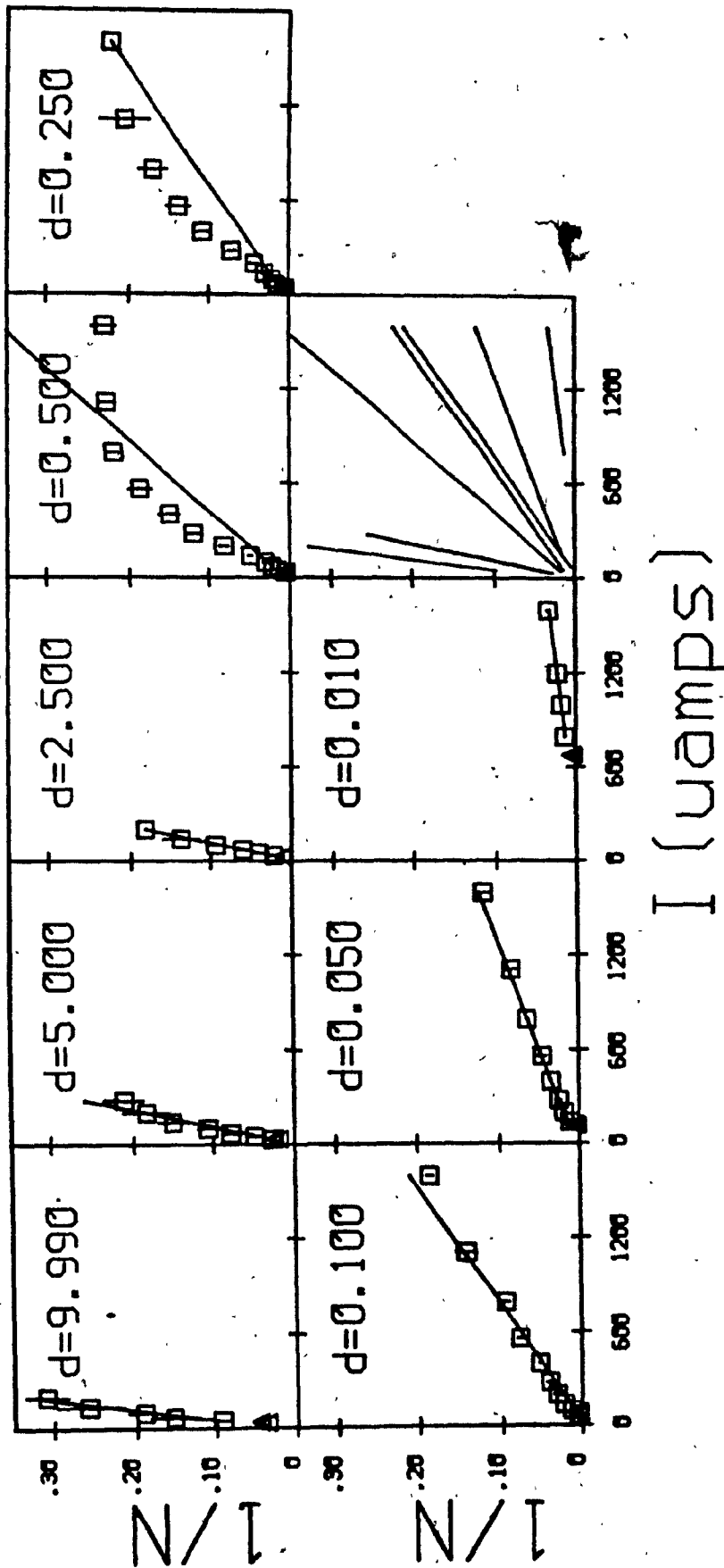


Figure 9a. The family of I/N versus I trade-off functions obtained for a series of pulse durations for subject 32. The pulse duration used for each trade-off function is indicated within each panel. The lower, right-hand panel presents the line segments for the various I/N versus I trade-off functions to highlight the changes in the slopes and the I_{min} values. The squares represent required number determinations with the vertical line indicating the 95 percent confidence interval. The triangles represent required current determinations with the horizontal line indicating the 95 percent confidence interval.

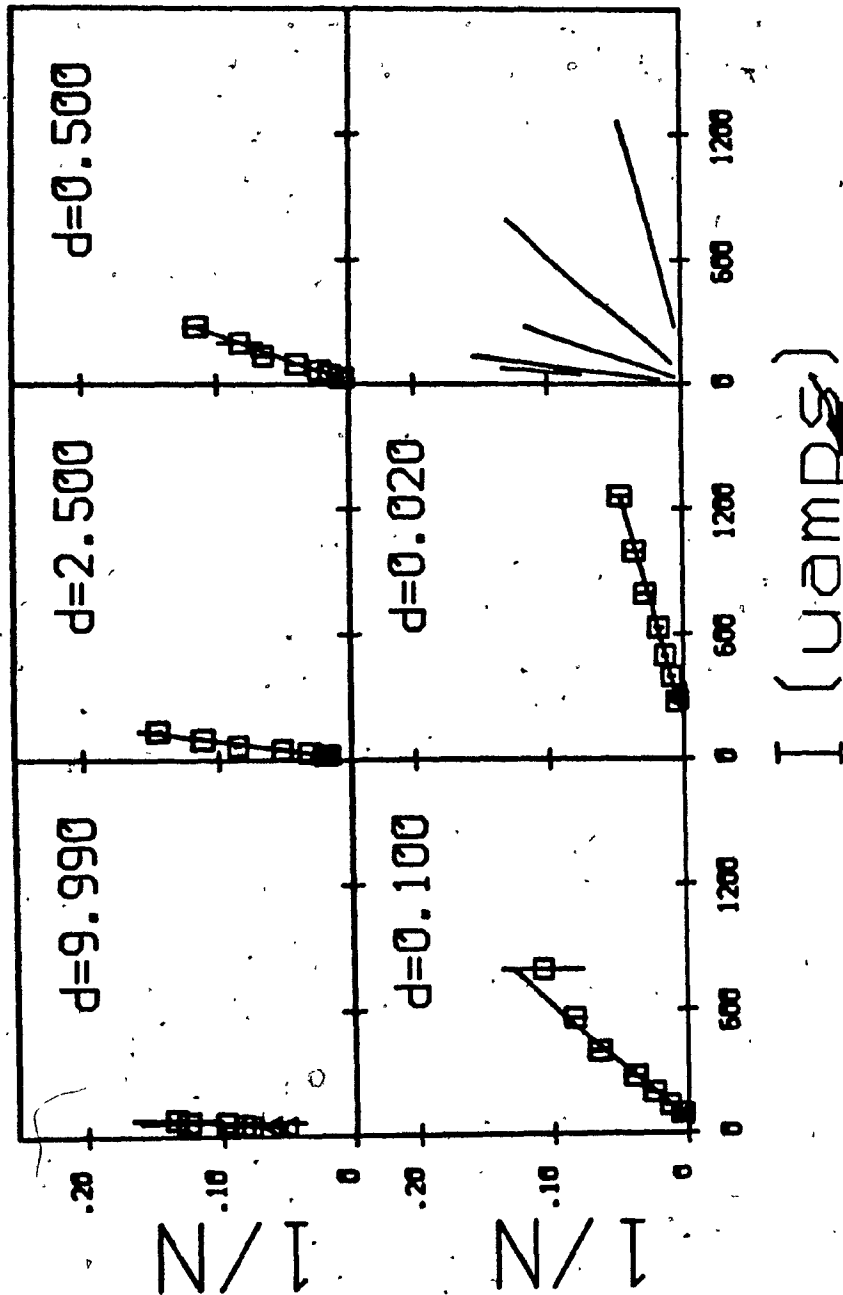


Figure 9b. The family of $1/N$ versus I trade-off functions obtained for a series of pulse durations for subject B2. The pulse duration used for each trade-off function is indicated within each panel. The lower, right-hand panel presents the line segments for the various $1/N$ versus I trade-off functions to highlight the changes in the slopes and the I_{min} values. The squares represent required number determinations with the vertical line indicating the 95 percent confidence interval. The triangles represent required current determinations with the horizontal line indicating the 95 percent confidence interval.

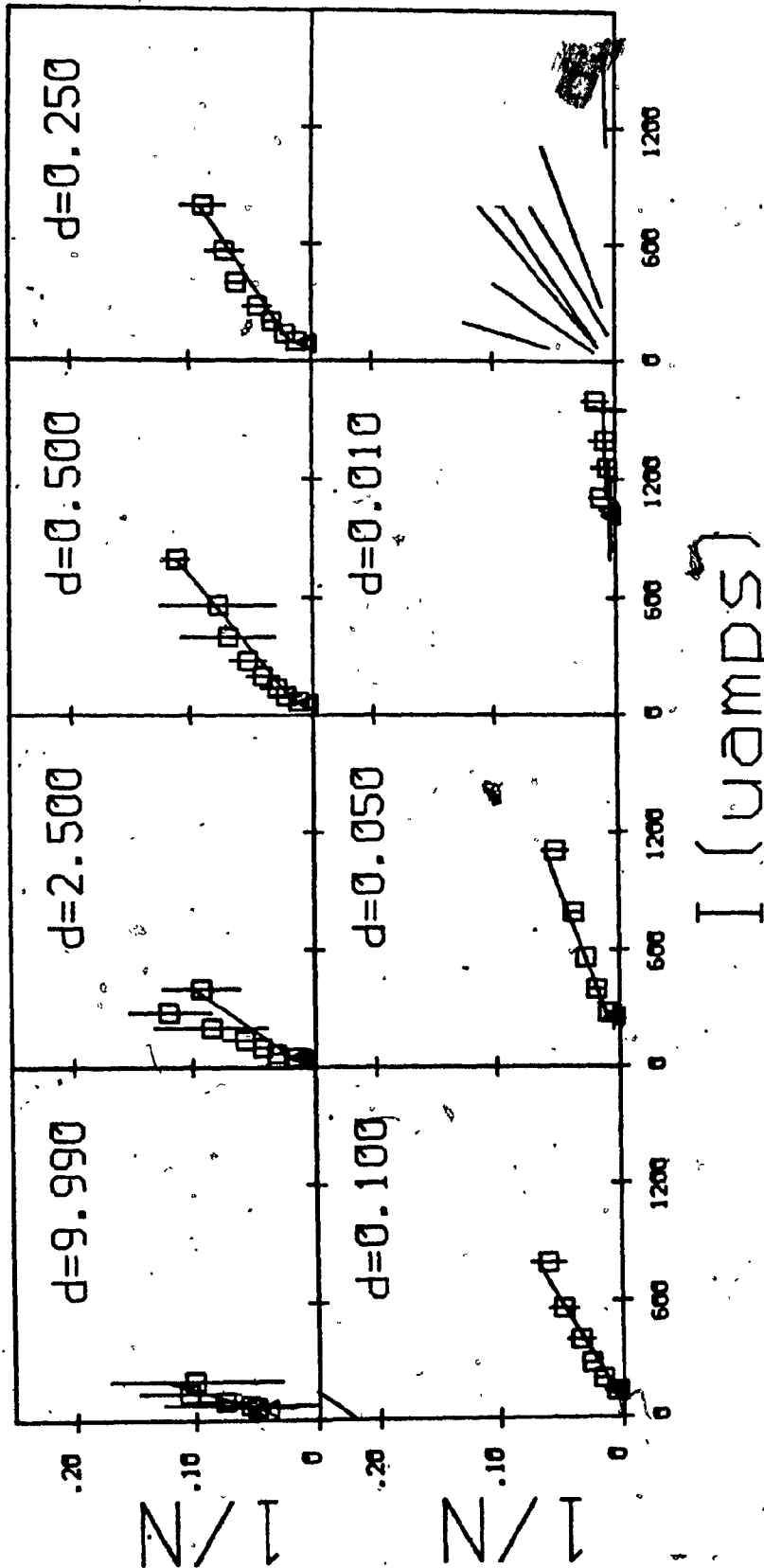


Figure 9c. The family of I trade-off functions obtained for a series of pulse durations for subject G1. The pulse duration used for each trade-off function is indicated within each panel. The lower, right-hand panel presents the line segments for the various I/N versus I trade-off functions to highlight the changes in the slopes and the I_{min} values. The squares represent required number determinations with the vertical line indicating the 95 percent confidence interval. The triangles represent required current determinations with the horizontal line indicating the 95 percent confidence interval.

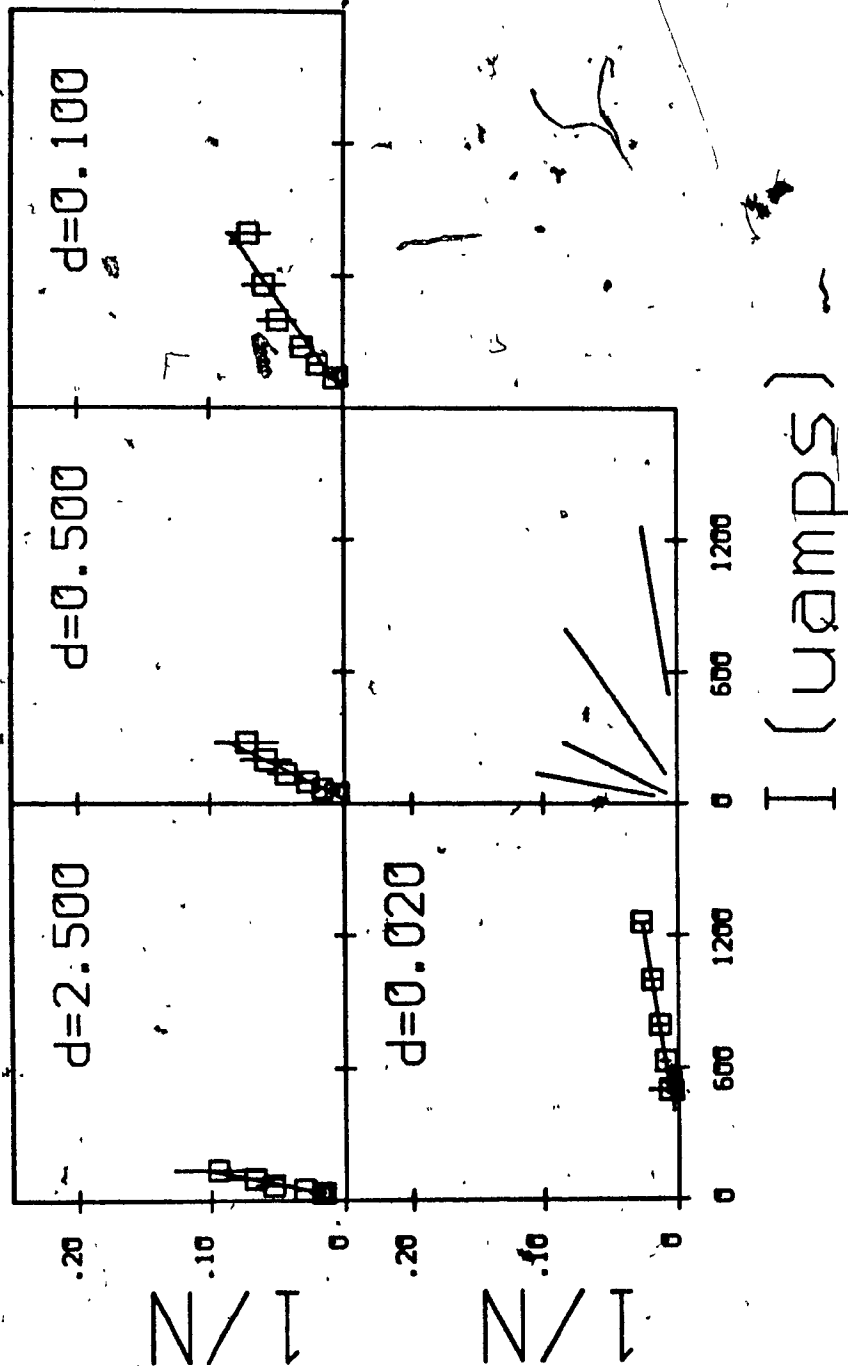


Figure 9d. The family of $1/N$ versus I trade-off functions obtained for a series of pulse durations for subject N1. The pulse duration used for each trade-off function is indicated within each panel. The lower, right-hand panel presents the line segments for the various $1/N$ versus I trade-off functions to highlight the changes in the slopes and the I_{min} values. The squares represent required number determinations with the vertical line indicating the 95 percent confidence interval. The triangles represent required current determinations with the horizontal line indicating the 95 percent confidence interval.

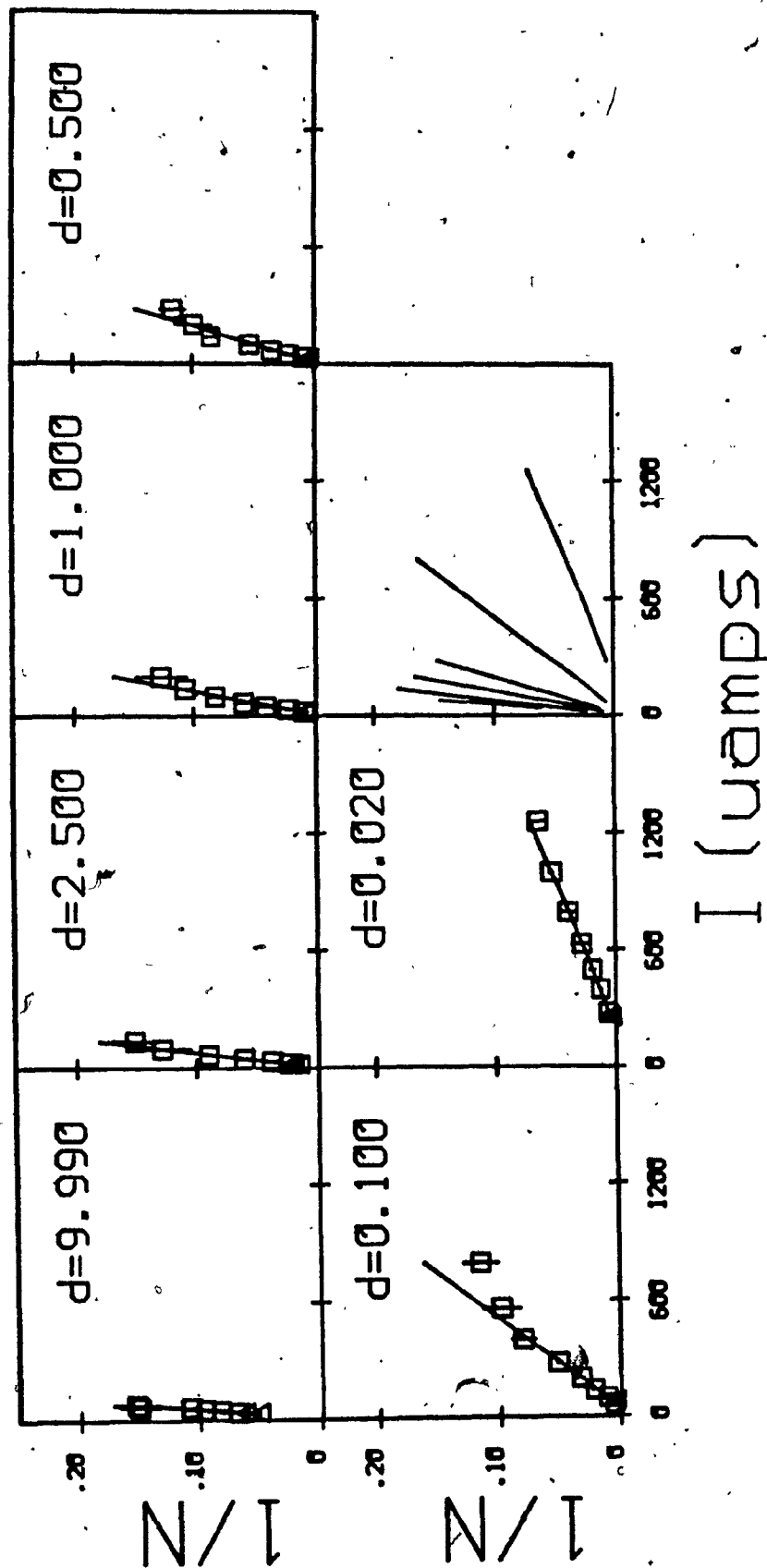


Figure 9e. The family of $1/N$ versus I trade-off functions obtained for a series of pulse durations for subject Y1. The pulse duration used for each trade-off function is indicated within each panel. The lower, right-hand panel presents the line segments for the various $1/N$ versus I trade-off functions to highlight the changes in the slopes and the I_{min} values. The squares represent required number determinations with the vertical line indicating the 95 percent confidence interval. The triangles represent required current determinations with the horizontal line indicating the 95 percent confidence interval.

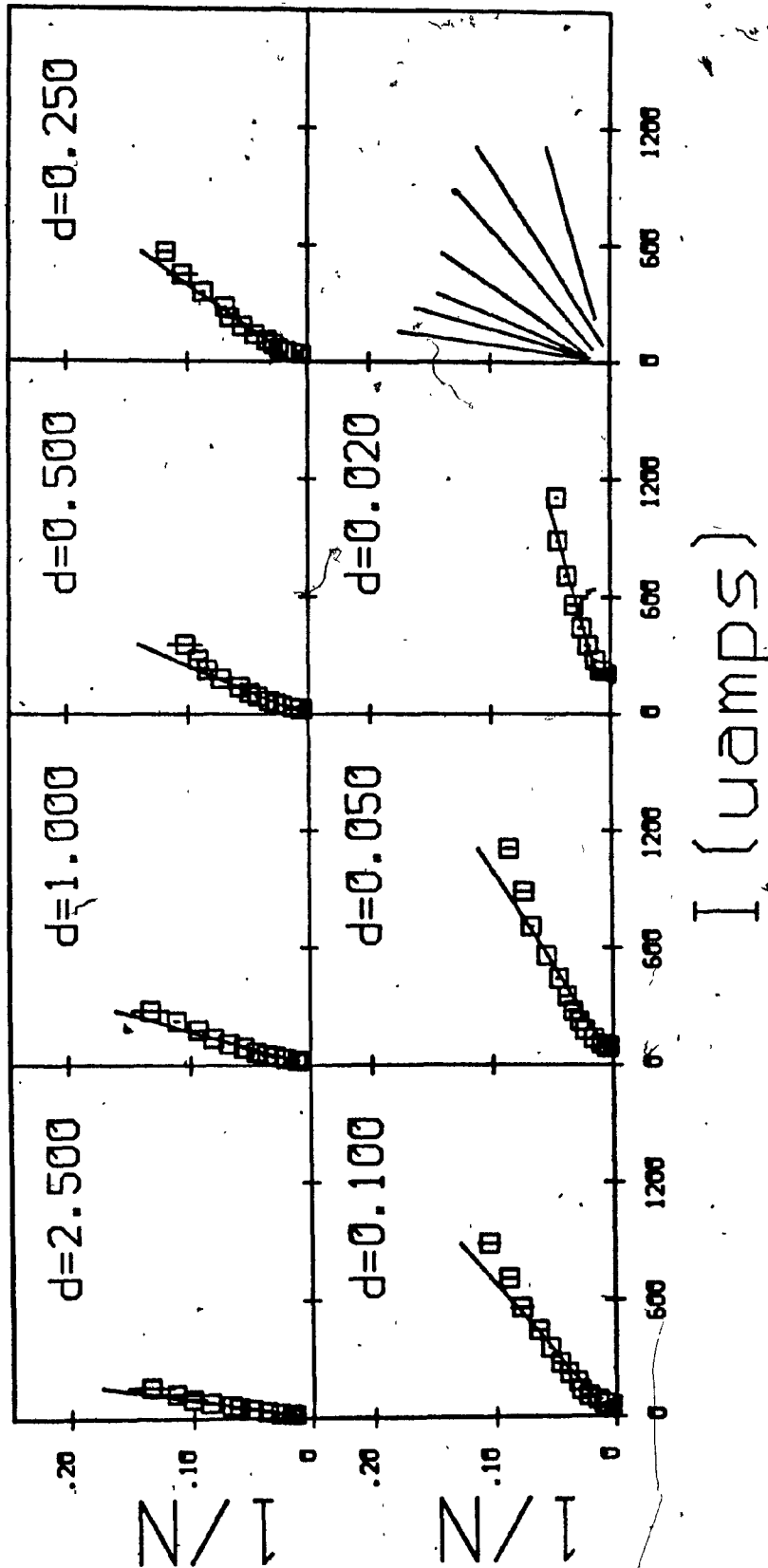


Figure 9f. The family of I trade-off functions obtained for a series of pulse durations for subject 2B2. The pulse duration used for each trade-off function is indicated within each panel. The lower, right-hand panel presents the line segments for the various I/N versus I trade-off functions to highlight the changes in the slopes and the I_{min} values. The squares represent required number determinations with the vertical line indicating the 95 percent confidence interval. The triangles represent required current determinations with the horizontal line indicating the 95 percent confidence interval.

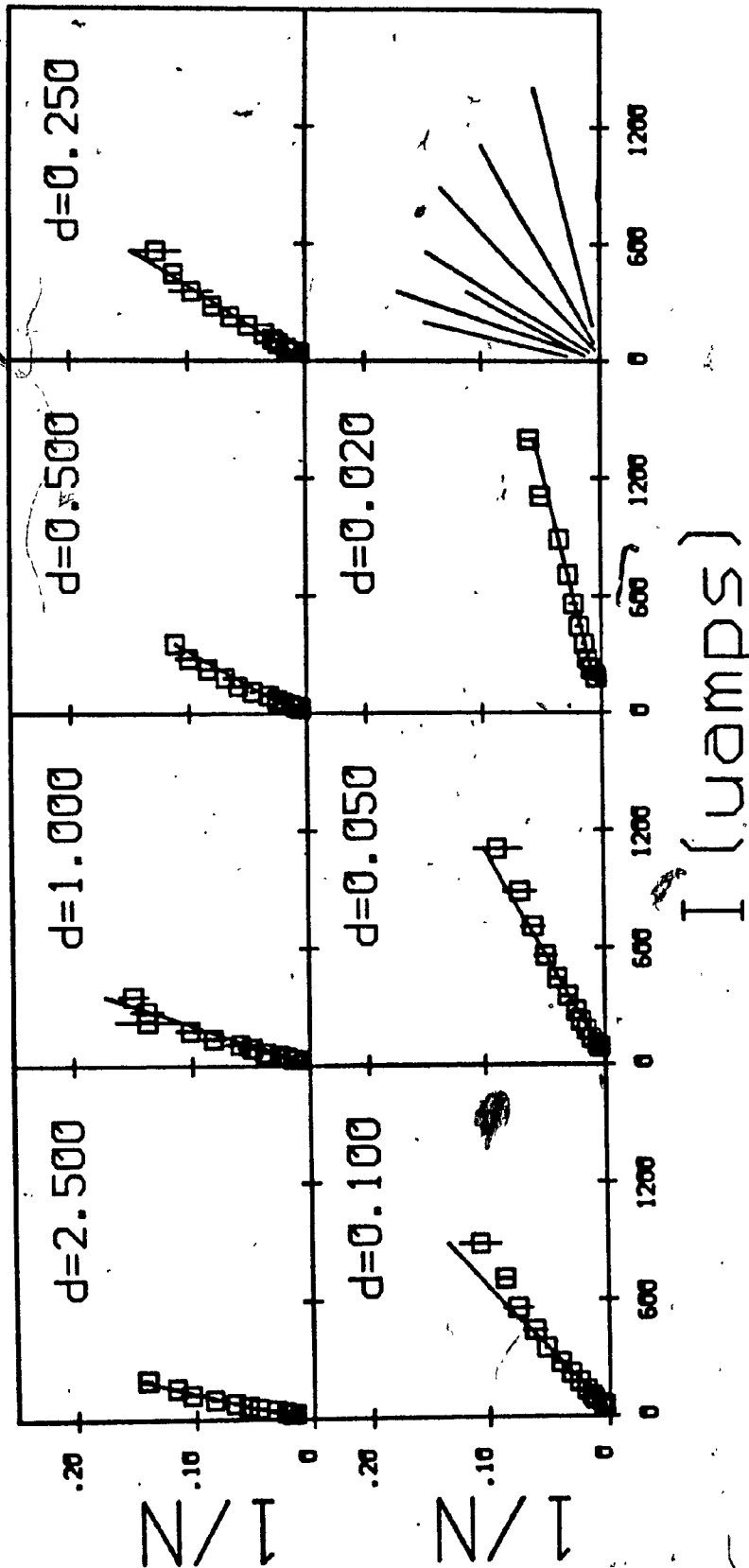


Figure 9g. The family of I/N versus I trade-off functions obtained for a series of pulse durations for subject 2G1. The pulse duration used for each trade-off function is indicated within each panel. The lower, right-hand panel presents the line segments for the various I/N versus I trade-off functions to highlight the changes in the slopes and the I_{min} values. The squares represent required number determinations with the vertical line indicating the 95 percent confidence interval. The triangles represent required current determinations with the horizontal line indicating the 95 percent confidence interval.

The range chosen for the abscissa was selected to facilitate comparison across pulse durations. However, the ability to discriminate between different data points is reduced at short pulse durations. To resolve this difficulty, the figures were redrawn with an expanded scale and with a more restricted range. Figures 11a and 11b show the data points and line segments, where appropriate, ranging between 0 and 0.016 rather than between 0 and 0.08 as in Figures 10a and 10b.

Charge-duration experiments

Required number determinations Figures 12a through 12f graphically represent the $1/N$ versus I trade-off functions for the six subjects run in this section of the charge-duration experiment. Each figure is composed of a series of panels. All but the lower right-hand panel represent the trade-off of the number of pulses and the current obtained with the single train duration indicated in the panel. The means of the required number determinations are represented by t_{ual} to the rheobase (R) of the strength-duration function for trains, while the y-intercept is equal to the product of the rheobase and the chronaxie (C) of the strength-duration function for trains. That is:

$$Q' = R \times D + R \times C \quad (25)$$

An estimate of the chronaxie was obtained by dividing the

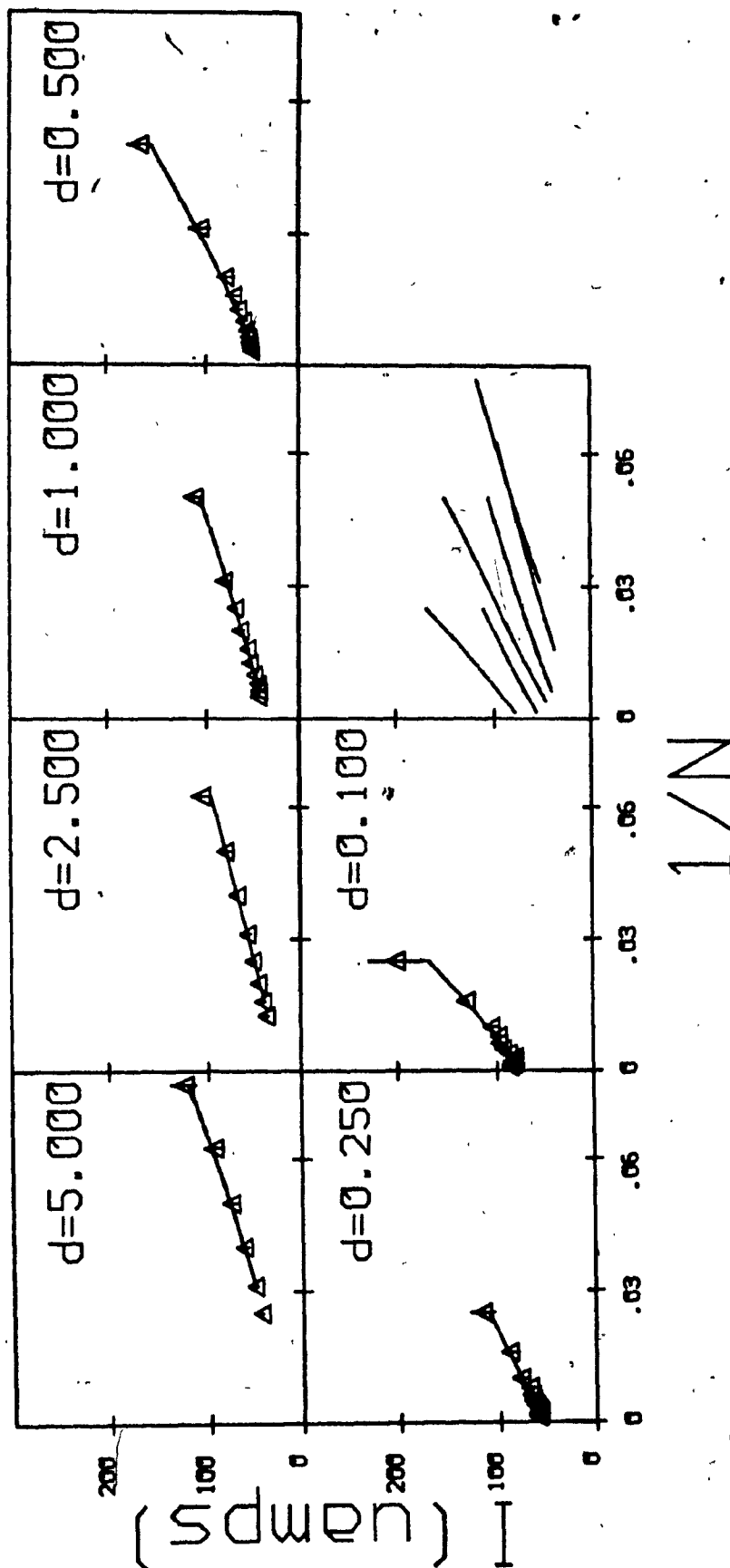


Figure 10a. The family of $1/N$ versus I trade-off functions obtained for a series of pulse durations for subject BL1. The pulse duration used for each trade-off function is indicated within each panel. The lower, right-hand panel presents the line segments for the various $1/N$ versus I trade-off functions to highlight the changes in the slopes and the I_{min} values. The triangles represent required current determinations with the vertical line indicating the 95 percent confidence interval.

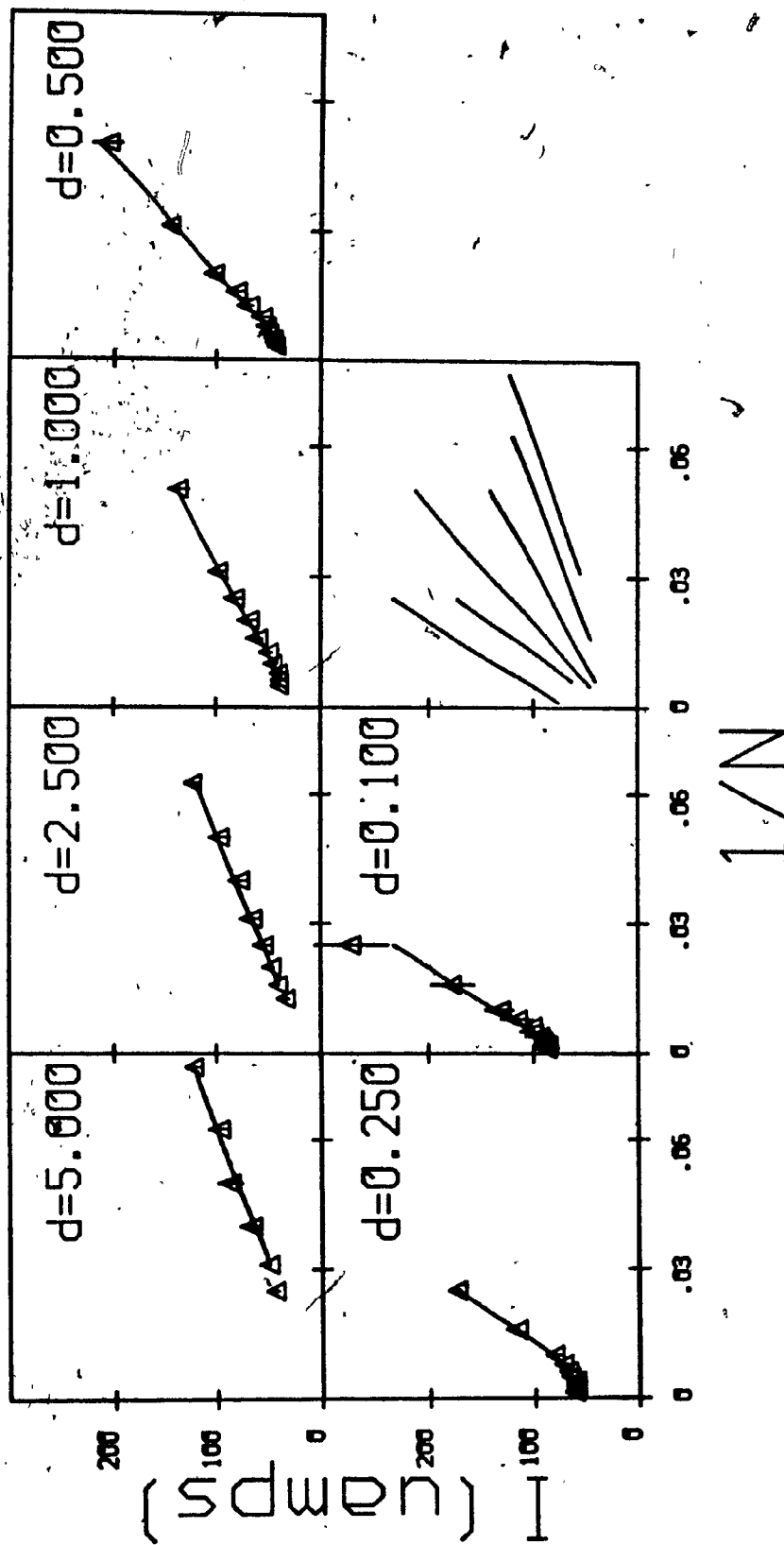


Figure 10b. The family of $1/N$ versus I trade-off functions obtained for a series of pulse durations for subject NB1. The pulse duration used for each trade-off function is indicated within each panel. The lower, right-hand panel presents the line segments for the various $1/N$ versus I trade-off functions to highlight the changes in the slopes and the I_{min} values. The triangles represent required current determinations with the vertical line indicating the 95 percent confidence interval.

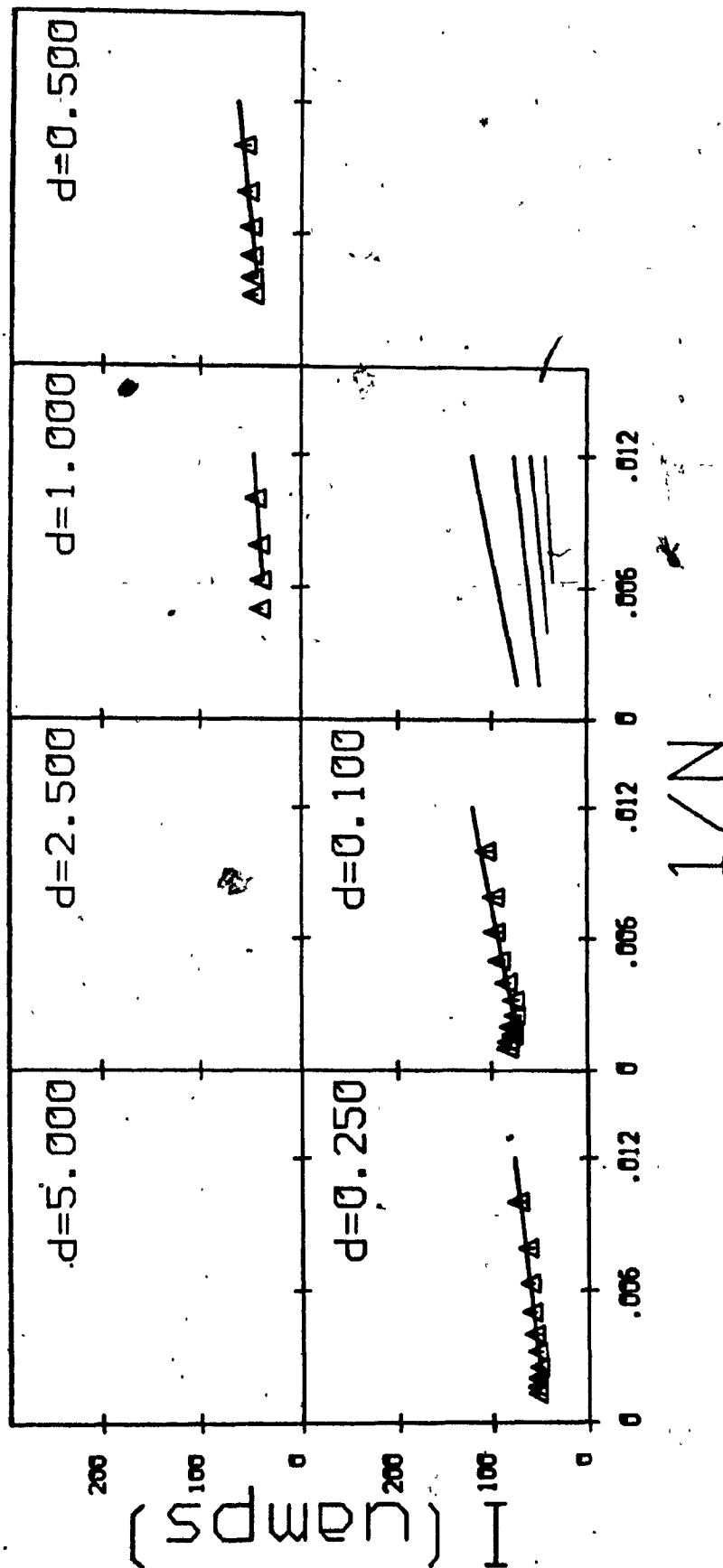
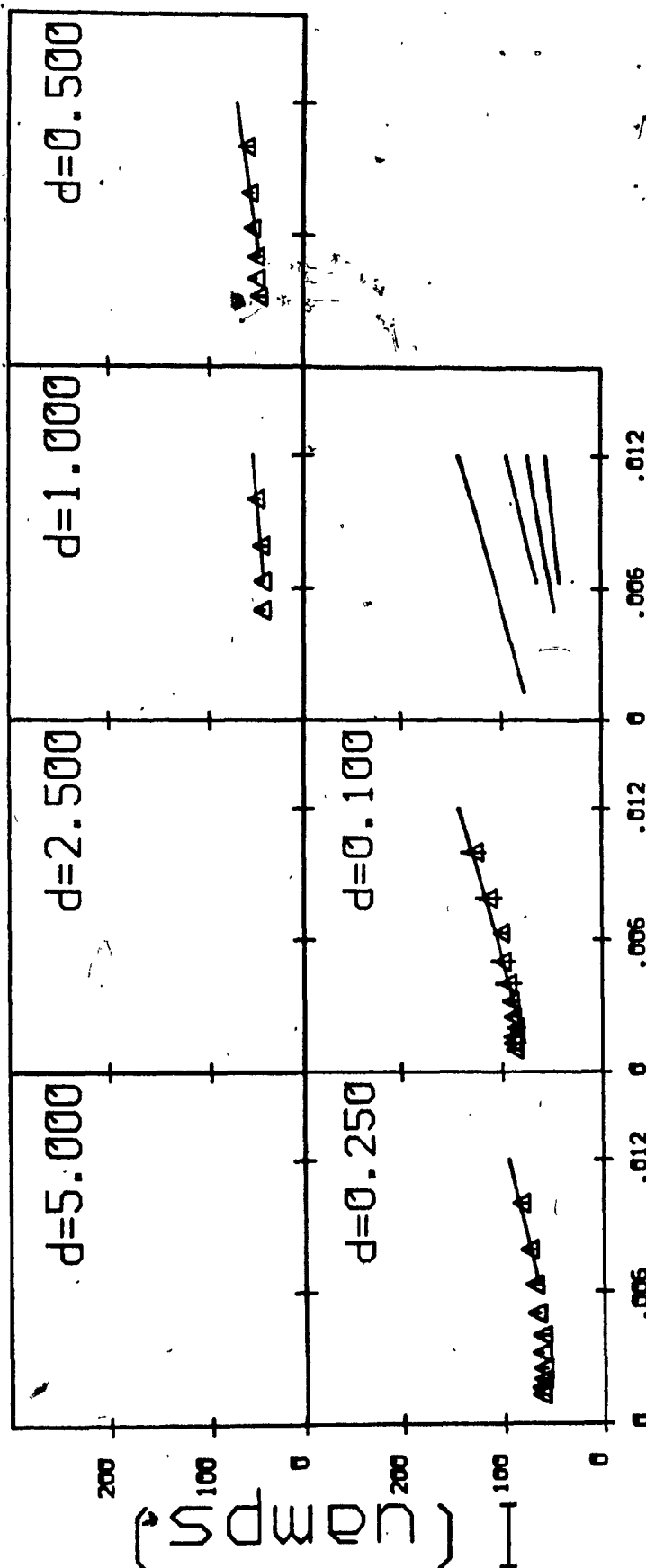


Figure 11a. Over the series of pulse durations tested for subject BL1, the data points and line segments are shown using the limited range of 0 to 0.016. The limited range was required to clearly show the data for high frequencies. The pulse duration used for each trade-off function is indicated within each panel. The absence of a line segment and/or data point means that the line was not defined and/or points were not collected over this range. The lower, right-hand panel presents the line segments for the various 1/N versus I' trade-off functions to highlight the changes in the slopes and the Imin values. The triangles represent required current determinations with the vertical line indicating the 95 percent confidence interval.



$$1/N$$

Figure 11b. Over the series of pulse durations tested for subject NB1, the data points and line segments are shown using the limited range of 0 to 0.016. The limited range was required to clearly show the data for high frequencies. The pulse duration used for each trade-off function is indicated within each panel. The absence of a line segment and/or data point means that the line was not defined and/or points were not collected over this range. The lower, right-hand panel presents the line segments for the various $1/N$ versus I trade-off functions to highlight the changes in the slopes and the I_{min} values. The triangles represent required current determinations with the vertical line indicating the 95 percent confidence interval.

range of values included in the regression analysis was bounded by the lowest and highest currents tested across all train durations. The lower right-hand panel of each figure presents the line segments for the various $1/N$ versus I trade-off functions so that the progressive changes in the slopes and the $(1/N)_c$ values may be more readily seen.

Required current determinations The results for the four subjects run in this version of the charge-duration experiment are shown graphically in Figures 13a through 13d. Each figure is composed of a series of panels. All but the lower right-hand panel represent the trade-off of the current and the number of pulses obtained with the single train duration indicated in the panel. The means of the required current determinations are represented by the triangles. Except where it is smaller than the symbol, the 95 percent confidence interval around each mean is indicated as a vertical line passing through each triangle. The line segment represents the line of best fit obtained from the weighted least squares linear regression of I on $1/N$ over the range of values used in the iterative, step-wise analysis. The lower right-hand panel of each figure presents the line segments for the various I versus $1/N$ trade-off functions so that the progressive changes in the slopes and the $(1/N)_c$ values may be more readily apparent.

The range chosen for the abscissa was selected to facilitate comparison across train durations. However, the

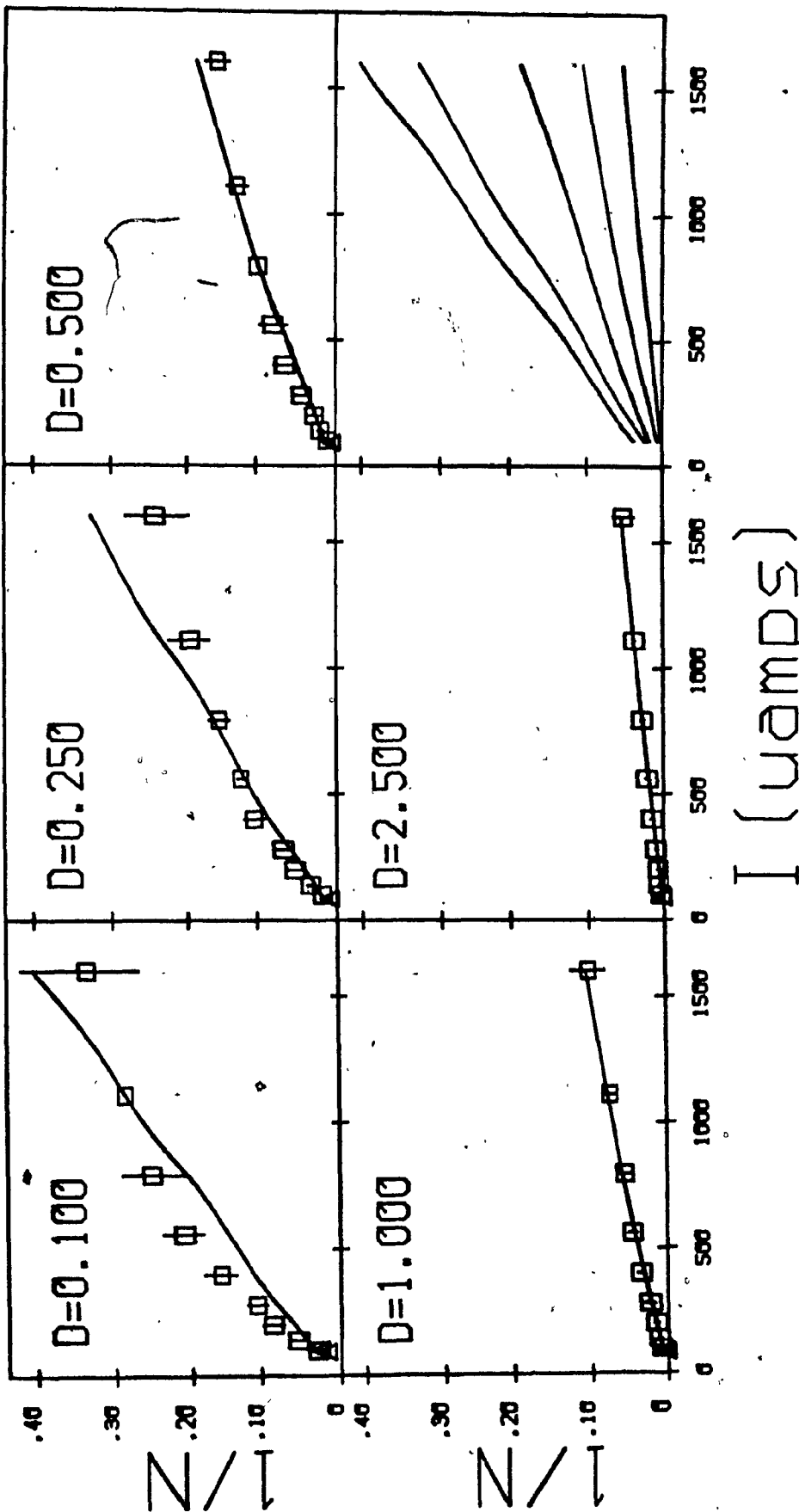
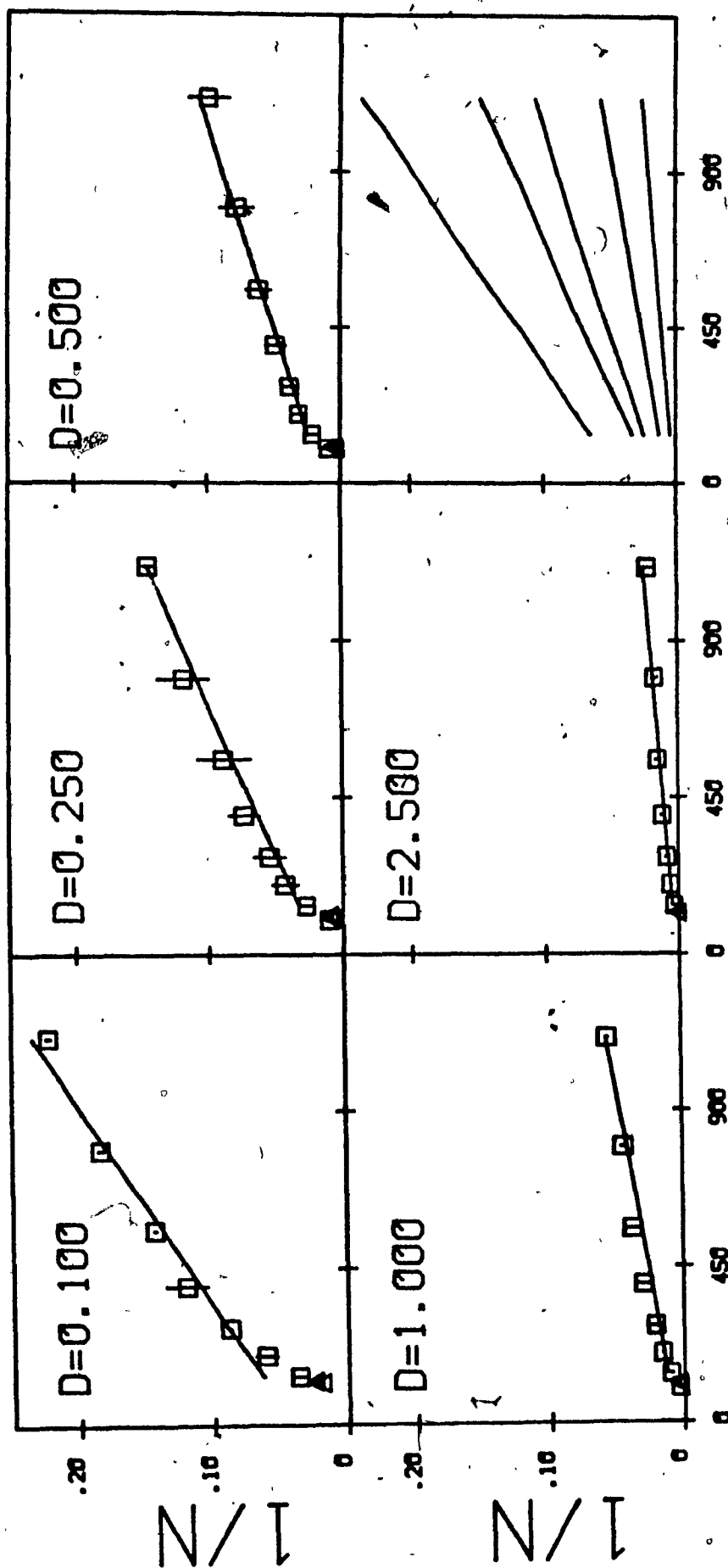
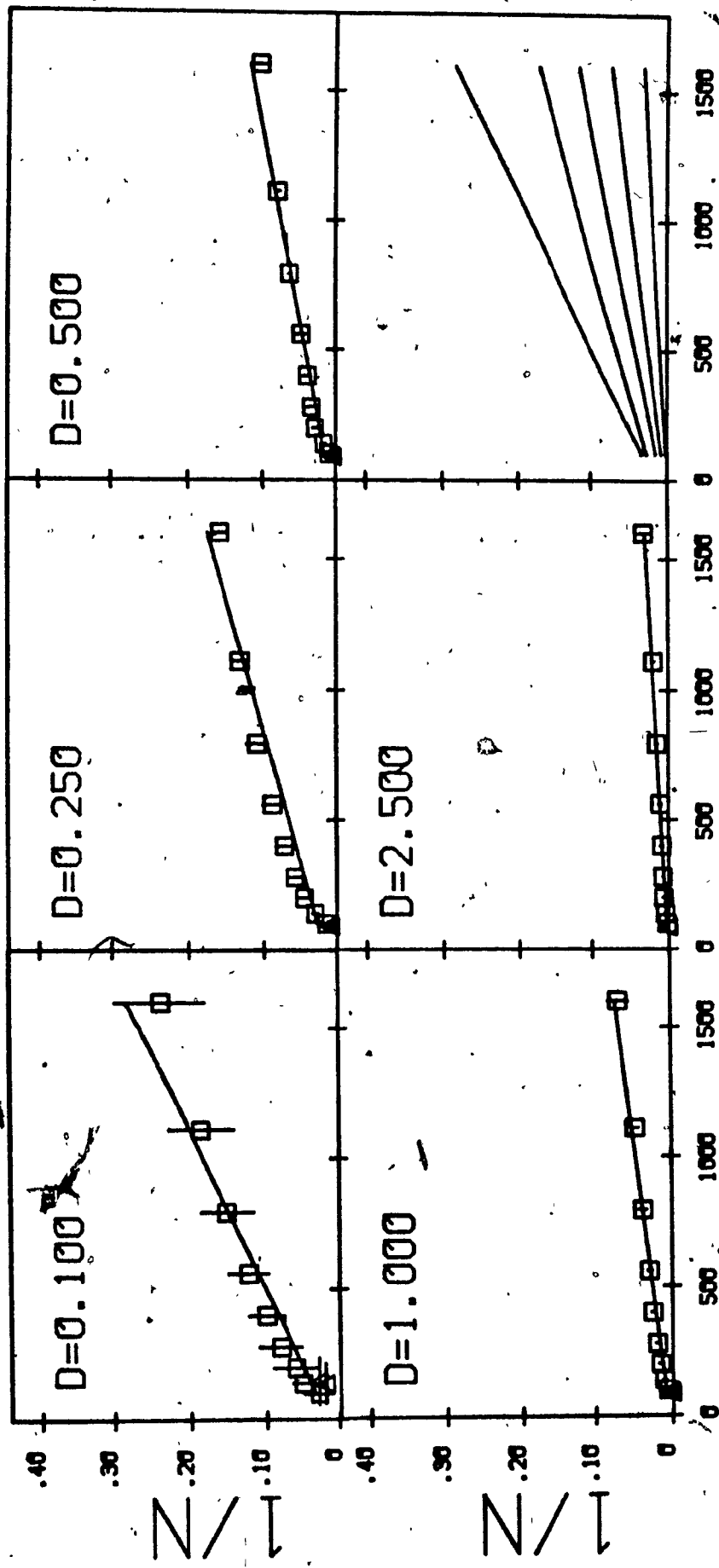


Figure 12a. The family of $1/N$ versus I trade-off functions obtained for a series of train durations for subject 32. The train duration used for each trade-off function is indicated within each panel. The lower, right-hand panel presents the line segments for the various $1/N$ versus I trade-off functions to highlight the changes in the slopes and the I_{min} values. The squares represent required number determinations with the vertical line indicating the 95 percent confidence interval. The triangles represent required current determinations with the horizontal line indicating the 95 percent confidence interval.



I (uamps)

Figure 12b. The family of I/N versus I trade-off functions obtained for a series of train durations for subject G2. The train duration used for each trade-off function is indicated within each panel. The lower, right-hand panel presents the line segments for the various I/N versus I trade-off functions to highlight the changes in the slopes and the I_{min} values. The squares represent required number determinations with the vertical line indicating the 95 percent confidence interval. The triangles represent required current determinations with the horizontal line indicating the 95 percent confidence interval.



I (uamps)

Figure 12c. The family of $1/N$ versus I trade-off functions obtained for a series of train durations for subject PC. The train duration used for each trade-off function is indicated within each panel. The lower, right-hand panel presents the line segments for the various $1/N$ versus I trade-off functions to highlight the changes in the slopes and the I_{min} values. The squares represent required number determinations with the vertical line indicating the 95 percent confidence interval. The triangles represent required current determinations with the horizontal line indicating the 95 percent confidence interval.

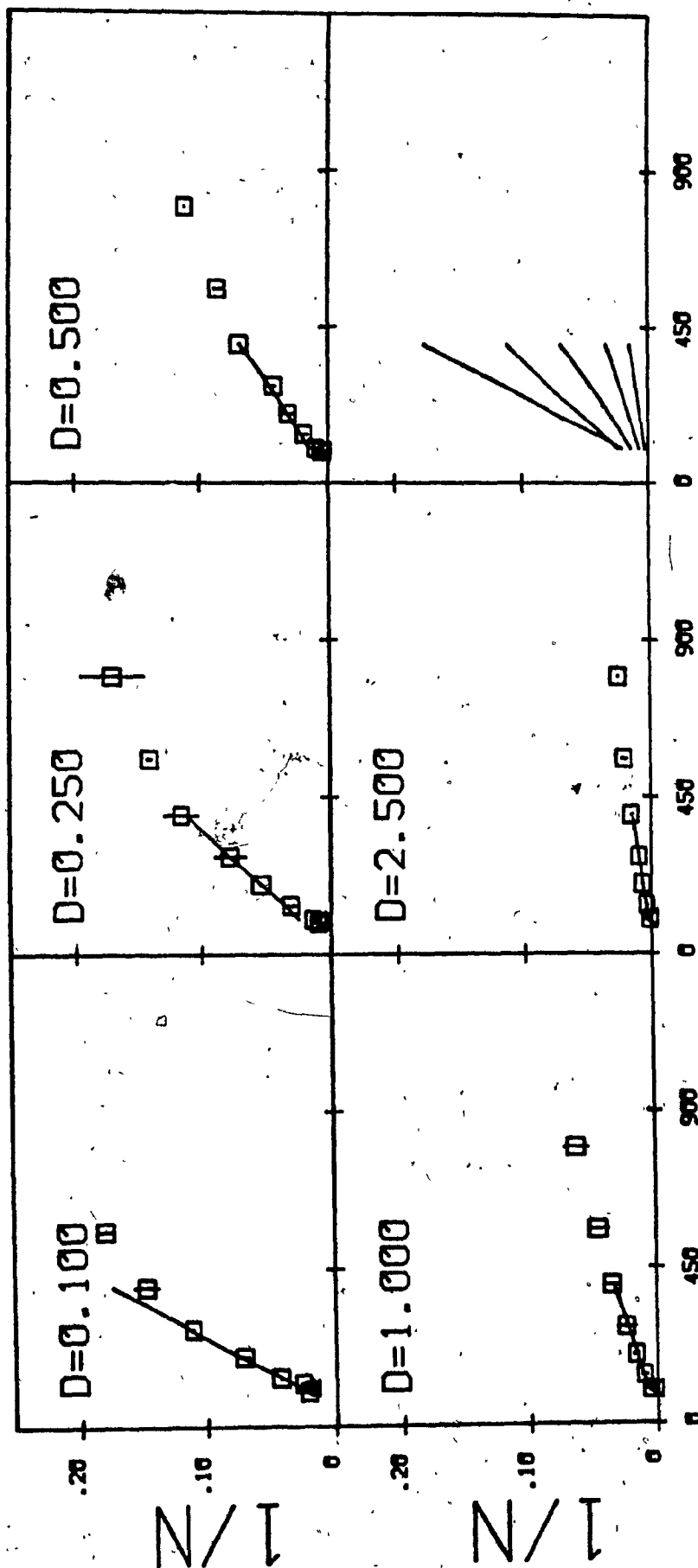


Figure 12d. The family of $1/N$ versus I trade-off functions obtained for a series of train durations for subject Y1. The train duration used for each trade-off function is indicated within each panel. The lower, right-hand panel presents the line segments for the various $1/N$ versus I trade-off functions to highlight the changes in the slopes and the I_{min} values. The squares represent required number determinations with the vertical line indicating the 95 percent confidence interval. The triangles represent required current determinations with the horizontal line indicating the 95 percent confidence interval.

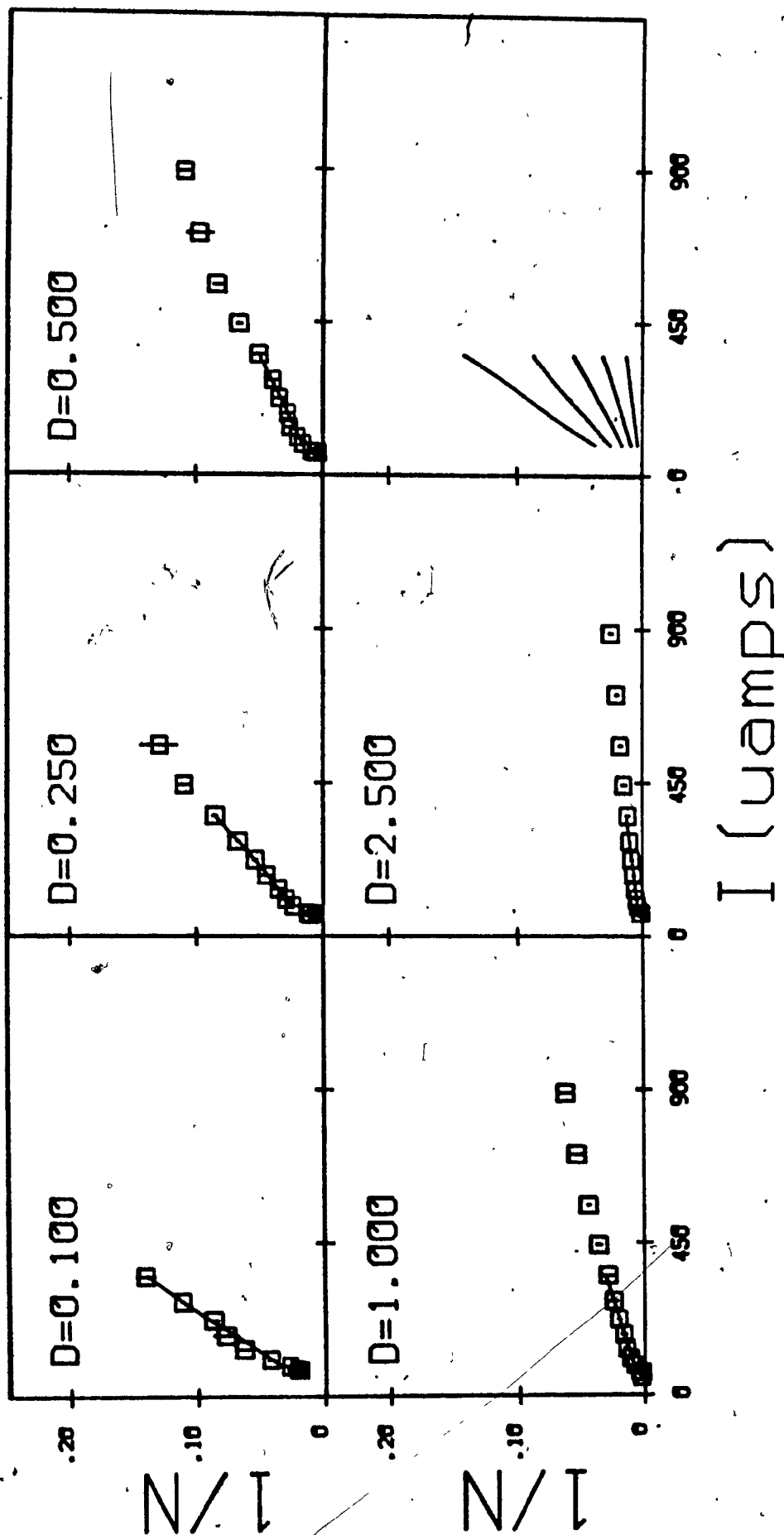


Figure 12e. The family of $1/N$ versus I trade-off functions obtained for a series of train durations for subject 2B2. The train duration used for each trade-off function is indicated within each panel. The lower, right-hand panel presents the line segments for the various $1/N$ versus I trade-off functions to highlight the changes in the slopes and the I_{min} values. The squares represent required number determinations with the vertical line indicating the 95 percent confidence interval. The triangles represent required current determinations with the horizontal line indicating the 95 percent confidence interval.

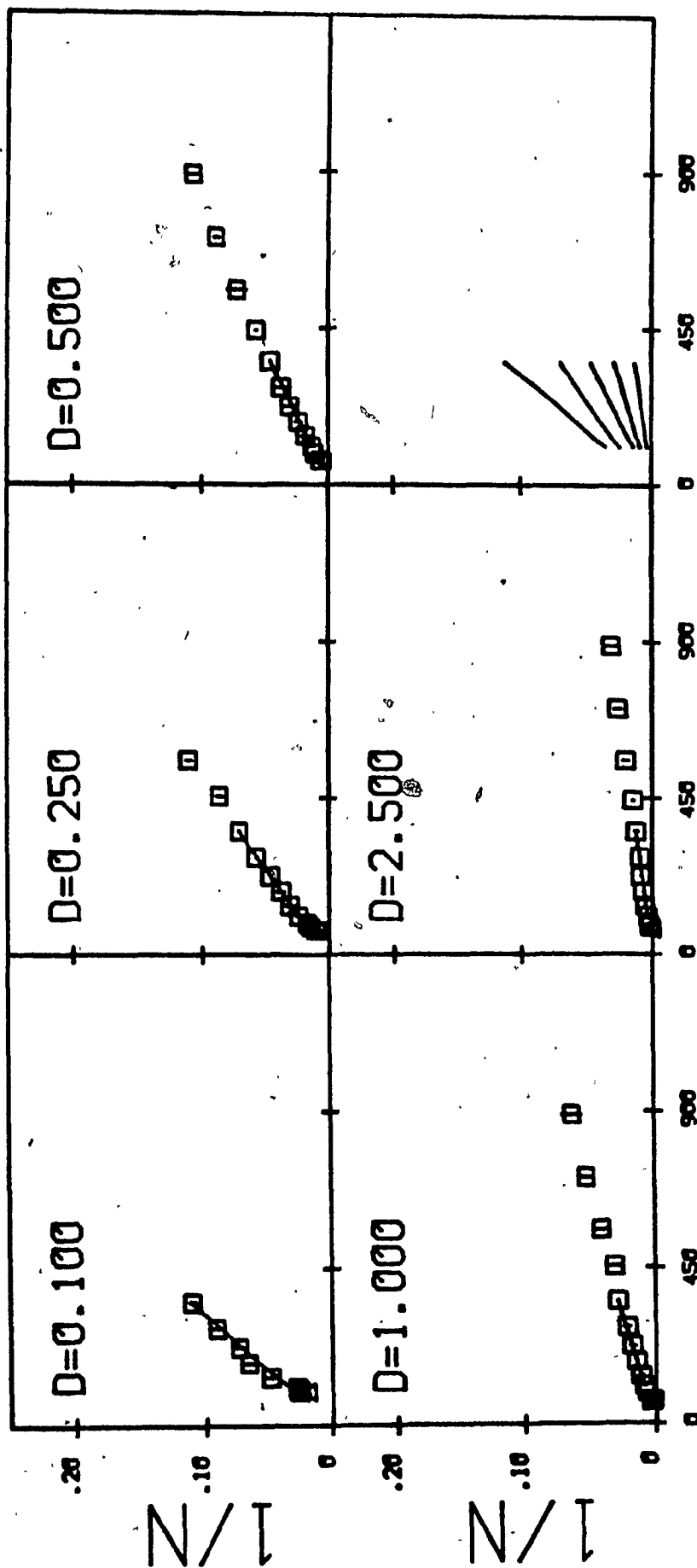


Figure 12f. The family of $1/N$ versus I trade-off functions obtained for a series of train durations for subject 2G1. The train duration used for each trade-off function is indicated within each panel. The lower, right-hand panel presents the line segments for the various $1/N$ versus I trade-off functions to highlight the changes in the slopes and the I_{min} values. The squares represent required number determinations with the vertical line indicating the 95 percent confidence interval. The triangles represent required current determinations with the horizontal line indicating the 95 percent confidence interval.

ability to discriminate between different data points was reduced at long train durations. To resolve this difficulty, the figures were redrawn with an expanded scale and a more restricted range. Figures 14a through 14d show the data points and line segments, where appropriate, ranging between 0 and 0.025 rather than between 0 and 0.125 as in Figures 13a through 13d.

II. Data analysis

The data analysis was designed to take into account two problematic aspects of the results, heteroscedasticity and non-linear trends.

The heteroscedasticity, unequal variance across the range of values determined, necessitated the use of a weighted regression. The weighting factor used was the reciprocal of the variance (Guest, 1961).

As explained in the introduction, it was expected that the linearity of the trade-off functions would break down both at high currents and at low currents. Such roll-offs pose a problem concerning which data points to include in the regression analysis.

With respect to the line segments fit to the $1/N$ versus I trade-off functions, two predictions arise from the extended model (Shizgal et al., 1980) for the

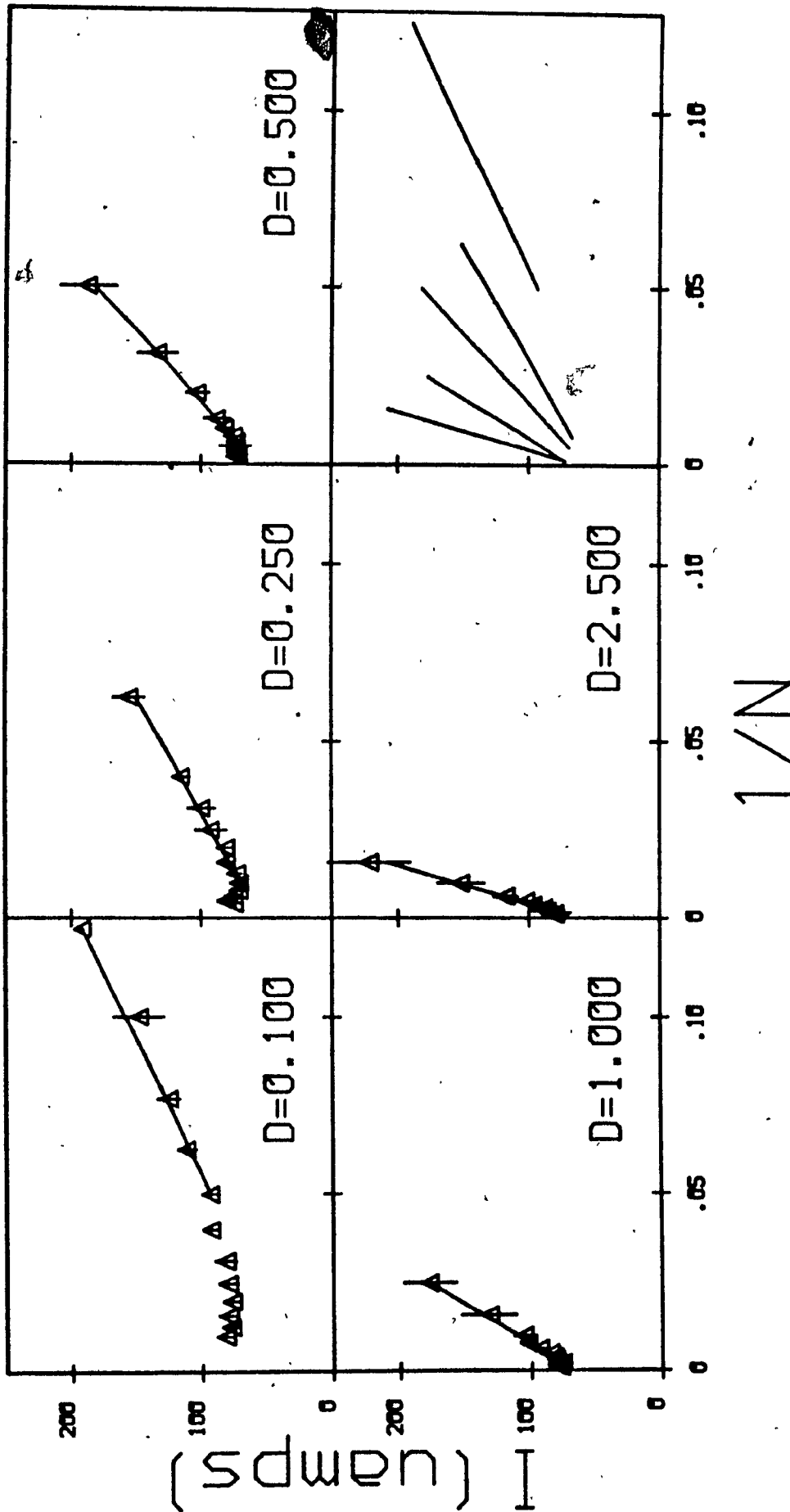


Figure 13a. The family of I trade-off functions obtained for a series of train durations for subject BL1. The train duration used for each trade-off function is indicated within each panel. The lower, right-hand panel presents the line segments for the various $1/N$ versus I trade-off functions to highlight the changes in the slopes and the I_{min} values. The triangles represent required current determinations with the vertical line indicating the 95 percent confidence interval.

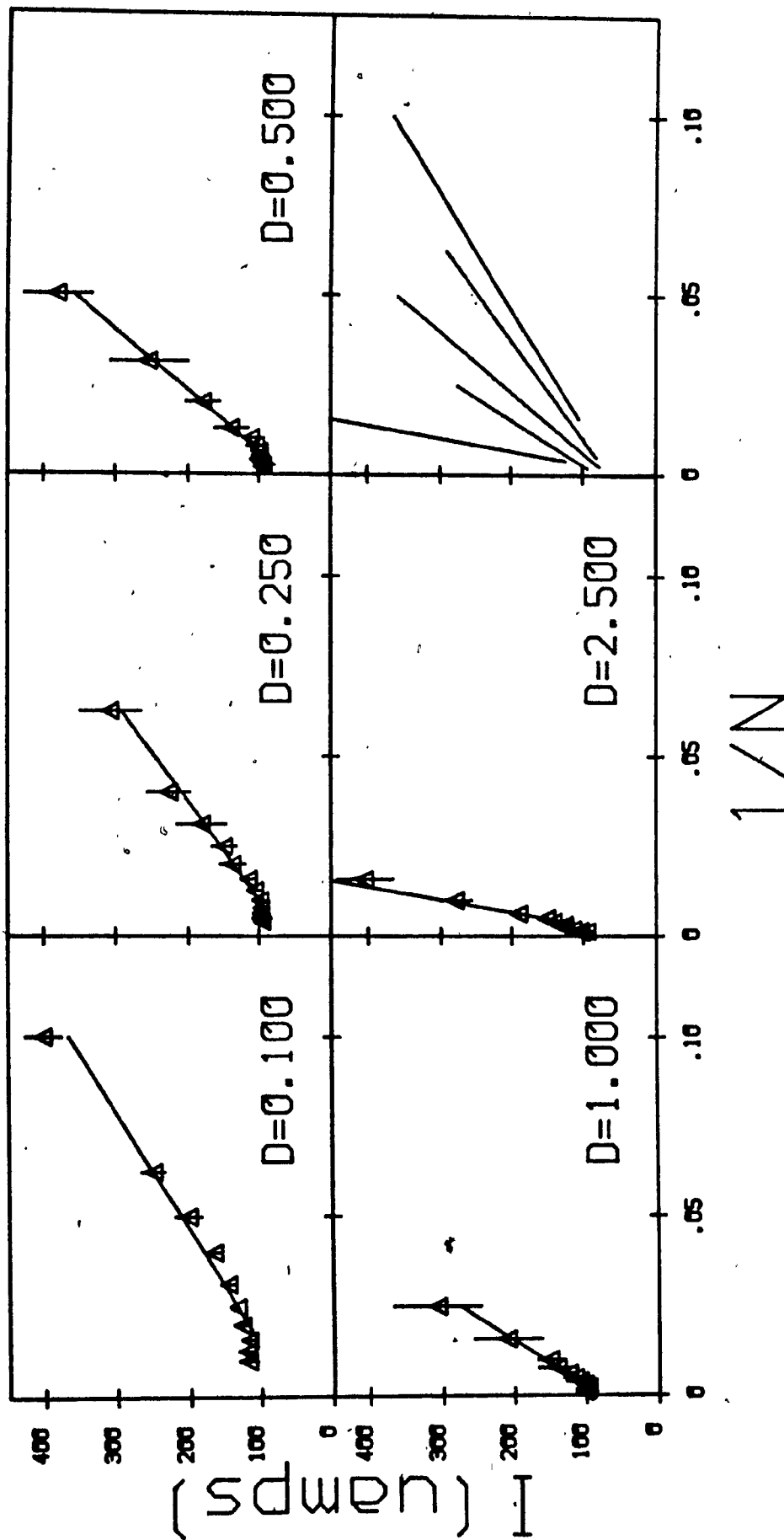


Figure 13b. The family of I versus $1/N$ trade-off functions obtained for a series of train durations for subject NBI. The train duration used for each trade-off function is indicated within each panel. The lower, right-hand panel presents the line segments for the various I/N versus I trade-off functions to highlight the changes in the slopes and the I_{min} values. The triangles represent required current determinations with the vertical line indicating the 95 percent confidence interval.

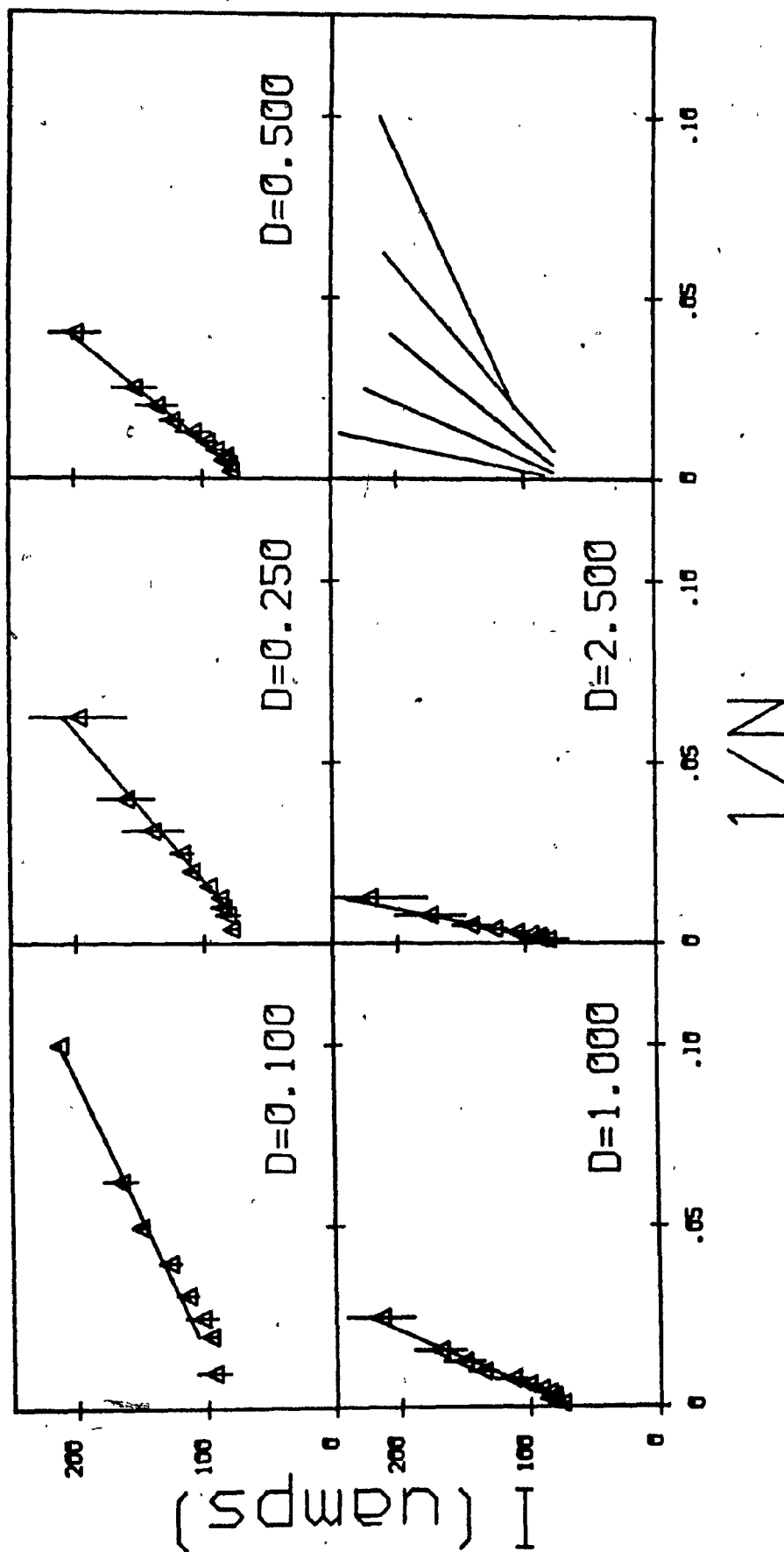


Figure 13c. The family of I versus $1/N$ trade-off functions obtained for a series of train durations for subject B1. The train duration used for each trade-off function is indicated within each panel. The lower, right-hand panel presents the line segments for the various $1/N$ versus I trade-off functions to highlight the changes in the slopes and the I_{min} values. The triangles represent required current determinations with the vertical line indicating the 95 percent confidence interval.

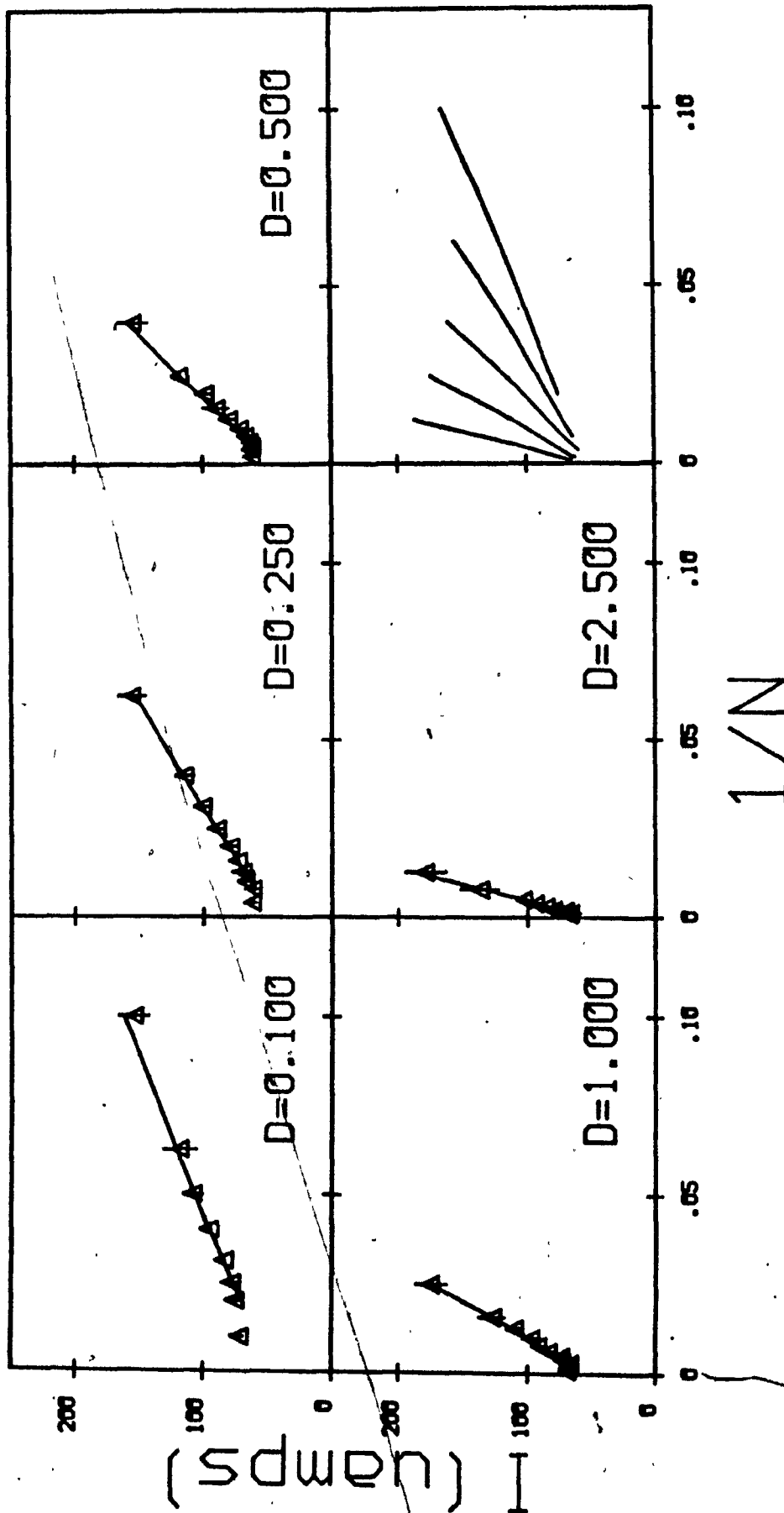


Figure 13d. The family of I versus $1/N$ trade-off functions obtained for a series of train durations for subject R2. The train duration used for each trade-off function is indicated within each panel. The lower, right-hand panel presents the line segments for the various $1/N$ versus I trade-off functions to highlight the changes in the slopes and the I_{\min} values. The triangles represent required current determinations with the vertical line indicating the 95 percent confidence interval.

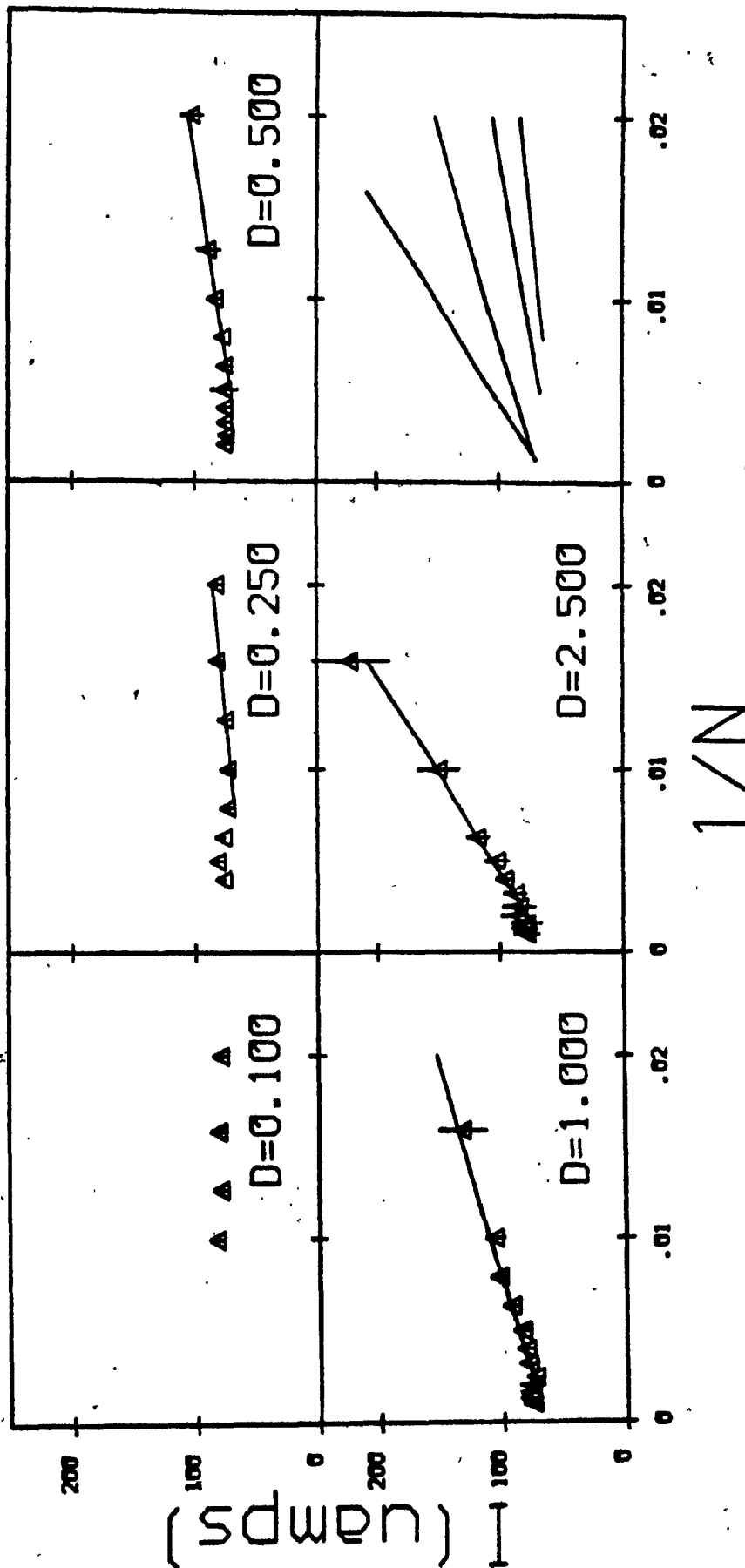


Figure 14a. Over the series of train durations tested for subject BL1, the data points and line segments are shown using the limited range of 0 to 0.025. The limited range was required to clearly show the data for high frequencies. The train duration used for each trade-off function is indicated within each panel. The absence of a line segment and/or data point means that the line was not defined and/or points were not collected over this range. The lower, right-hand panel, presents the line segments for the various 1/N versus 1 trade-off functions to highlight the changes in the slopes and the 1/N values. The triangles represent required current determinations with the vertical line indicating the 95 percent confidence interval.

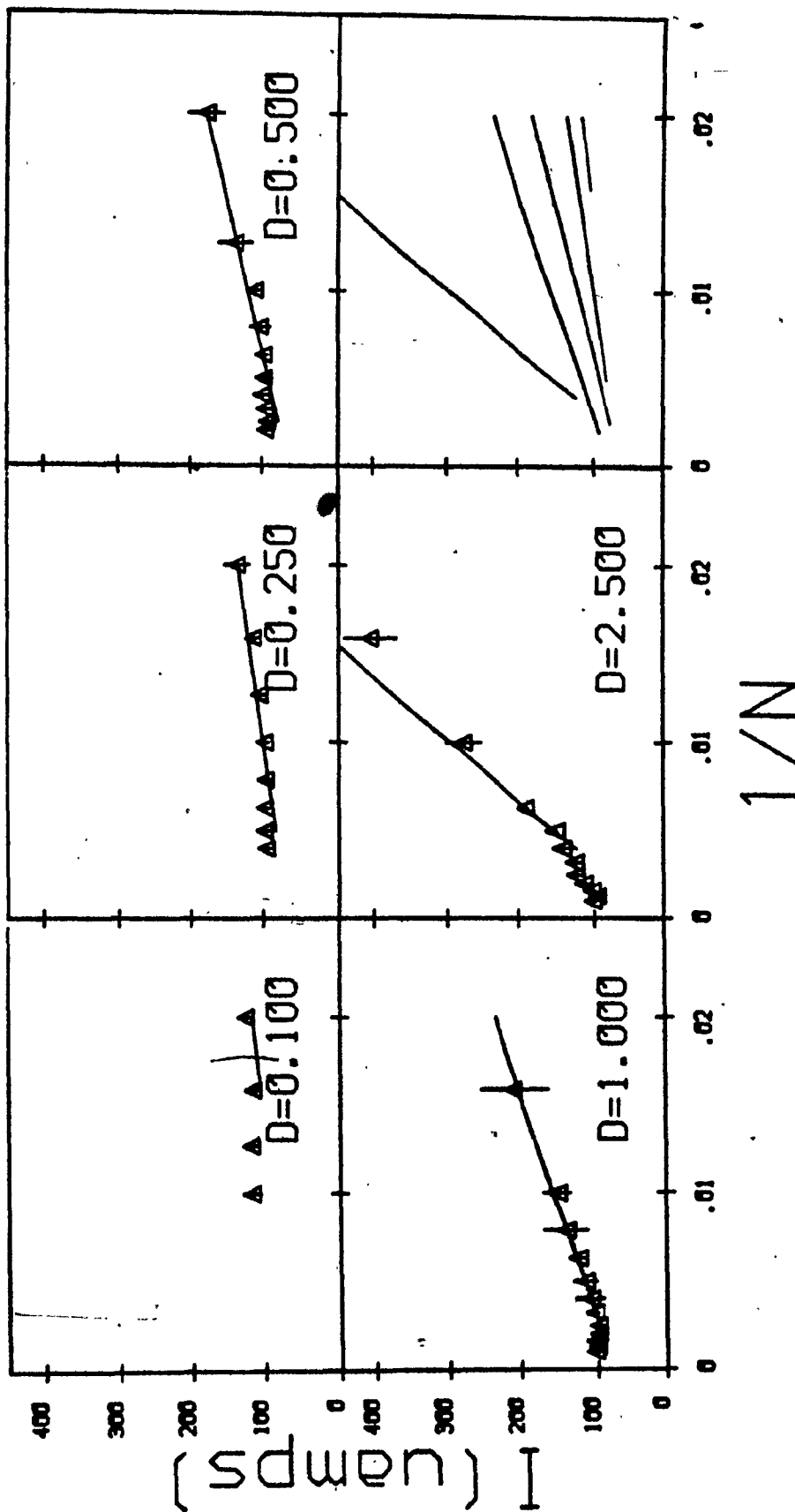


Figure 14b. Over the series of train durations tested for subject NBI, the data points and line segments are shown using the limited range of 0 to 0.025. The limited range was required to clearly show the data for high frequencies. The train duration used for each trade-off function is indicated within each panel. The absence of a line segment and/or data point means that the line was not defined and/or points were not collected over this range. The lower, right-hand panel presents the line segments for the various $1/N$ versus I trade-off functions to highlight the changes in the slopes and the I_{min} values. The triangles represent required current determinations with the vertical line indicating the 95 percent confidence interval.

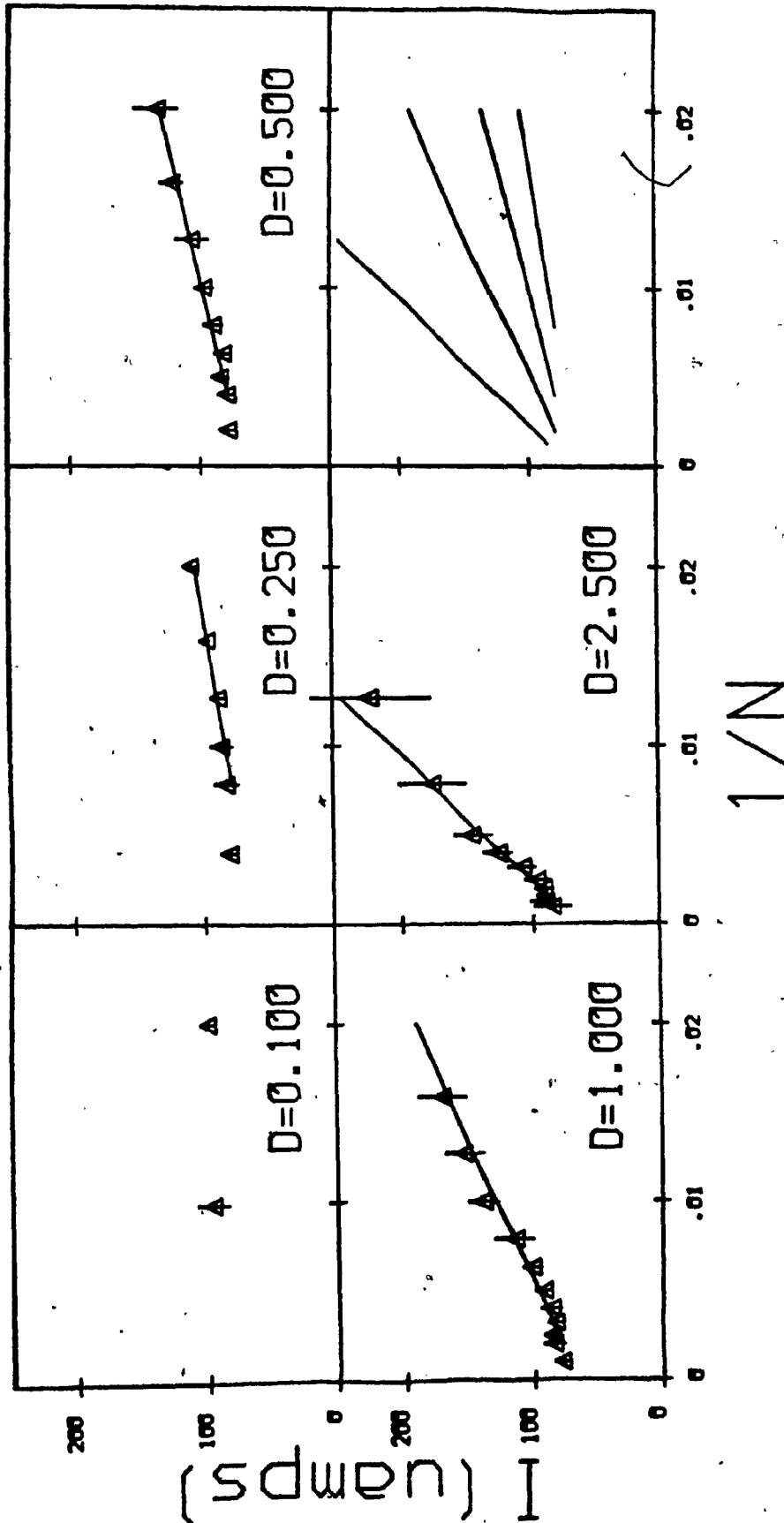


Figure 14c. Over the series of train durations tested for subject B1, the data points and line segments are shown using the limited range of 0 to 0.025. The limited range was required to clearly show the data for high frequencies. The train duration used for each trade-off function is indicated within each panel. The absence of a line segment and/or data point means that the line was not defined and/or points were not collected over this range. The lower, right-hand panel presents the line segments for the various $1/N$ versus I trade-off functions to highlight the changes in the slopes and the I min values. The triangles represent required current determinations with the vertical line indicating the 95 percent confidence interval.

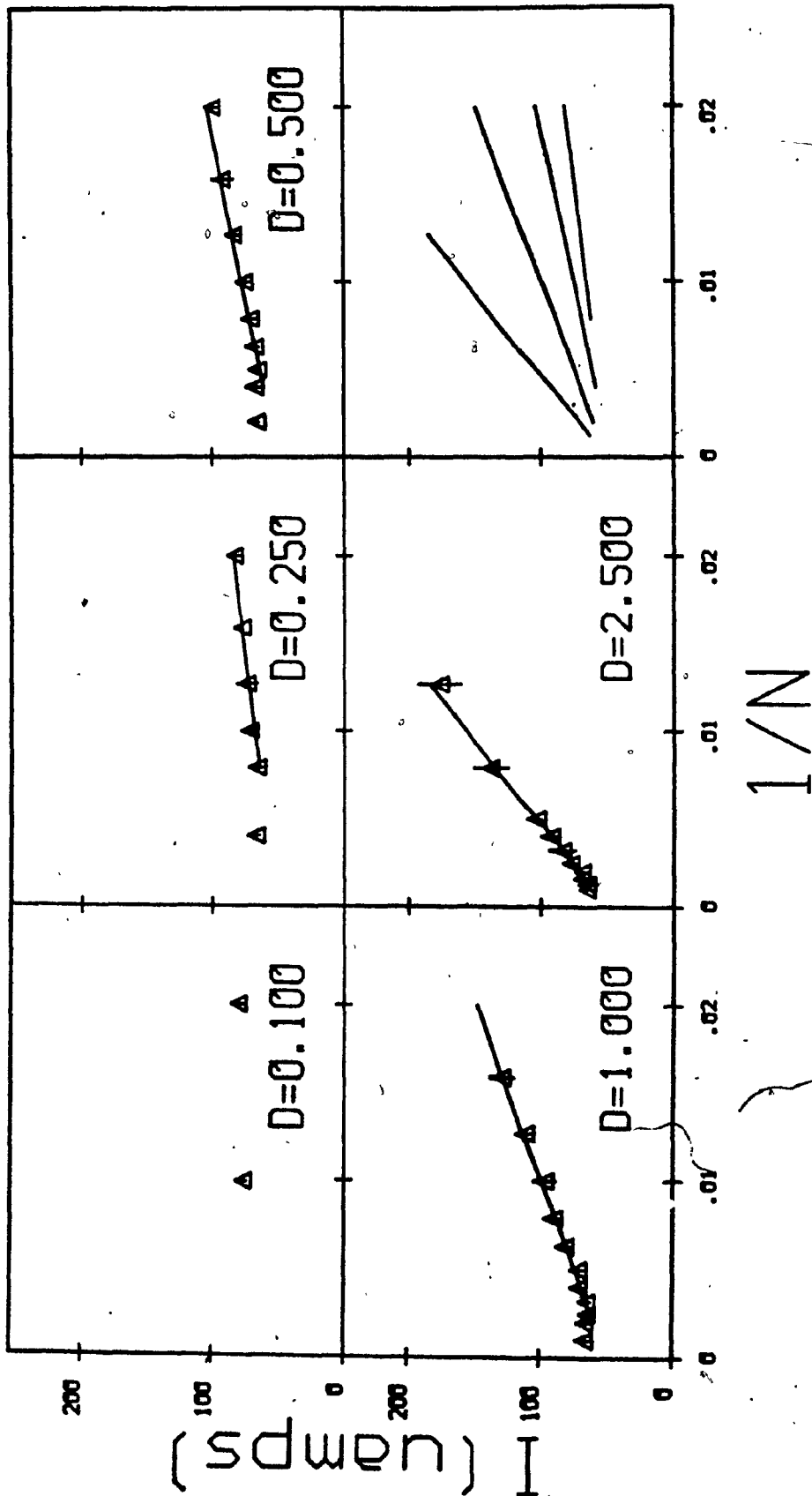


Figure 14d. Over the series of train durations tested for subject R2, the data points and line segments are shown using the limited range of 0 to 0.025. The limited range was required to clearly show the data for high frequencies. The train duration used for each trade-off function is indicated within each panel. The absence of a line segment and/or data point means that the line was not defined and/or points were not collected over this range. The lower, right-hand panel presents the line segments for the various $1/N$ versus 1 trade-off functions to highlight the changes in the slopes and the main values. The triangles represent required current determinations with the vertical line indicating the 95 percent confidence interval.

charge-duration experiments. First, it is predicted that there is a linear segment over the middle range of currents plus two non-linear segments at both extremities that are due to the low and high frequency roll-offs. Second, it is predicted that the roll-offs occur at consistently the same currents for all train durations for any one subject.

To test these predictions, a non-arbitrary, iterative analysis was performed on the data for each subject. Briefly, it started with three successive, "seed" currents and added additional currents when certain criteria, outlined below, were met. Also, the analysis was constructed to include the same range and number of currents across train durations. All possible combinations of three starting currents were analyzed.

It was hypothesized on the basis of the extended model that the analysis would encompass the largest number of points when the seed currents were intermediate in value. Further, it was hypothesized that when seeded with points from any part of the linear segment, the analysis would tend to converge on the same set of points. The analysis involved four steps which are detailed below.

Step 1 involved fitting a weighted regression line to seed values for each train duration. For the first iteration, three seed values were used. The seed values were the data points corresponding to successive currents that

had been used in all five train durations. A slope and a y-intercept for each train duration was established. Step 2 involved transforming all the $1/N$ values. This was done by first subtracting the corresponding y-intercept and then dividing by the corresponding slope, effectively collapsing the data across train durations. Step 3 involved fitting a single weighted regression line to the collapsed data points corresponding to the seed currents. Step 4 involved using the regression line to calculate the predicted values of $1/N$ for the next highest and the next lowest currents as well as the 95 percent confidence intervals surrounding the predicted values of $1/N$. A one-tailed, 95 percent confidence interval was placed around the predicted $1/N$ values since the extended model proposes that the roll-offs decrease the value of $1/N$. If the 95 percent confidence interval about the mean $1/N$ values observed for either or both of these currents overlapped with the 95 percent confidence interval about the corresponding predicted values, then the number of seed values was appropriately increased, and the analysis was reinitiated at Step 1.

This procedure was continued until all points had been tested or until both points tested in Step 4 fell outside the confidence interval.

When the iterative analysis terminated for a particular set of seed values, the five slopes for the untransformed trade-off functions corresponding to the five train

durations were used to calculate the charge-duration function. The charge-duration function is derived by calculating the regression line that relates the effective charge (Q') to train duration (D). As outlined in the introduction, Q' is equal to the pulse duration (d) divided by the slope of the $1/N$ versus I trade-off function. The slope of the charge-duration function is equal to the rheobase (R) of the strength-duration function for trains, while the y-intercept is equal to the product of the rheobase and the chronaxie (C) of the strength-duration function for trains. That is:

$$Q' = R \times D + R \times C \quad (25)$$

An estimate of the chronaxie was obtained by dividing the y-intercept of the charge-duration function by the slope.

Table 2 shows the chronaxie estimates and the number of data used in the iterative, linear regressions for the six subjects run in the required number variant of the charge-duration experiment. The first prediction was that the analysis would encompass the largest number of values when it originated in the middle. It may be seen that this prediction was satisfied only by subjects PC and 2G1. There does not appear to be any consistent pattern in the data analysis for the other four subjects. While the form of Table 2 makes this difficult to discern, there was some convergence for some animals.

Table 2

The chronaxies and the number of points used in the weighted least squares linear regression for all possible combinations of three successive, starting currents. The current listed in the table represents the middle value of the three starting currents. Chronaxie values are in seconds.

Rat no.	Current (microamperes)									
	110	140	180	200	225	280	400	560	795	1110
32	---	.10 (5)	---	.047 (4)	---	.047 (4)	.13 (5)	.43 (5)	.43 (5)	.45 (4)
PC	---	.15 (3)	---	.067 (3)	---	.26 (7)	.26 (7)	.30 (6)	.30 (6)	.30 (6)
2G1	---	.41 (4)	.14 (5)	---	.14 (5)	.07 (4)	---	---	---	---
2B2	.25 (3)	.10 (6)	.11 (5)	---	.11 (5)	.11 (5)	---	---	---	---
Y1	---	.28 (3)	---	.19 (4)	---	.29 (3)	.44 (4)	---	---	---
G2	---	---	---	.25 (3)	---	.38 (3)	.40 (4)	.15 (4)	.15 (4)	---

As the results in Table 2 show, the iterative analysis was not able to consistently identify a central, linear segment on the $1/N$ versus I trade-off functions. The results depended very strongly on the choice of seed values. Therefore, it was decided to include all the data points in the analysis for the required number variants of the strength-duration and charge-duration experiments. The consequences of using an arbitrary procedure would be very serious because the chronaxie values depend so strongly on the selection of points.

Since the current varies as a function of pulse duration, the analysis employed for the charge-duration data was not applied to the strength-duration data. At present, an analogous strategy is being developed for the strength-duration data.

The same rule could not be applied to the required current variants of the strength-duration and charge-duration experiments, because the influence of the high-frequency roll-off was predicted to be greatest over the range of values tested. For these experiments, an iterative analysis was performed which varied slightly from the procedure outlined above. Each analysis started from the three largest $1/N$ values and progressed towards the lowest. The regression lines were calculated separately for each duration. Therefore, each regression line tends to vary with

respect to the range of values included in each analysis.

III. Statistical analysis

The alpha level employed in these experiments was .05. However, since five ANOVAs were performed on each data set, the level of significance was set to .01.

Strength-duration experiments

Required number determinations Table 3 through Table 6 show the numerical results derived from the regression analysis for the seven subjects run in this variant of the strength-duration experiment.

In Table 3, a progressive decrease in the slope with decrements of pulse duration may be noted. An ANOVA was performed on the slopes for four pulse durations: 2.500, 0.500, 0.100, and 0.020 msec. These four pulse durations were used since all subjects except rat nos. 32 and G1 had been run at all these durations. Estimates for the two missing values were obtained using the procedure outlined by Kirk (1968, pg. 146). This procedure was followed for calculating all ANOVAs in the required number version of the strength-duration experiments. The result ($F=26$, $df=3,22$, $p<.001$) indicates that there is a significant main effect of pulse duration on the slope of the trade-off function.

The value of the y-intercept ($(1/N)_0$) shown in Table 3

Table 3

The slope and y-intercept $((1/N)_0)$ values derived from the required number strength-duration experiment. (All values are expressed as $10E-3$.)

	Rat no.						
	32	N1	G1	Y1	B2	2B2	2G1
Pulse duration (msec)							
Slope (units = (pulses x microamperes)-1)							
9.990	1.5	---	0.54	2.1	2.1	---	---
5.000	0.94	---	---	---	---	---	---
2.500	0.95	0.82	0.23	1.4	1.2	1.1	0.71
1.000	---	---	---	0.89	---	0.57	0.49
0.500	0.22	0.34	0.13	0.55	0.45	0.39	0.30
0.250	0.14	---	0.11	---	---	0.23	0.27
0.100	0.13	0.11	0.094	0.22	0.18	0.14	0.16
0.050	0.075	---	0.059	---	---	0.10	0.092
0.020	---	0.027	---	0.067	0.043	0.047	0.040
0.010	0.024	---	0.0053	---	---	---	---
Y-intercept (units = (pulses)-1)							
9.990	22	---	17	-25	-28	---	---
5.000	- 4.6	---	---	---	---	---	---
2.500	- 8.0	-12	6.4	- 9.3	-12	-4.3	7.3
1.000	---	---	---	-13	---	-1.2	-3.1
0.500	6.9	- 8.5	5.6	- 7.1	-10	4.6	4.3
0.250	6.2	---	6.1	---	---	9.1	-2.6
0.100	- 4.6	- 7.0	- 6.4	- 8.5	-10	3.9	-4.1
0.050	4.0	---	- 5.4	---	---	-3.2	-2.6
0.020	---	- 6.9	---	-13	- 6.6	1.5	-0.32
0.010	- 6.4	---	1.8	---	---	---	---

does not appear to change in any systematic manner with pulse duration. An ANOVA ($F=0.69$, $df=3,22$, $p>.20$) indicates that there is no main effect of pulse duration on the value of $(1/N)_o$.

One result of using the effective current rather than the total current is that the $1/N$ versus I trade-off function is linear rather than scalar. The model predicts that the y-intercept should be negative and non-zero. To test this assumption, a mean y-intercept value was calculated using the y-intercepts determined for each pulse duration for all seven subjects run in this experiment. A one-tailed, 95 percent confidence interval was then placed around the y-intercept. The mean value was $-2.9 \times 10E-3$ while the upper-limit of the confidence interval was $-0.55 \times 10E-3$. Since this value does not overlap zero, it would appear that the prediction of the model was supported.

Table 4 shows the average I_{min} values obtained during the required number version of the strength-duration experiment. In general, the value of I_{min} tends to decrease as pulse duration is increased. However, at the longest pulse duration (9.990 msec) there is a tendency for the value of I_{min} to increase. An ANOVA ($F=34$, $df=3,22$, $p<.001$) indicates that there is a significant main effect of pulse duration on I_{min} .

The x-intercept, I_o , values obtained are shown in Table

Table 4

The mean minimum current values (I_{min}) in microamperes derived from the required number strength-duration experiment.

Pulse duration (msec)	Rat no.						
	32	N1	G1	Y1	B2	2 B2	2 G1
9.990	37	---	62	38	45	---	---
5.000	33	---	---	---	---	---	---
2.500	28	36	46	22	28	21	26
1.000	---	---	---	26	---	26	32
0.500	41	55	64	33	38	30	27
0.250	51	---	88	---	---	39	41
0.100	81	150	140	78	91	62	62
0.050	12	---	250	---	---	100	97
0.020	---	500	---	26	280	210	180
0.010	680	---	1000	---	---	---	---

5. The tendency for I_o to decrease with increments of pulse duration may be noted. An ANOVA ($F=6.8$, $df=3,22$, $p<.005$) on the four pulse durations indicates a significant main effect of pulse duration on I_o .

Table 6 indicates the $1/N$ values ($(1/N)_c$) corresponding to I_{min} . The subscript, c , stands for the hypothetical "corner" which is formed by the intersection of the linear portion of the $1/N$ versus I trade-off function and a vertical line corresponding to I_{min} . There is a tendency for the $(1/N)_c$ value to decrease with decrements of pulse duration. An ANOVA yielded a significant main effect of pulse duration on $(1/N)_c$ ($F=36$, $df=3,22$, $p<.001$).

To summarize, a significant main effect of pulse duration on four of the five measures derived from the $1/N$ versus I trade-off function was observed. These measures were a) the slope of the trade-off function, b) I_{min} , c) I_o , and d) $(1/N)_c$. There was no significant main effect of pulse duration on $(1/N)_o$, the y-intercept. The four significant effects are predicted by the extended model. The extended model predicts that $(1/N)_o$ should only vary if there were multiple firings or if the substrate were composed of multiple sub-populations.

Required current determinations Table 7 shows the numerical results for the two subjects run in this variant of the strength-duration experiment.

Table 5

The x-intercept (I_0) in microamperes derived from the required number strength-duration experiment.

	Rat no.						
	32	N1	G1	Y1	B2	2B2	2G1
Pulse duration (msec)							
9.990	-14	---	-31	12	14	---	---
5.000	4.9	---	---	---	---	---	---
2.500	8.4	13	-28	6.9	10	3.9	-10
1.000	---	---	---	15	---	- 2.1	6.2
0.500	-31	25	-42	13	22	-12	-14
0.250	-45	---	-57	---	---	-39	9.6
0.100	35	62	68	39	57	-28	26
0.050	-53	---	92	---	---	31	28
0.020	---	260	---	190	150	-33	8.1
0.010	270	---	-350	---	---	---	---

Table 6

The $1/N$ values $((1/N)c)$ corresponding to I_{min} in the required number strength-duration experiment. (All values are expressed as $10E-3$ with units of (pulses)-1.)

Pulse duration (msec)	Rat no.						
	32	N1	G1	Y1	B2	2B2	2G1
9.990	.78	---	50.	55	63	---	---
5.000	27	---	---	---	---	---	---
2.500	19	19	17	21	22	19	26
1.000	---	---	---	9.6	---	14	13
0.500	16	10	14	11	7.4	16	13
0.250	13	---	16	---	---	18	8.5
0.100	6.2	9.5	6.3	8.4	6.1	13	5.5
0.050	13	---	9.3	---	---	7.1	6.4
0.020	---	6.2	---	4.3	5.6	11	7.0
0.010	9.6	---	7.3	---	---	---	---

Table 7

Data derived from the required current strength-duration experiment for rat nos. NB1 and BL1. (The units for the slope are pulses x microamperes.)

Rat no. NB1

Pulse duration (msec)	Slope	Y-intercept (uamps)	(1/N)c (x 10E-3) ((pulses)-1)	Imin (uamps)	X-intercept (x 10E-3) ((pulses)-1)
5.000	1500	5	27	46	- 3.5
2.500	1700	17	11	35	-10
1.000	2300	25	7.1	41	-11
0.500	3800	25	5.3	45	- 6.7
0.250	5900	24	6.2	60	- 4.1
0.100	6800	66	3.0	86	- 9.8

Rat no. BL1

Pulse duration (msec)	Slope	Y-intercept (uamps)	(1/N)c (x 10E-3) ((pulses)-1)	Imin (uamps)	X-intercept (x 10E-3) ((pulses)-1)
5.000	1500	3	27	44	- 2.3
2.500	1300	17	14	35	-14
1.000	1500	30	7.9	42	-20
0.500	2300	36	5.6	49	-15
0.250	2500	51	3.0	58	-20
0.100	4000	70	3.7	85	-18

At the time of the experiment, it was believed that, by increasing the train duration from 0.500 sec to 1.000 sec, better estimates of I_{min} would be obtained. Since then, it has been realized that this is an erroneous interpretation of the model. To understand how these results compare to those obtained from the required number version of the strength-duration experiment, it is necessary to understand how they were obtained. It may be recalled that Equation 17 expresses the reciprocal of the required number of pulses ($1/N$) as a function of the current (I) with train duration constant. That is,

$$\begin{aligned} 1/N(d,D,I) &= 1/N_f \times k / k(d) \times I \\ &- 1/N_f \times k / k(d) \times I_o(d). \end{aligned} \quad (17)$$

When this equation is solved for I , one obtains

$$I = 1 / (1/N_f \times k / k(d)) \times 1/N + I_o(d). \quad (26)$$

Equation 26 represents the situation where the required current is obtained as the number of pulses is varied. The slopes of the two functions contain the same terms except that the slope of the required current function is the reciprocal of the slope of the required number function. In the required number experiment, it was hypothesized that the slope of the trade-off function would increase with increments of pulse duration. Since the slope of the

required current function is the reciprocal of the slope of the required number function, its slope should decrease with increments of pulse duration. The y-intercept of the required current function is simply I_0 while the x-intercept is $(1/N)_0$.

Due to the fact that only two subjects were run in this experiment no statistical analysis of the results was performed. In studying the results in Table 7, it may be seen that the slope decreases with increments of pulse duration. This is consistent with the results from the required number experiment. There is a tendency for I_0 to decrease with increments of pulse duration which is also similar to the pattern noted above for the required number experiment. As in the required number determinations, the average minimum current (I_{min}) may be seen to decrease with increments of pulse duration except at the longest pulse duration. The current at the longest pulse duration tends to be greater than the current at the next two shorter pulse durations. The value of $(1/N)_0$ (the y-intercept for the required number experiments) does not show any particular tendency to vary with changes in pulse duration. This is also similar to the result noted in the required number experiment. However, the pattern previously noted for $(1/N)_c$ is not as clearly seen in Table 7 as in Table 6. That is, the data from subject no. BL1 tend to show this pattern while the data from subject no. NB1 do not.

To summarize, the results of the required current determinations tend to correspond, for the most part, to the results obtained from the required number determinations.

A non-linear curve fitting program was used to calculate two strength-duration curves for the pulse duration data, one based on the slope of the $1/N$ versus I trade-off function, and the other based on I_{min} (Cuthbert and Wood, 1980; Tee, Note 5). The hyperbolic and exponential functions fit to the data were, respectively:

$$\log(\text{slope}) \text{ or } \log(I_{min}) = \log(r(1 + c/d)) \quad (27)$$

$$\text{and } \log(\text{slope}) \text{ or } \log(I_{min}) = \log(r/(1 - \exp(-d/\tau))) \quad (28),$$

where r is the rheobase of the strength-duration curve,
and c is the chronaxie of the strength-duration curve.

The program was designed to find values of r and c in Equation 27 or r and τ in Equation 28 that provide the minimum residual sum of squares. As outlined in the introduction, the chronaxie (c) of the exponential function is 0.693τ . The logarithm was used to equate the standard errors of the slope or I_{min} across pulse duration.

The rheobase and chronaxie estimates derived from the hyperbolic and exponential functions for the I_{min} values are

shown in Table 8. The Chi² estimate provides a measure of how well a given function fits the data. It may be seen that the hyperbola provides a better fit to the data for five out of the nine subjects run in the strength-duration experiment when I_{min} is used. The rheobase and chronaxie estimates derived from the hyperbolic and exponential functions for the slope of the trade-off functions are shown in Table 9. In using the slope to estimate the chronaxies and rheobases, the hyperbola provides a better fit to the data than the exponential for all subjects.

Using the chronaxie estimates derived from the hyperbolic function, estimates based on I_{min} were found to be significantly less than estimates based on the slope ($t=5.1$, $df=8$, $p<.0005$). However in comparing the results in Table 8 to those in Table 9, it may be seen that regardless the function being fit to the data, the curves based on I_{min} have lower chronaxies than those based on the slope of the trade-off functions.

These results are shown graphically for two subjects in Figures 15 and 16. Each figure shows the hyperbolic functions based on I_{min} and the slope. The curves in each figure are forced to have a rheobase of 1.0 by dividing each value by the corresponding rheobasic current. A difference in chronaxie is shown as a disparity between the curves. In both figures, it may be seen that the strength-duration curve based on I_{min} has a shorter chronaxie than the one

Table 8

Comparison of the rheobase (r) and the chronaxie (c) estimates for the strength-duration function for I_{min} when using a hyperbola or an exponential function to determine the line of best fit. The smaller the Chi sq., the better the fit.

Hyperbola

Subject no.	r (uamps)	c (usec)	Chi sq.
32	31	150	0.34
N1	33	300	0.015
G1	50	190	0.075
Y1	26	180	0.22
B2	33	150	0.15
2B2	21	180	0.013
2G1	26	130	0.053
NB1	38	130	0.052
BL1	38	130	0.034

Exponential

Subject no.	r (uamps)	c (usec)	Chi sq.
32	35	100	0.34
N1	40	190	0.062
G1	56	130	0.073
Y1	28	130	0.19
B2	36	120	0.14
2B2	25	120	0.089
2G1	30	90	0.095
NB1	41	120	0.059
BL1	42	110	0.059

Table 9

Comparison of the rheobase (r) and the chronaxie (c) estimates for the strength-duration function for the slope of the trade-off functions when using a hyperbola or an exponential function to determine the line of best fit. The smaller the Chi sq., the better the fit. (The units for the rheobase (r) are pulses x microamperes.)

Hyperbola

Subject no.	r	c (usec)	Chi sq.
32	850	890	1.4
N1	990	790	0.033
G1	2700	460	0.95
Y1	570	670	0.27
B2	530	1000	0.17
2B2	1000	510	0.37
2G1	1500	330	0.12
NB1	1500	510	0.22
BL1	1300	210	0.075

Exponential

Subject no.	r	c (usec)	Chi sq.
32	960	610	1.7
N1	1300	450	0.069
G1	3200	290	1.2
Y1	670	440	0.51
B2	630	640	0.31
2B2	1300	320	0.55
2G1	1900	200	0.26
NB1	1700	370	0.33
BL1	1500	170	0.14

based on the slope.

Charge-duration experiments

Required number determinations Table 10 shows the slopes and the y-intercepts ($(1/N)_0$) corresponding to the various train durations used for the six subjects run in this experiment. It can be clearly seen that the slope decreases as train duration is increased. An ANOVA indicated that there was a significant main effect of train duration on the slope of the $1/N$ versus I trade-off function ($F=15$, $df=4,25$, $p<.001$). Contrary to the prediction of the model, the ANOVA indicated that there was no significant main effect of train duration on $(1/N)_0$ ($F=0.43$, $df=4,25$, $p>.20$).

The average minimum current (I_{min}) values are shown in Table 11. It may be noted that the currents corresponding to the train durations between 0.250 and 2.500 sec tend to cluster around one value whereas the current corresponding to 0.100 sec tend to be higher. However, the minimum current corresponding to a train duration of 2.500 sec was not obtained using the same frequency as had been used for the four other train durations. This was because the maximum number of pulses that the equipment could produce was 999. This corresponded to a frequency of 400 Hertz whereas the maximum frequency used for the other train durations was 500 Hertz. In order to more accurately investigate the relationship between frequency and current, the currents corresponding to the highest frequency run at all train

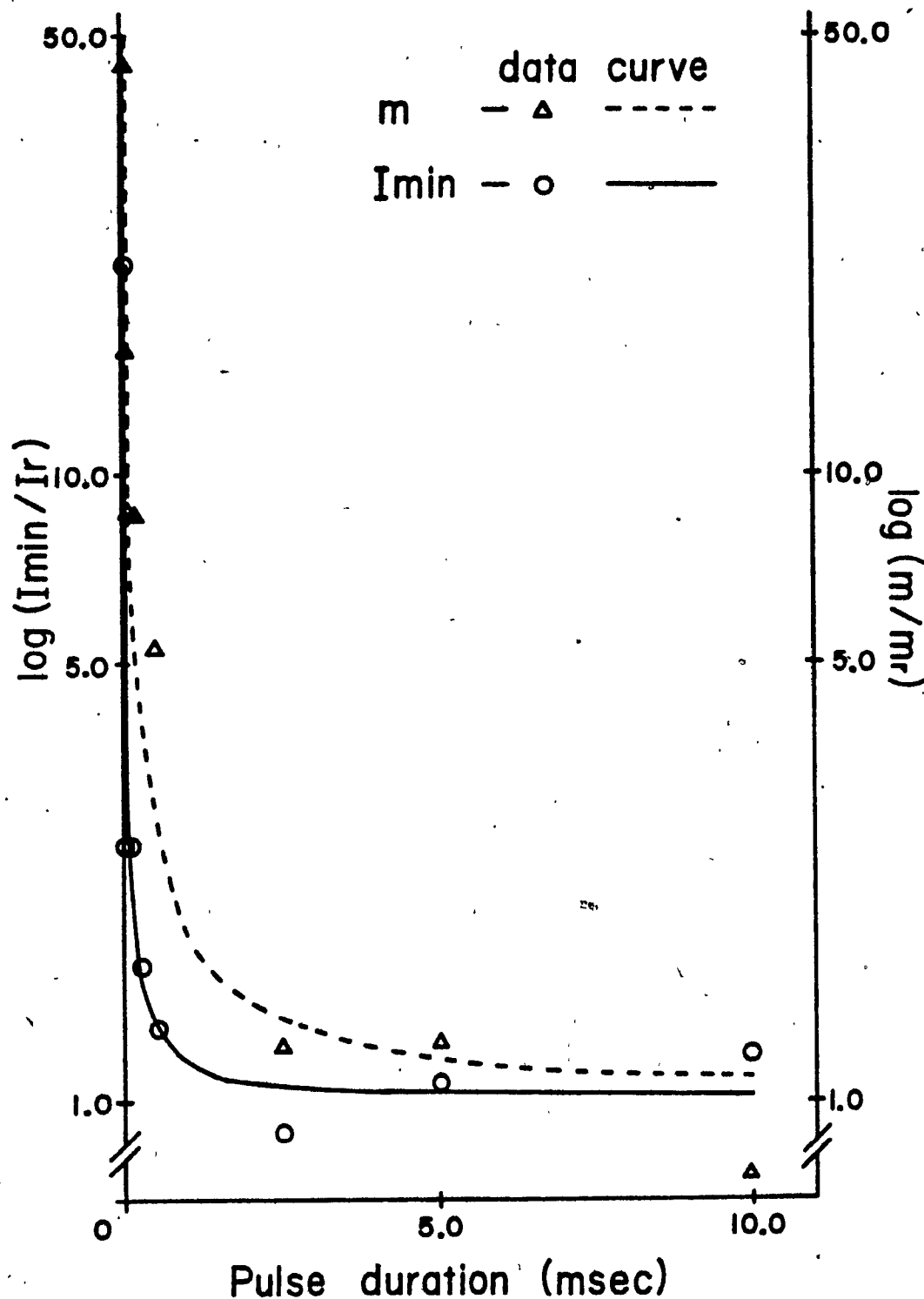


Figure 15. Hyperbolic functions based on I_{min} and the slope (m) of the $1/N$ versus I trade-off function for subject no. 32, selected at random from the required number variant of the strength-duration experiment. By dividing each value by the corresponding rheobasic current, both curves are forced to have a rheobase of 1.0. A difference in chronaxie is shown as a disparity between the curves. The strength-duration curve based on I_{min} may be seen to have a shorter chronaxie than the one based on the slope.

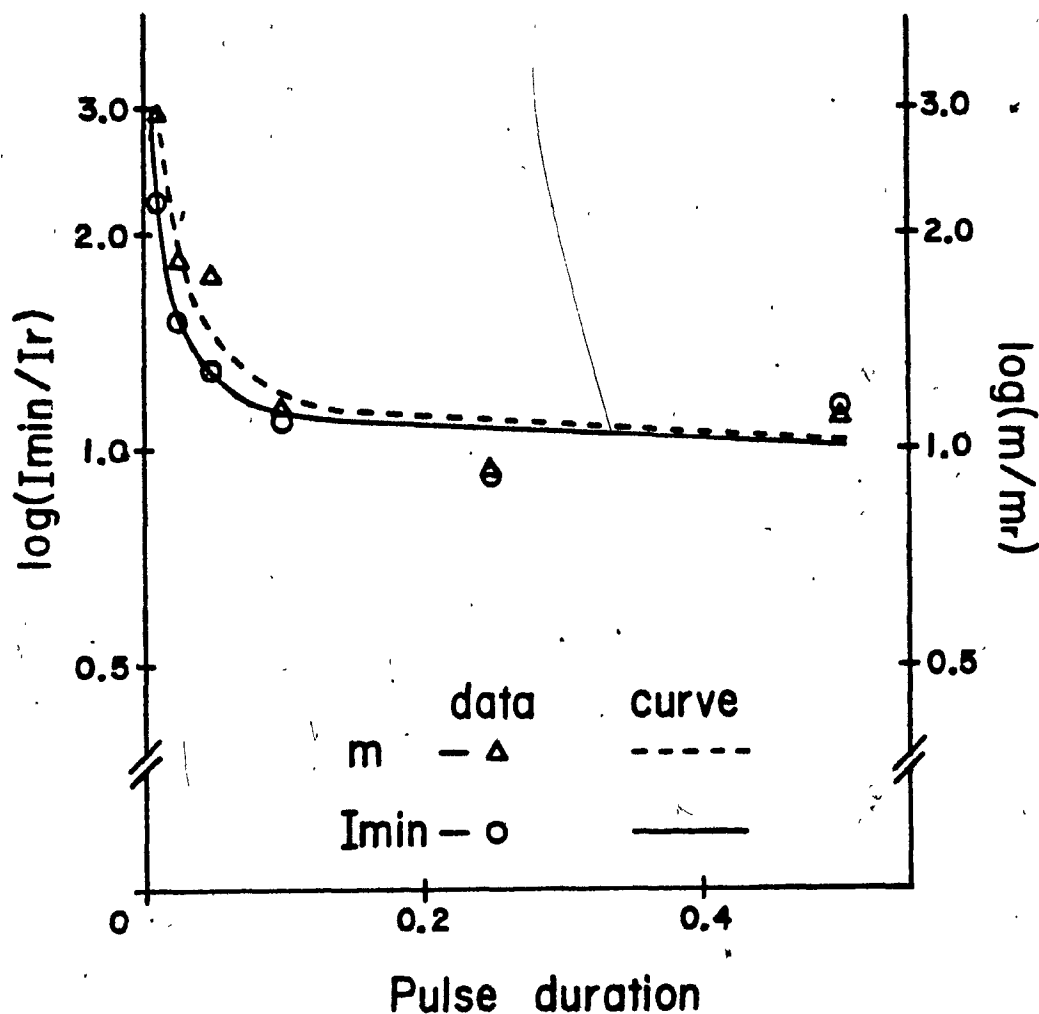


Figure 16. Hyperbolic functions based on I_{\min} and the slope (m) of the $1/N$ versus I trade-off function for subject no. BL1, selected at random from the required current variant of the strength-duration experiment. By dividing each value by the corresponding rheobasic current, both curves are forced to have a rheobase of 1.0. A difference in chronaxie is shown as a disparity between the curves. The strength-duration curve based on I_{\min} may be seen to have a shorter chronaxie than the one based on the slope.

Table 10

The slope and y-intercept $((1/N)o)$ values derived from the required number charge-duration experiment. (All values are expressed as $10E-3$.)

Train duration (sec)	Rat no.					
	32	PC	G2	Y1	2B2	2G1
Slope (units = (pulses x microamperes) ⁻¹)						
0.100	0.25	0.17	0.18	0.50	0.39	0.32
0.250	0.21	0.10	0.12	0.26	0.23	0.19
0.500	0.12	0.069	0.083	0.19	0.14	0.13
1.000	0.068	0.044	0.044	0.094	0.084	0.076
2.500	0.031	0.019	0.022	0.050	0.035	0.036
Y-intercept (units = (pulses) ⁻¹)						
0.100	10	17	39	-28	2.2	-2.5
0.250	0.19	18	18	1.9	6.2	2.0
0.500	4.9	9.4	14	-5.1	5.1	-0.59
1.000	0.53	4.4	7.8	-1.4	2.6	0.31
2.500	0.21	1.0	2.2	-2.8	1.3	-0.40

durations were determined (see Table 12). As in Table 11, the same pattern is manifested when frequency is held constant. That is, the I_{min} values corresponding to train durations between 0.250 and 2.500 sec tend to cluster around the same current while the currents for a 0.100 sec train tend to be higher.

All subjects run in the charge-duration experiments except two were used in this analysis. The two subjects were excluded since the maximum frequency used did not correspond to that used by the other subjects. The results from the two variants of the procedure could be combined because I_{min} was determined in the same way in both variants. First, the I_{min} values from each session for each subject were converted to z-scores. An ANOVA ($F=6.6$, $df=4,155$, $p<.001$) indicated that there was a significant main effect of train duration on the value of I_{min} .

The x-intercept (I_0) values obtained are shown in Table 13. There does not appear to be any discernable variation in the data as a function of train duration, an impression that was confirmed by an ANOVA: The main effect of train duration on I_0 was not significant ($F=0.21$, $df=4,25$, $p>.20$). The extended model predicts that the x-intercept should be positive and non-zero. To test this assumption, the mean x-intercept for all train durations for the six subjects run in this experiment was calculated. This yielded a value of -50 uamps. Hence, this prediction of the model was not

Table 11

The mean minimum current values (I_{min}) in microamperes derived from the required number charge-duration experiment.

Train duration (sec)	Rat no.					
	32	PC	G2	Y1	2B2	2G1
0.100	95	140	120	110	79	98
0.250	88	92	110	95	68	70
0.500	90	90	98	95	65	69
1.000	85	87	110	98	67	66
2.500	90	88	120	100	70	74

Table 12

The mean current values in microamperes derived from the required number charge-duration experiment corresponding to the highest frequency (400 hertz) run at all train durations.

Train duration (sec)	Rat no.					
	32	PC	G2	Y1	2B2	2G1
0.100	100	150	130	120	81	100
0.250	88	95	110	100	70	70
0.500	90	95	110	95	70	70
1.000	90	95	110	100	69	66
2.500	90	88	120	100	70	74

supported.

Table 14 indicates the $1/N$ values $((1/N)c$) corresponding to I_{min} . Clearly, $(1/N)c$ decreases with increments of train duration. The results of an ANOVA ($F=28$, $df=4,25$, $p<.001$) indicate that there was a significant main effect of train duration on $1/N$.

To summarize, statistical analysis indicated that there was a significant main effect of train duration on the slope of the trade-off function, I_{min} and $(1/N)c$. There was no significant main effect of train duration on the y-intercept $((1/N)o)$ or on the x-intercept (I_o) . The extended model predicts the three significant effects and the finding that there is no effect of train duration on I_o . However, the finding that there is no effect of train duration on $(1/N)o$ is not predicted by the extended model.

Required current determinations The numerical results for the four subjects run in this version of the charge-duration experiment are indicated in Tables 15 through 19.

Table 15 indicates the slopes and the y-intercepts (I_o) obtained. A progressive increase in the slope with increments of train duration may be noted. An ANOVA indicated that there was a significant main effect of train duration on the slope of the I versus $1/N$ trade-off functions ($F=7.9$, $df=4,15$, $p<.005$). No discernable pattern

Table 13

The x-intercept (I_0) in microamperes derived from the required number charge-duration experiment.

Train/ duration (sec)	Rat no.					
	32	PC	G2	Y1	2B2	2G1
0.100	-40	-100	-220	55	- 5.5	7.7
0.250	- 0.89	-180	-150	-7.4	-27	-10
0.500	-41	-140	-170	27	-37	4.6
1.000	- 7.7	-100	-180	15	-31	- 4.1
2.500	- 6.8	- 52	-100	55	-38	-11

Table 14

The $(1/N)c$ values corresponding to I_{min} from the required number charge-duration experiment. (All values are expressed as $10E-3$ with units of (pulses) $^{-1}$.)

	Rat no.					
	32	PC	G2	Y1	2B2	2G1
Train duration (sec)						
0.100	34	41	61	29	33	29
0.250	19	27	30	26	21	15
0.500	16	16	22	13	14	8.1
1.000	6.3	8.2	13	7.8	8.1	5.3
2.500	3.0	2.7	4.9	2.4	3.8	2.3

was noted for the y-intercept. An ANOVA indicated that there was no significant main effect of train duration on I_o ($F=0.68$, $df=4,15$, $p>.20$).

The extended model predicts that the y-intercept, I_o , should be significantly greater than zero. To test this assumption, a mean y-intercept was calculated and a one-tailed, 95 percent confidence interval was placed around it. The mean value was 56 uampers while the lower-limit of the confidence interval was 50. This result supports the prediction of the model.

The minimum current (I_{min}) values are shown in Table 16. The currents corresponding to the highest frequency (400 hertz) run at all train durations are shown in Table 17.

The statistical analysis for I_{min} has been discussed in the required number variant of the charge-duration experiment.

The x-intercept ($(1/N)_o$) are shown in Table 18. It may be noted that there is a tendency for the value of $(1/N)_o$ to increase with increments of train duration. An ANOVA ($F=6.2$, $df=4,15$, $p<.005$) shows that there was a significant main effect of train duration on $(1/N)_o$.

Table 19 indicates the $1/N$ values ($(1/N)_c$) corresponding to I_{min} . It may be noted that there is a

Table 15

The slope value and the y-intercept (I_0) in microamperes derived from the required current charge-duration experiment.

Slope (units = pulses x microamperes)

Train duration (sec)	Rat no.			
	R2	B1	BL1	NB1
0.100	1100	1300	1300	3100
0.250	1700	2400	1600	3600
0.500	2800	3500	2500	5900
1.000	4900	6300	4400	7900
2.500	11000	14000	9400	28000

Y-intercept (units = microamperes)

Train duration (sec)	Rat no.			
	R2	B1	BL1	NB1
0.100	51	81	27	55
0.250	49	58	53	64
0.500	47	64	56	63
1.000	51	65	66	78
2.500	49	66	59	11

Table 16

The mean minimum current values (I_{min}) in microamperes derived from the required current charge-duration experiment.

	Rat no.			
	R2	B1	BL1	NB1
Train duration (sec)				
0.100	74	96	78	120
0.250	64	79	72	95
0.500	63	78	72	93
1.000	65	77	76	98
2.500	65	84	79	95

Table 17

The mean current values (I) in microamperes derived from the required current charge-duration experiment corresponding to the highest frequency (400 hertz) run at all train durations.

	Rat no.			
	R2	B1	BL1	NB1
Train duration (sec)				
0.100	80	110	80	130
0.250	69	85	72	98
0.500	63	84	74	98
1.000	65	86	76	98
2.500	65	84	79	110

Table 18

The x-intercept $((1/N)_0)$ values derived from the required current charge-duration experiment. (All values are expressed as $10E-3$ with units of (pulses) $^{-1}$.)

Train duration (sec)	Rat no.			
	R2	B1	BL1	NB1
0.100	-45	-61	-20	-18
0.250	-29	-24	-34	-18
0.500	-17	-18	-22	-11
1.000	-10	-10	-15	- 9.9
2.500	- 4.6	- 4.8	- 6.3	- 0.38

tendency for the value of $(1/N)c$ to decrease with increments of train duration. An ANOVA shows that there was a significant main effect of train duration on the value of $(1/N)c$ ($F=11$, $df=4,15$, $p<.001$).

To summarize, a significant main effect of train duration was found on a) the slope of the I versus $1/N$ trade-off function, b) the x-intercept $((1/N)_0)$, and c) $(1/N)c$. No significant main effect of train duration on the y-intercept (I_0) was found. All of these findings are predicted by the extended model.

Using Equation 24, the required charge was calculated for each train duration. The charge-duration function was derived by determining the least-squares linear regression of the required charge on the train duration:

$$Q' = m \times D + b. \quad (29)$$

Gallistel (1978) described the charge-duration function in terms of the parameters of the underlying strength-duration function. In this case, the strength-duration function is defined for trains instead of for pulses.

According to Gallistel (1978), the slope is equal to the rheobase (R) of the charge-duration function while the y-intercept is equal to the product of the rheobase (R) and the chronaxie (C). Therefore, the chronaxie of the charge-

Table 19

The $1/N$ values ($(1/N)c$) corresponding to I_{min} derived from the required current charge-duration experiment. (All values are expressed as $10E-3$ with units of (pulses)-1.)

Train duration (sec)	Rat no.			
	R2	B1	BL1	NB1
0.100	21	11	39	20
0.250	9.0	8.6	12	8.7
0.500	5.7	4.0	6.4	5.2
1.000	3.0	1.9	2.1	2.6
2.500	1.5	1.2	2.1	3.0

duration function may be determined by dividing the y-intercept by the slope. Table 20 shows the values determined using the procedure described above. In addition, chronaxie and rheobase estimates were calculated for the present data using the procedure outlined by Gallistel (1978).

Figures 17a and 17b represent the charge-duration curves based on the effective current for two subjects selected at random: one from the required number variant and the other from the required current variant.

A t-test was performed to determine whether the procedure outline by Shizgal (Note 3) using the corrected current and the procedure outlined by Gallistel (1978) using the total current (Q) yielded different estimates of the chronaxies for the charge-duration functions. The difference between the mean chronaxie estimates was not statistically different at the .05 level ($t=1.0$, $df=18$, $p>.10$). A t-test was also performed comparing the mean chronaxie estimates from this experiment to those obtained by Gallistel (1978). It was found that the mean chronaxie of 0.45 seconds, obtained by Gallistel (1978), was significantly greater than the mean chronaxie of 0.21 seconds obtained in the present experiment ($t=5.9$, $df=20$, $p<.001$).

IV. Histology

The location of the electrode tips (Figure 18) was

Table 20

Comparison of charge-duration functions using the effective current (Shizgal, Note 3) and using the total current (Gallistel, 1978). The slope (m), y-intercept (b), and the correlation coefficient (r) for the two charge-duration functions for each subject are indicated. The estimates of the rheobase (R) in microcoulombs and of the chronaxie (C) in seconds are also shown.

$$Q' = m \times D + b$$

Subject no.	m	b	r	R	C
Y1	0.74	0.20	0.99	0.74	0.27
G2	1.6	0.46	1.0	1.6	0.29
PC	1.9	0.47	1.0	1.9	0.25
32	1.2	0.25	1.0	1.2	0.21
2G1	1.0	0.26	1.0	1.0	0.26
2B2	1.1	0.16	1.0	1.1	0.15
NB1	1.1	0.05	0.98	1.1	0.05
BL1	0.34	0.09	1.0	0.34	0.25
R2	0.40	0.08	1.0	0.40	0.19
B1	0.52	0.10	1.0	0.52	0.19

$$Q = m \times D + b$$

Subject no.	m	b	r	R	C
Y1	1.0	0.11	1.0	1.0	0.11
G2	1.2	0.18	1.0	1.2	0.16
PC	1.4	0.22	1.0	1.4	0.16
32	1.0	0.18	1.0	1.0	0.18
2G1	0.90	0.21	1.0	0.90	0.23
2B2	0.76	0.14	1.0	0.76	0.18
NB1	1.8	0.94	0.93	1.8	0.54
BL1	1.3	0.67	0.91	1.3	0.46
R2	1.2	0.37	0.98	1.2	0.30
B1	1.6	0.45	0.99	1.6	0.28

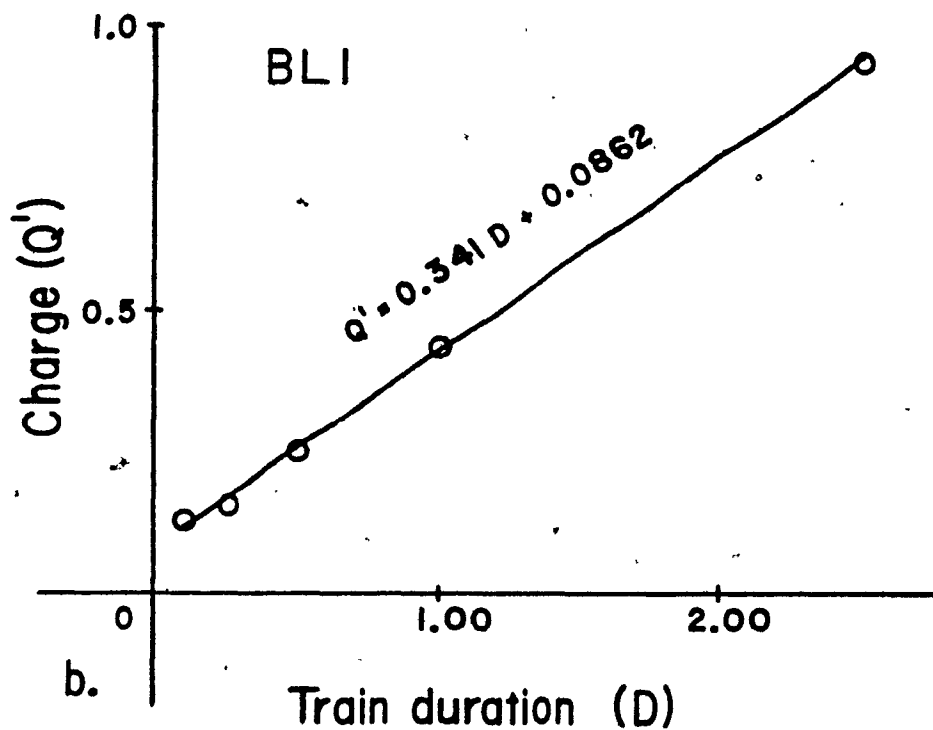
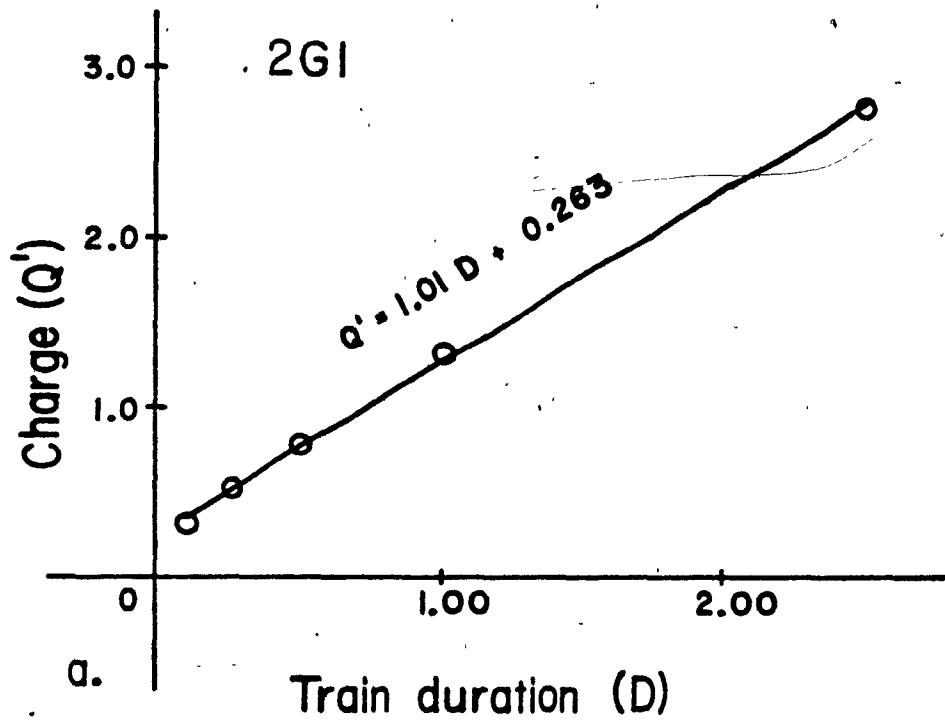


Figure 17. Charge-duration curves for two subjects selected at random. The upper panel (a) shows the curve for subject no. 2G1 from the required number variant, while the lower panel (b) shows the curve for subject no. BL1 from the required current variant of the experiment. The charge-duration function is indicated above each curve.

verified with reference to the Pellegrino, Pellegrino, and Cushman (1970) stereotaxic atlas. All the electrode tips appeared to lie in the general region of the LH, between 0.2 and 1.2 mm posterior to bregma. The electrode tip for subject Y1 bordered the fornix while the electrode tip for subject 2B2 was just below the zona incerta. No histological results are available for rat G2.

Discussion

The present series of experiments had several objectives. First, these experiments were designed to test the ability of the extended model to predict changes in the families of I/N versus I trade-off functions generated by varying pulse duration and train duration. Second, it was hypothesized that the pulse duration experiments would aid in distinguishing between two hypotheses that have been proposed to account for the discrepancy between behaviourally- and electrophysiologically-derived strength-duration curves. Third, it was hypothesized that the pulse duration experiments might remove the influence of multiple firing from the chronaxie estimates obtained from behaviourally-derived strength-duration curves, thereby rendering these curves more comparable to electrophysiological results. Finally, it was hypothesized that the train duration experiments might remove the contribution of the electrode scar (Shizgal et al., Note 4) from charge-duration curves. The discussion will focus successively on

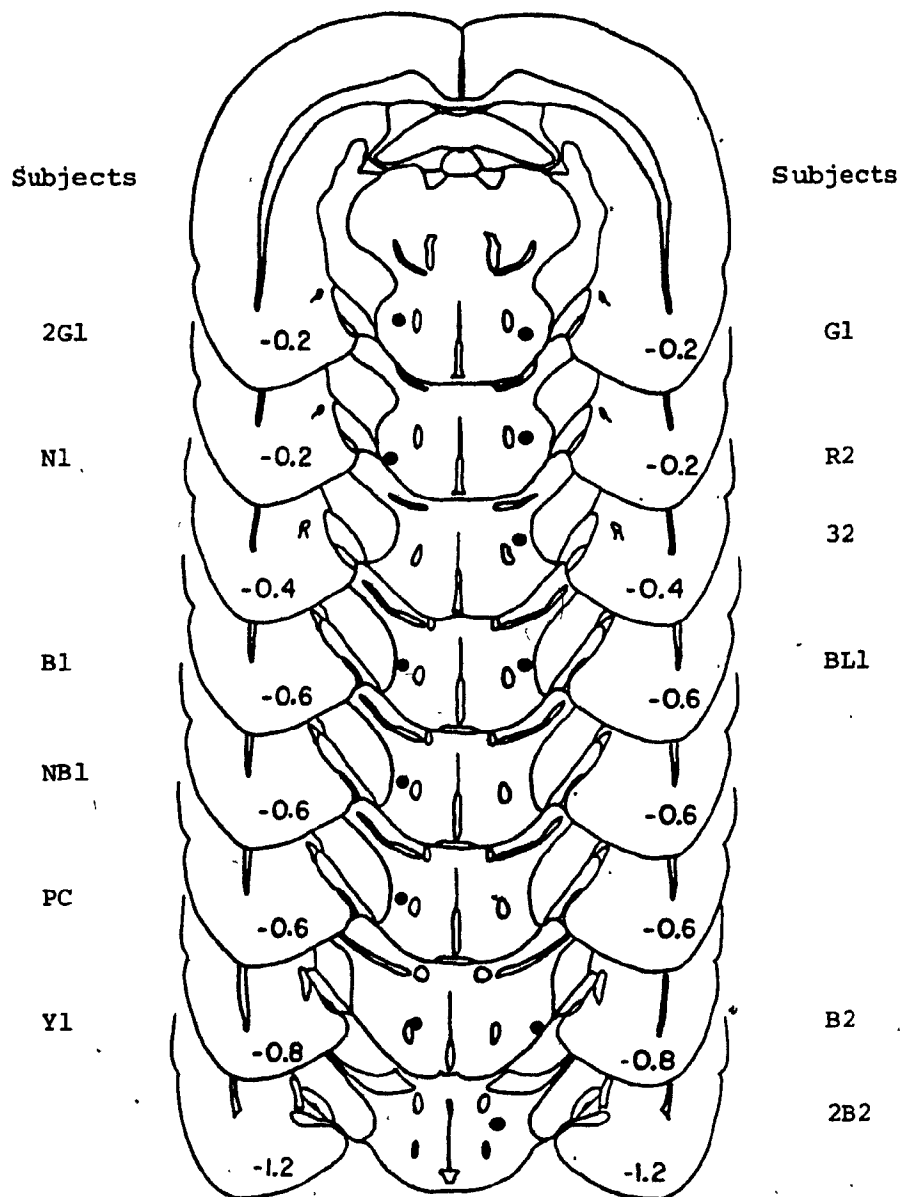


Figure 18. Electrode placements for all subjects are shown on tracings from the Pellegrino et al. (1970) atlas. The electrode tip for subject no. G2 could not be located.

each of these issues followed by an overall summary.

I. The 1/N versus I trade-off functions

In 1978, Gallistel proposed a minimal model of how electrical stimulation of the brain results in behaviour directed toward obtaining more stimulation. Building on this, Shizgal et al. (Note 4) investigated the relationship between the stimulation parameters in terms of the anatomical and physiological characteristics of the reward substrate. The term, extended model, refers to the most recent version of these models (Gallistel et al., 1981; Shizgal, Note 3). Equation 12, developed earlier, provides the mathematical representation of the extended model:

$$\begin{aligned} 1/N^0 &= w_1(d,F)/Nf(D) \times k_2/k_1(d) \times (w_2(d,I) \times I) \\ &- w_1(d,F)/Nf(D) \times k_2/k_1(d) \times I_0(d) \end{aligned} \quad (12)$$

This formidable looking equation is actually rather simple, predicting a linear relationship between 1/N and I over a central range of currents, and a breakdown in this linearity at extreme currents. The extended model predicts that certain parameters derived from the 1/N versus I trade-off function vary in systematic ways as either pulse duration or train duration is varied. These parameters are the slope, $I_0(d)$, $(1/N)_0$, I_{min} , and the 1/N value $((1/N)_c)$ corresponding to I_{min} . The experimental results and the significance of these results for each of these parameters

will be reviewed individually.

Linearity

While a straight line accounts for a very large proportion of the variance, there is often no section of the $1/N$ versus I trade-off function that is consistently and clearly flat. That is, the trade-off functions often appear to be continuous curves with the degree of curvature varying regionally.

The extended model predicts that some central portion of the trade-off function is flat. There are several possible reasons that could account for the observed non-linearity. First, the cross-sectional shape of the stimulation field may be best represented by a geometric form other than the circle prescribed. A circle is often used as an approximation to the shape of the region excited by extracellular stimulation via a monopolar electrode (Ranck, 1975). In the BSR paradigm, it is assumed that proportional changes in the current produce proportional changes in the number of stimulated neurons. However, if the impedance in the brain is too anisotropic, then the shape of the field may be more complex, and the relationship between $1/N$ and I would not be linear. Second, the electrode tip may be located some distance from the centre of the cable. In such cases, Yeomans et al., (Note 6) have proposed that there is a curvilinear relationship between $1/N$ and I .

Specifically, they predict that the degree of curvature depends on the distance between the location of the electrode tip and the centre of the cable. For example, the curvature would be greatest when the electrode tip is located outside the cable (Yeomans et al., Note 6). Third, the excitability of the neurons in the cable may vary. If so, the packing constant would become a function of the current, and bend the $1/N$ versus I trade-off function. Furthermore, different sub-populations may vary in their ability to follow high stimulation frequencies. This would tend to exaggerate the high frequency roll-off, and extend it over a greater range of currents. Any one or a combination of these violations of the assumptions could account for the observed non-linearity. With so many possible violations, there does not appear to be any obvious, non-arbitrary strategy that could correct the assumptions of the model and linearize the data.

The slope

One of the major propositions of the extended model (Shizgal et al., Note 4) concerns the slope of the $1/N$ versus I trade-off function. Shizgal et al. (Note 4) suggested dividing the slope into three components representing anatomical and physiological characteristics of the reward substrate. The three factors were: a) the reciprocal of the required number of firings ($1/N_f(D)$); b) the packing constant (k_2) representing the number of reward

neurons per square millimeter; and c) the current-distance constant ($k_1(d)$). The two weighting factors, $w_1(d,F)$ and $w_2(d,I)$, were added to represent the effect of high- and low-frequency roll-offs and multiple firing (Shizgal, Note 3).

In the pulse duration experiments, the train duration was constant. Over the linear portion of the curve at short pulse durations, the slope of the trade-off function becomes $1/Nf \times k_2/k_1(d)$. That is, the extended model predicts that only $k_1(d)$ is affected by manipulations of pulse duration. Since increases in pulse duration are similar to increases in the current, the extended model predicts that, for a given current, increases in pulse duration increase the number of reward neurons brought to threshold. The increase in the number of stimulated neurons necessitates a decrease in the number of pulses required to maintain a criterial level of behaviour, and thus increases the slope.

This prediction was largely supported by the results. Over a substantial range of pulse durations, increments in pulse duration produced systematic increments in the slope.

In the charge-duration experiments, pulse duration was held constant, and thus, the slope of the trade-off function becomes $1/Nf(D) \times k_2/k_1$. Note that only $Nf(D)$ is affected by manipulations of train duration. According to the leaky integrator model, increases in train duration decrease the

per pulse effectiveness of the stimulation. For a given current, increases in train duration will necessitate an increase in the number of pulses required to produce a critical number of firings. Therefore, an increase in the train duration should be manifested as a decrease in the slope of the $1/N$ versus I trade-off function.

This prediction was also clearly borne out by the results. As train duration was increased over a 25-fold range, the slope systematically decreased.

To this point, the discussion has focused on the orderliness of the changes in the slope. The form and parameters of the functions relating the slope to the pulse duration and train duration are discussed in detail below.

$I_0(d)$

Another major prediction of the extended model concerns $I_0(d)$, the wasted current. Shizgal et al. (Note 4) propose that not all of the current is effective in stimulating the reward neurons. To better model the relationship between $1/N$ and I , they suggested that a correction factor must be subtracted from the total current since the electrode is not a point source and some current is wasted due to its dilution by the electrode tip and surrounding scar tissue. The wasted current is the correction factor. The addition of a term to represent the wasted current changes the scalar

relationship between $1/N$ versus I (Gallistel, 1974; 1978) to a linear relationship.

The extended model predicts that $I_0(d)$ is a function of pulse duration but is not a function of train duration. It is also predicted that $I_0(d)$ is positive and deviates significantly from zero.

As predicted, $I_0(d)$ was found to be a function of pulse duration but not a function of train duration. Since $I_0(d)$ varies as a function of pulse duration, the data from the charge-duration experiment were used to test the relationship between $I_0(d)$ and zero. In the required number variant, the mean $I_0(d)$ value was negative. In the required number variant, the mean $I_0(d)$ value was positive and deviated significantly from zero. Thus, the prediction of the extended model was supported in one variant but not the other.

This seemingly contradictory finding can be understood by recalling how $I_0(d)$ is derived. A weighted, linear regression line is fit to pairs of $1/N$ and I values, and the $I_0(d)$ value is determined by extrapolating the current corresponding to a $1/N$ value of zero. This makes $I_0(d)$ subject to two sources of error: a random error due to its relative position to the mean and a systematic error resulting from the inclusion of data biased by either low- or high-frequency roll-offs.

The finding that $I_o(d)$ is negative in the required number variant will be discussed with respect to the two sources of error. To aid in the discussion of the random error, it should be recalled that in any linear regression analysis, the variance associated with a predicted value increases with the distance of its abscissal value from the mean. In the required number variant, a large range of currents was tested and all the data points were used in the regression analysis. Compared to the required current variant, this tended to shift the mean along the abscissa away from the origin. Since the predicted $I_o(d)$ values are small compared to the mean currents tested in the required number variant, there is a large amount of variance associated with $I_o(d)$. In addition, the largest currents tested tended to decrease the slope of the trade-off function because of the effect of the low-frequency roll-off. This change in the slope systematically biased the estimates of $I_o(d)$ toward small or negative values. Taken together, the random and systematic error may be responsible for the failure to obtain estimates of $I_o(d)$ that were significantly greater than zero.

In the required current variant, the opposite forces are at work. A smaller range of lower currents was used. This tended to decrease or eliminate the effect of the low-frequency roll-off. Moreover, a larger number of high frequency points were determined. Hence, the high-frequency

roll-off, which increases the slope, was more pronounced. The smaller current range reduces the variance about $I_0(d)$; the high-frequency roll-off systematically biases $I_0(d)$ toward larger and positive values. Consequently, it is not surprising that the $I_0(d)$ estimates obtained from the required current variant were significantly greater than zero.

The systematic biases inherent in each variant preclude an objective assessment of this aspect of the model. Another possibility to keep in mind is that the true value of the wasted current might be small given the electrode size and stimulation site. If so, accurate estimates would be difficult to obtain under the conditions of this experiment.

$(1/N)_0$

The prediction of a negative $(1/N)_0$ value follows from the predictions that there is a linear relationship between $1/N$ and I , and that $I_0(d)$ value is positive. Since $(1/N)_0$ varies to a greater extent as a function of train duration, this hypothesis was tested using $(1/N)_0$ values obtained in the strength-duration experiment. As predicted, the $(1/N)_0$ value was found to be negative and significantly different than zero.

In Equation 12, $(1/N)_0$ is equal to $-w_1(d,F)/N_f(D) \times k_2/k_1(d) \times I_0(d)$. For short pulse durations, $w_1(d,F)$ has a

value of unity over the linear portion of the curve. In that case, the extrapolated value of $(1/N)_0$ becomes $-1/Nf(D) \times k_2/k_1(d) \times I_0(d)$.

With train duration constant, the $(1/N)_0$ value is simplified to $-1/Nf \times k_2/k_1(d) \times I_0(d)$. Changes in $k_1(d)$ as a function of pulse duration are offset by changes in $I_0(d)$. Therefore for short pulse durations, the extended model (Shizgal et al., Note 4) predicts that $(1/N)_0$ is constant. At long pulse durations, the extended model predicts that the reward neurons fire repetitively and $w_1(d, F)$ is assigned a value greater than one and increases in proportion to the increase in frequency with which the neurons fire repetitively. When the constant, $-1/Nf(D) \times k_2/k_1(d) \times I_0(d)$ is multiplied by the weighting factor, $w_1(d, F)$, the value of $(1/N)_0$ decreases. Therefore for long pulse durations, the $(1/N)_0$ value decreases with increments of pulse duration. These predictions were not supported.

For a constant, short pulse duration, the $(1/N)_0$ value simplifies to $-1/Nf(D) \times k_2/k_1 \times I_0$. As discussed with respect to the slope, $Nf(D)$ increases ($1/Nf(D)$ decreases) with increments of train duration. No significant main effect of train duration on $(1/N)_0$ was found in the required number variant in the train duration experiment. However, a significant main effect was found in the required current variant. Thus, the prediction was supported in one variant but not the other.

The failure of several predictions concerning $(1/N)_o$ may well be due to the factors responsible for the uncertainty associated with $I_o(d)$. That is, since $(1/N)_o$ is an extrapolated point, it suffers from the same sources of error as $I_o(d)$.

I_{min}

The extended model (Shizgal et al., Note 4) predicts that there is a minimum current, I_{min} , below which behaviour will not be elicited. Further, I_{min} is predicted to be both a function of pulse duration and train duration.

With train duration constant, I_{min} is predicted to decrease with increments of pulse duration provided that the pulse durations are short. Long pulse durations are hypothesized either to elicit repetitive firing or to recruit additional sub-populations that have long chronaxies. The extended model predicts that the influence of repetitive firing is similar to a change in frequency. If this is correct, then I_{min} should asymptote and the $(1/N)_c$ values corresponding to I_{min} should increase. The extended model predicts that the recruitment of additional sub-populations within the cable is similar to a change in k , the packing constant. If this is correct, then I_{min} should continue to decrease and the $(1/N)_c$ values corresponding to I_{min} should increase.

A significant main effect of pulse duration on I_{min} was found. However, for several subjects, the I_{min} value associated with the longest pulse duration was greater than the I_{min} value associated with the second longest pulse duration. Neither the multiple firing nor the multiple sub-population hypothesis predicts these results.

One possible explanation for the increase in I_{min} concerns F_{max} . As pulse duration increases, the amount of time required between pulses to discharge the brain-electrode interface increases. Therefore, the maximum frequencies that could be run decreased with increments in pulse duration. It is possible that at the long pulse durations, F_{max} could not be reached because of charge build-up. That is, the experimenter avoided testing the higher frequencies because of the possibility of lesioning the stimulation site. If F_{max} was not reached, then the $1/N$ versus I trade-off functions at the long pulse durations were truncated at the low current intensities. That is, an artificial limit imposed by the charge build-up may have made it impossible to attain I_{min} .

An analysis is currently underway that is designed to determine whether I_{min} has been overestimated. The analysis involves examining the shape of the high-frequency roll-off in a standardized, transformed space. It is expected that a failure to have attained I_{min} will manifest itself in the

absence or attenuation of the high-frequency roll-off.

One possible strategy for reducing the charge build-up is to use less polarizable electrodes. For example, a platinum-iridium cathode and a sintered, silver/silver-chloride pellet anode may perform better than the electrodes used in this experiment.

When frequency and pulse duration are held constant, the extended model predicts that the required current varies with train duration. It is assumed that with the current equal to I_{min} , the frequency is fixed at F_{max} . Hence, I_{min} should vary with train duration. Unfortunately, a limitation of the equipment prevented a direct test of this prediction. Such a test was approximated by computing the required current at a fixed frequency of 400 hertz. The current value corresponding to the shortest train duration was significantly greater than the current values for the other train durations.

The impressively linear charge-duration functions derived by Gallistel (1978) predict hyperbolic changes in I_{min} as a function of train duration. The observation that the required current for a frequency of 400 hertz often increased when the train duration was lengthened from 0.5 sec to 2.5 sec is inconsistent with a hyperbolic trend. This may be related to the covariance of task difficulty and train duration. At short train durations, the subjects

vigorously pressed the lever, sometimes reaching rates of 6-7 presses per second. However at long pulse durations, the subject's behaviour was different. This was especially evident when I_{min} was approached during the 2.500 sec train. The subject would press the bar, and then initiate another response only after the train finished. In some cases, the motoric effects of the stimulation appeared to turn the subject away from the lever. It is possible that these effects slightly shifted the threshold. That is, as the task became more difficult, the subject required a larger reward to elicit a bar press. Another possibility that could account for the failure to find the hyperbolic relationship concerns F_{max} . If the maximum frequency that the stimulated fibres are able to follow declines as train duration increases, then more fibres would have to be excited to ensure a criterial level of performance. This would necessitate an increase in the current.

$(1/N)_c$

The $1/N$ value corresponding to the intersection of the regression line and a line drawn vertically from I_{min} is predicted to be a function of pulse duration and train duration. This general prediction of the extended model was supported for both the strength-duration and the charge-duration experiments. The more specific prediction that the relationship between $(1/N)_c$ and I_{min} could discriminate between multiple firing or multiple sub-populations will be

discussed below.

The fate of the principal predictions: A summary

The relationship between $1/N$ and I appears to be curvilinear. However, a linear function is a close approximation to the data, particularly over the central range of currents. The inability to find a clearly consistent linear segment might be due to oversimplified assumptions concerning the geometric properties of the substrate and the stimulation field as well as the homogeneity of the substrate.

In the two variants of the pulse duration and train duration experiments orderly changes in the slope of the $1/N$ versus I trade-off functions were noted. Specifically, the slope of the trade-off function increases with pulse duration and decreases with train duration. The orderliness of the changes over the range of pulse durations and train durations tested appears to support the hypothesis of the extended model (Shizgal et al., Note 4) that the slope of the trade-off may be conceived of as a composite of anatomical and physiological factors.

The predictions concerning I_0 and $(1/N)_0$ tended to be supported in the required current variants, but not in the required number variants. These contradictory findings were hypothesized to arise from systematic and random errors that

bias the results in the direction of the predictions in the required current variants and to bias the results in the direction opposite to the predictions in the required number variants. Another reason why I_0 and $(1/N)_0$ may be so sensitive to these errors could be that the contribution of the wasted current is small.

As predicted, I_{min} was found to be a function of pulse duration. However, I_{min} tended to increase at the longest pulse durations. This last finding may be due to charge build-up at the brain-electrode interface. In addition, the results supported the prediction that I_{min} would vary with train duration. The unexpected increase in I_{min} at the longest train durations may have been due to interfering movements induced by the stimulation.

The prediction that $(1/N)_c$ is a function of pulse duration and train duration was supported.

It should be remembered that in the strength-duration experiment, only four pulse durations from the required number variant were used in the statistical analysis since not all subjects were run at the same pulse durations. Therefore, the conclusions concerning the five predictions for that experiment are not as definitive as would be desired.

The gross predictions of the extended model have

generally been borne out by the experiments. Some of the finer predictions have fared less well. It is not clear to what degree this is due to shortcomings of the model or the experimental techniques. Whereas this section dealt with the adequacy of the model, the next section uses the model to derive higher-order trade-off functions. According to the model, these higher-order functions estimate fundamental characteristics of the B&R substrate.

II. Multiple firing versus multiple sub-populations

Shizgal and his co-workers have proposed that the directly stimulated substrate for self-stimulation of the medial forebrain bundle includes myelinated axons (Bielajew and Shizgal, 1982; Shizgal et al., 1980; Shizgal, Kiss, and Bielajew, 1982). If the substrate is entirely comprised of such fibres, then there is a discrepancy between behaviourally-derived (Matthews, 1977) and electrophysiological-derived (cited by Ranck, 1975) chronaxie estimates. Matthews (1977) hypothesized that the difference may be due to the influence of multiple firing or multiple sub-populations. Since each hypothesis predicts a different effect of pulse duration on the family of $1/N$ versus I trade-off functions, the extended model (Shizgal et al., Note 4) should make possible a discrimination between these two hypotheses.

At long pulse durations, the multiple firing hypothesis predicts that the I_{min} values reach an asymptote while the

slopes continue to change. If so, chronaxie estimates based on the slope should be greater than those based on I_{min} .

At first glance, the results appear to support this prediction. The mean chronaxie estimate based on I_{min} was 0.13 msec, while the mean chronaxie estimate based on the slope was 0.60 msec. However, this result may be artifactual. If as argued above, I_{min} was overestimated at long pulse durations, then the corresponding chronaxie estimates would be underestimated. That is, if I_{min} was overestimated, then any strength-duration curve based on I_{min} would reach asymptote earlier and would have a shorter chronaxie. Hence, the build-up of charge at the brain-electrode interface may be indirectly responsible for the chronaxie difference.

An analogous argument can be made concerning the prediction that $(1/N)c$ increases at long pulse durations. The experimentally-derived results are in accordance with the predicted changes but could be explained by a procedural artifact - the restriction on testing high frequencies when using long pulse durations.

The predictions of the multiple firing hypothesis concerning I_0 and $(1/N)_0$ were not supported. The failure to find an effect of pulse duration on I_0 and $(1/N)_0$ may be due to their small magnitude or to the large variability inherently associated with them.

At long pulse durations, the multiple sub-population hypothesis predicts that the I_{min} values continue to decrease at the same rate as the slopes continue to increase. This was not observed. As noted above, there is a discrepancy in the chronaxie estimates based on I_{min} and the slope. Nonetheless, this discrepancy does not necessarily undermine the multiple sub-population hypothesis because of the possible procedural artifact.

Like the multiple firing hypothesis, the multiple sub-population hypothesis predicts that $(1/N)_c$ increases with pulse duration. While the data bear out this prediction, this could be due to procedural rather than physiological factors.

As in the case of the multiple firing hypothesis, the predictions concerning I_0 and $(1/N)_0$ were not supported. The failure to find an effect of pulse duration on these two parameters has already been discussed.

Theoretically, the extended model permits a discrimination to be made between the multiple firing and the multiple sub-populations hypotheses. The experimentally-derived results best fit the multiple firing hypothesis, but this may be due to a procedural artifact. As discussed above, this problem could be circumvented by using less polarizable electrodes.

While the present experiments could not conclusively distinguish between the two hypotheses, Milner and Laferriere (1982) have published data that they believe support the multiple sub-population hypothesis. The basis of their work is the following pair of assumptions: a) the strength-duration curves of the individual reward-related neurons are exponential in shape and b) the long chronaxie elements have a greater behavioural weight than the short chronaxie elements. To test these assumptions, Milner and Laferriere determined strength-duration curves for neurons at sites in the LH and the periaqueductal grey (PAG). When a single exponential function was fit to the data at either site, a large discrepancy between the predicted points and the experimentally-derived points was found at the long pulse durations. In order to account for this large discrepancy in terms of the multiple firing hypothesis, Milner and Laferriere (1982) concluded that the reward neurons would have to fire four to five times for a 1 msec pulse. They felt that this was unrealistic.

There is experimental support for the role of myelinated neurons with short chronaxies in BSR (Gallistel et al., 1981; Shizgal et al., 1980). Such neurons are likely to have short chronaxies (Ranck, 1975). In order to account for their data, Milner and Laferriere concluded that some proportion of the stimulated neurons must have longer chronaxies. In support of this notion, they showed that

their results were well described by fitting one exponential function to the data for the pulse durations between 0.1 - 0.4 msec and another to the data for pulse durations between 0.4 - 2.0 msec. They concluded that long chronaxie elements play a proportionally larger role at the longer pulse durations.

However, as outlined in the introduction, cable theory and the Hodgkin-Huxley theory of axonal excitability argue that a lumped resistor-capacitor model of the membrane, which predicts a simple exponential relationship between current and pulse duration, is oversimplified. Deviations from simple exponential behaviour could be due to such parameters as non-linear membrane resistance or accommodation (Noble and Stein, 1976).

This means that strength-duration curves for single neurons are not necessarily best described by an exponential function. It should be recalled that the strength-duration curves of some of Matthews' (1978) units could be best described by an exponential function, others by a hyperbolic function, whereas others were described equally well by both or well described by neither. Also, Matthews found that 2 out of the 27 units studied responded with two or three action potentials for pulses of more than 2 msec. While the units studied by Matthews (1978) were not necessarily part of the BSR substrate, it would appear that neurons at sites that support self-stimulation display characteristics that

could account for the results obtained by Milner and Laferriere (1982) without using a multiple sub-population model.

At this moment, there does not appear to be any experimental evidence that definitively distinguishes between the multiple firing and the multiple sub-population hypotheses. Tests of the plausibility of these hypotheses may be carried out via electrophysiological recording. This could involve matching candidate reward neurons to a list of behaviourally-derived electrophysiological characteristics and then using pulses of long duration to test for repetitive firing.

It would not be surprising if both hypotheses were correct. It is known that a wide variety of axons will fire repetitively during prolonged depolarizations (Connor, Walter, and McKown, 1977). On the other hand, West and Wolstencroft (1983) obtained very long chronaxie estimates for unmyelinated axons in the mammalian central nervous system, estimates long enough to account for the present results. Furthermore, Yeomans (1979) unequal pulse study provides independent support for the multiple sub-population model by showing that recovery occurs gradually even when steps are taken to minimize the contribution of the absolute refractory period.

III. A non-arbitrary, strength-duration curve

It was proposed that the pulse duration experiments might permit the influence of multiple firing to be eliminated from the chronaxie estimates obtained from behaviourally-derived strength-duration curves. This was seen as an important goal because multiple firing does not contribute to electrophysiologically-derived curves. Chronaxie estimates corrected in this way should render the two types of curves more comparable. Hence, this correction should increase the likelihood that electrophysiological recording studies will aid in identifying the neural elements subserving BSR.

Given the uncertainty surrounding the determination of I_{min} , the need for such a correction is presently unclear.

IV. The charge-duration curve

One of the reasons for doing the train duration experiments was to determine the form and parameters of the charge-duration function. Previous researchers (Gallistel, 1978; Huston et al., 1976) have found a linear relation between the required charge and the train duration. However, previous research has not taken into account the wasted current proposed by Shizgal et al. (Note 4).

A strong, linear relationship was found between the

effective charge and train duration. The correlation coefficients for these functions ranged between 0.98 and 1.00. The striking linearity of the charge-duration function is an important constraint on models of temporal integration in the BSR substrate. That is, any proposed model must be able to account for the linear relationship that exists between charge and input duration.

In the introduction, temporal integration within the BSR substrate was modelled as a leaky integrator. However, as pointed out by Gallistel et al. (1981), the linearity of the charge-duration function is inconsistent with a simple leaky integrator model such as the one proposed by Edmonds et al. (1974), but is compatible with more complex leaky integrator models (Norman and Gallistel, 1978).

Having established that the form of the charge-duration function is indistinguishable from a straight line, the significance of its parameters can now be discussed. The parameter that Gallistel (1978) has taken to be the most meaningful is the ratio of the y-intercept and the slope. This ratio is the chronaxie of the strength-duration function for trains, the function obtained by dividing the charge values by the train duration. Gallistel (1978) has argued that the chronaxie of the strength-duration function for trains is related to the time course of temporal integration, and is one of the fundamental parameters describing the reward substrate.

A significant difference was found between chronaxie estimates obtained in the present experiment and in Gallistel's (1978) study. The difference could arise from the use of different paradigms or from the use of different procedures to calculate the charge.

To determine whether the differences were due to the paradigms, it would be necessary to test the same subjects in both an alley way and a Skinner box. Such a comparison has not yet been made.

To determine whether the differences are due to the procedures used to calculate the charge, chronaxie estimates based on the effective current (Shizgal et al., Note 4) and the total current (Gallistel, 1978) were calculated for all subjects run in the charge-duration experiments (see Table 20). No significant difference was found between mean chronaxie estimates derived from either of the two analyses when all the subjects were compared. This would tend to support the hypothesis that the difference in chronaxie estimates is due to the paradigm rather than the procedure to calculate the charge.

However, it may be recalled that I_0 was -50 uamps in the required number variant and was 56 uamps in the required current variant. As discussed earlier, I_0 is underestimated in the required number variant due to low-frequency roll-off

and overestimated in the required current variant due to the high-frequency roll-off. The possibility that errors in estimating the wasted current might influence the analysis can be assessed by comparing chronaxie estimates based on the required number variant and the required current variant.

It may be recalled that Table 20 compared the chronaxie estimates based on the effective charge and the total charge. In that table, the data for the first six subjects are the results from the required number variant, while the data for the last four subjects are ~~the~~ results from the required current variant.

A statistical comparison of the means or medians was not performed due to the small number of subjects. The discussion below uses the median values to describe differences between groups of chronaxie estimates without attempting to assess the significance of these differences.

When the effective charge (Q') is used to derive chronaxie estimates from the charge-duration function, the median values for the required number and required current variants are 0.26 and 0.19 sec, respectively. Since there is considerable overlap between the two distributions, this difference is probably not very meaningful. Despite the opposing biases inherent within the two variants, it would appear that the effective current yields comparable

chronaxie estimates.

When the total charge is used to derive chronaxie estimates, the median values for the required number and required current variants are 0.17 and 0.38 sec, respectively. The difference between these median estimates may be meaningful since there is no overlap between the two distributions. Contrary to the finding for the effective charge, chronaxie estimates based on the total charge appear to be sensitive to the magnitude of the wasted current.

The two median chronaxie estimates based on the total charge, 0.17 and 0.38 sec, straddle the median chronaxie estimates based on the effective charge, 0.26 and 0.19. This suggests that the total charge is more sensitive than the effective charge to the low- and high-frequency roll-offs. That is, in the required number variant where the effect of the low-frequency roll-off should be greatest, the total charge yields a smaller chronaxie estimate, while the opposite is true in the required current variant.

Furthermore, when Gallistel (1978) derived his charge-duration function, he set the frequency and determined the current required to yield a criterial response. This is similar to the paradigm employed here in the required current variant. The median chronaxie estimate obtained by Gallistel was 0.44 sec with a range of 0.28-0.61 sec. When the total charge was used to determine the charge-duration

function in the present required current experiment, the median chronaxie was 0.38 sec with a range of 0.28-0.54 sec. These results appear similar. They appear even more similar when compared to estimates based on the effective charge. The median chronaxie was 0.19 sec with a range of 0.05-0.25 sec.

This last finding would tend to support the hypothesis that the difference in chronaxie estimates is a result of the different procedures used in calculating the charge rather than a result of the differences in the paradigms.

In summary, a linear charge-duration function was obtained when the corrected current was used to compute the required charge. This is consistent with the findings of previous researchers (Gallistel, 1978; Huston et al., 1976). A discrepancy between the chronaxie estimates obtained in the present experiment and in Gallistel's (1978) study was noted. This difference may result from the different paradigms used in each study. However, it appears more likely that the discrepancy stems from the inclusion of the wasted current in Gallistel's calculations. The procedure used here not only attempts to factor out the wasted current, but also may be less sensitive to the systematic deviations from linearity observed at low and high frequencies.

V. Overview

Electrical stimulation of the brain has been proposed as a tool for characterizing neural circuits so that they can be identified and linked to the behaviours they subserve. In order to use this tool effectively, it is necessary to understand how the stimulation parameters affect the activity of the reward substrate. The extension of Gallistel's (1978) model that has been proposed by Shizgal et al., (Note 4) relates the stimulation parameters through the use of anatomical and physiological constructs that, in turn, describe substrate characteristics.

The object of the present research was two-fold. First, the extended model was evaluated by examining the family of $1/N$ versus I trade-off functions generated when pulse duration and train duration were varied. Second, the parameters of the $1/N$ versus I trade-off functions were used to establish higher-order, trade-off functions in order to characterize the BSR substrate.

The extended model proposes that the slope of the $1/N$ versus I trade-off function can be divided into three anatomical and physiological variables. The orderliness of the changes in the slope following manipulations of parameters that should independently affect two of these variables is consistent with this hypothesis.

Also, the extended model proposes that there is a linear relationship between $1/N$ and I over some range of currents. Inherent within the idea of linearity are two concepts: that a straight line provides a reasonable description of the relationship between $1/N$ and I over the central range of behaviourally effective currents, and that some of the stimulating current is wasted since the electrode tip is not a point source. While no section of the $1/N$ versus I trade-off function appears to be consistently and clearly flat, a straight line accounts for a very large proportion of the variance. It appears that in this paradigm, estimates of the wasted current include substantial random and systematic errors. Consequently, it was impossible to firmly establish the importance of the wasted current.

Finally, increments in pulse duration and train duration are predicted to produce decrements in I_{min} , the current below which behaviour cannot be elicited regardless of the stimulation frequency. Such effects were observed but were reversed both at long pulse durations and long train durations.

In summary, the gross predictions of the extended model were supported for the most part, while some of the finer predictions were not. It appears that the extension of Gallistel's model sheds some light on the relationship between $1/N$ and I . The derivation of higher-order trade-off

functions from these data attempted to make use of these insights.

In the strength-duration experiments, the establishment of higher-order, trade-off functions depended on determining an accurate estimate of I_{min} . Due to a procedural artifact, I_{min} may have been overestimated at long pulse durations. Therefore, it was not possible to accurately estimate the chronaxie of the strength-duration function for pulses. Consequently, it was not possible to distinguish between the two hypotheses that have been proposed to account for the unusually long chronaxie estimates obtained in self-stimulation experiments. A platinum cathode and a sintered, silver/silver-chloride anode combination may reduce electrode polarization and make it possible to more accurately determine I_{min} at long pulse durations.

In the charge-duration experiments, trade-off functions were derived by determining the relationship between the effective charge and the train duration. The striking linear relationship that has also been noted by previous researchers imposes a quantitative constraint upon any proposed model of temporal integration. For example, in its present form, the simple leaky integrator model proposed by Edmonds et al., (1974) cannot account for temporal integration within the reward substrate since this model can not account for the linear charge-duration function.

A significant difference between the chronaxie estimates obtained in the present experiment and in Gallistel's (1978) study was noted. This discrepancy may be due to the procedure used to calculate the charge. The procedure used here, which attempts to factor out the waste current, may be less sensitive to systematic errors.

It would appear that the extended model contributes to understanding how stimulation parameters affect the activity of the substrate for rewarding MFB stimulation. In turn, this may increase the effectiveness with which the BSR paradigm can be used to characterize neural circuits subserving reward.

Reference notes

1. Mundl, W. Internal communications, 1975.
2. Sax, L.D., and Gallistel, C.R. Temporal integration in self-stimulation: A paradox. (In preparation).
3. Shizgal, P. A model of spatial and temporal integration in the substrate for brain stimulation reward. (In preparation).
4. Shizgal, P., Howlett, S., and Corbett, D. Behavioral inference of current-distance relationships in rewarding electrical stimulation of the rat hypothalamus. Poster presented at the meeting of the Canadian Psychological Association, Quebec City, June, 1979.
5. Tee, O. Department of Chemistry, Concordia University. A Basic program for Apple computers: Non-linear least squares regression analysis.
6. Yeomans, J.S., Pearce, R., Wen, D., and Hawkins, R. Localization of a midbrain circling substrate by means of current-frequency trade off data. (In preparation).

References

Bielajew, C., and Shizgal, P. Behaviorally derived measures of conduction velocity in the substrate for rewarding medial forebrain bundle stimulation. Brain Research, 1982, 237, 107-119.

Caggiula, A.R., and Hoebel, B.G. "Copulation-reward site" in the posterior hypothalamus. Science, 1966, 153, 1284-1285.

Connor, J.A., Walter, D., and McKown, R. Neural repetitive firing: Modifications of the Hodgkin-Huxley axon suggested by experimental results from crustacean axons. Biophysical Journal, 1977, 18, 81-102.

Cornsweet, T.N. Visual perception. New York: Academic Press, 1970.

Cuthbert, D., and Wood, F.S. Fitting equations to data: Computer analysis of multifactor data (2nd ed.). New York: John Wiley and Sons, 1980.

Deutsch, J.A., Chisholm, D., and Mason, P.A. Adaptation to rewarding brain stimuli of differing amplitude. Behavioral and Neural Biology, 1980, 29, 359-364.

Edmonds, D.E., Stellar, J.R., and Gallistel, C.R. Parametric

analysis of brain stimulation reward in the rat: II. Temporal summation in the reward system. Journal of Comparative and Physiological Psychology, 1974, 87, 860-869.

Gallistel, C.R. Note on temporal summation in the reward system. Journal of Comparative and Physiological Psychology, 1974, 87, 870-875.

Gallistel, C.R. Motivation as central organizing process: The psychophysical approach to its functional and neurophysiological analysis. In J. Cole and T. Sonderegger (Eds.), Nebraska Symposium on Motivation, 1975a, 22, 183-250.

Gallistel, C.R. Spatial and temporal summation in the neural circuit subserving brain-stimulation reward. In A. Wauquier and E.T. Rolls (Eds.), Brain-stimulation reward. New York: American Elsevier Publishing Company, Inc., 1975b.

Gallistel, C.R. Self-stimulation in the rat: Quantitative characteristics of the reward pathway. Journal of Comparative and Physiological Psychology, 1978, 92, 977-998.

Gallistel, C.R., Shizgal, P., and Yeomans, J.S. A portrait of the substrate for self-stimulation. Psychological

Review, 1981, 88, 228-273.

Gallistel, C.R., Stellar, J.R., and Bubis, E. Parametric analysis of brain stimulation reward in the rat: I. The transient process and the memory-containing process. Journal of Comparative and Physiological Psychology, 1974, 87, 848-859.

Guest, P.G. Numerical methods of curve fitting. Cambridge: Cambridge University Press, 1961.

Hill, A.V. Excitation and accommodation in nerve. Proceedings of the Royal Society B, 1936, 119, 305-355.

Hodgkin, A.L., and Huxley, A.F. Currents carried by sodium and potassium ions through the membrane of the giant axon of Loligo. Journal of Physiology, 1952a, 116, 449-472.

Hodgkin, A.L., and Huxley, A.F. The components of membrane conductance in the giant axon of Loligo. Journal of Physiology, 1952b, 116, 473-496.

Hodgkin, A.L., and Huxley, A.F. The dual effect of membrane potential on sodium conductance in the giant axon of Loligo. Journal of Physiology, 1952c, 116, 497-506.

Hodgkin, A.L., Huxley, A.F., and Katz, B. Measurement of

current-voltage relations in the membrane of the giant axon of Loligo. Journal of Physiology, 1952, 116, 424-448.

Hodgkin, A.L., and Rushton, W.A.H. The electrical constants of a crustacean nerve fibre. Proceedings of the Royal Society, B, 1946, 133, 444-476.

Hoebel, B.G. Inhibition and disinhibition of self-stimulation and feeding: Hypothalamic control and postingestional factors. Journal of Comparative and Physiological Psychology, 1968, 66, 89-100.

Hoebel, B.G. Feeding and self-stimulation. Annals of the New York Academy of Sciences, 1969, 157, 758-778.

Hoebel, B.G. Brain reward and aversion systems in the control of feeding and sexual behavior. In J.K. Cole and T.B. Sonderegger (Eds.), Nebraska Symposium on Motivation, (Vol. 22). Lincoln: University of Nebraska Press, 1975.

Hoebel, B.G., and Teitelbaum, P. Hypothalamic control of feeding and self-stimulation. Science, 1962, 135, 375-377.

Hoebel, B.G., and Thompson, R.D. Aversion to lateral hypothalamic stimulation caused by intragastric feeding

on obesity. Journal of Comparative and Physiological Psychology, 1969, 68, 536-543..

Huston, J.P., Mills, A.W., and Huston, R. Strength-duration function of hypothalamic self-stimulation. Behavioral Biology, 1972, 7, 383-390.

Kandel, E.R. Nerve cells and behavior. Scientific American, 1970, 223(1), 57-70.

Lapicque, L. Considerations prealables sur la nature du phenomene par lequel l'electricite excite les nerfs. Journale de physiologie et de pathologie generale, 1907, 9, 565-578.

Lucas, K. On summation of propagated disturbances in the claw of Astacus, and on the double neuro-muscular system of the adductor. Journal of Physiology (London), 1917, 51, 1-35.

Margules, D.L., and Olds, J. Identical "feeding" and "rewarding" systems in the lateral hypothalamus of rats. Science, 1962, 135, 374-375.

Matthews, G. Neural substrate for brain stimulation reward in the rat: Cathodal and anodal strength-duration properties. Journal of Comparative and Physiological Psychology, 1977, 91, 858-874.

Matthews, G. Strength-duration properties of single units driven by electrical stimulation of the lateral hypothalamus in rats. Brain Research Bulletin, 1978, 3, 171-174.

Milner, P.M. and Laferriere, A. Strength-duration characteristics of lateral hypothalamic and periaqueductal gray reward-path neurons. Physiology and Behavior, 1982, 29, 857-863.

Mundl, W.J. A constant-current stimulator. Physiology and Behavior, 24, 1980, 991-993.

Noble, D., and Stein, R.B. The threshold conditions for initiation of action potentials by excitable cells. Journal of Physiology (London), 1966, 157, 129-162.

Norman, M.F., and Gallistel, C.R. What can one learn from a strength-duration experiment. Journal of Mathematical Psychology, 1978, 18, 1-24.

Olds, J., and Milner, P. Positive reinforcement produced by electrical stimulation of septal area and other regions of rat brain. Journal of Comparative and Physiological Psychology, 1954, 47, 419-427.

Pearson, K.G. The control of walking. Scientific American,

1976, 235(6), 72-86.

Pellegrino, L.J., Pellegrino, A.S., and Cushman, A.J. A stereotaxic atlas of the rat brain (2nd ed.). New York: Plenum Press, 1979.

Ranck, J.B., Jr. Which elements are excited in electrical stimulation of mammalian central nervous system: A review. Brain Research, 1975, 98, 417-440.

Roeder, K.D. Nerve cells and insect behavior (Rev. ed.). Cambridge: Harvard University Press, 1976.

Rolls, E.T., Burton, M.J., and Mora, F. Neurophysiological analysis of brain-stimulation reward in the monkey. Brain Research, 1980, 194, 339-357.

Rushton, W.A.H. The time factor in electrical excitation. Biological Reviews, 1935, 10, 1-17.

Shizgal, P., Bielajew, C., Corbett, D., Skelton, R., and Yeomans, J. Behavioral methods for inferring anatomical linkage between rewarding brain stimulation sites. Journal of Comparative and Physiological Psychology, 1980, 94, 227-237.

Shizgal, P., Kiss, I., and Bielajew, C. Psychophysical and electrophysiological studies of the substrate

for brain stimulation reward. In B.G. Hoebel and D. Novin^o (Eds.), The neural basis of feeding and reward. Brunswick, Maine: Haer Institute, 1982.

Ward, H.P. Stimulus factors in septal self-stimulation. American Journal of Physiology, 1959, 196, 779-782.

West, D.C., and Wolstencroft, J.H. Strength-duration characteristics of myelinated —and non-myelinated bulbospinal axons in the cat spinal cord. Journal of Physiology, 1983, 337, 37-50.

Yeomans, J.S. Quantitative measurement of neural post-stimulation excitability with behavioral methods. Physiology and Behavior, 1975, 15, 593-602.

Yeomans, J.S. The absolute refractory periods of self-stimulation neurons. Physiology and Behavior, 1979, 22, 911-919.

